HEAT CONDUCTION IN HEAT-GENERATING UNIDIRECTIONAL COMPOSITES

A THESIS

Presented to

The Faculty of the Division of Graduate Studies

by

Thomas Lawler Wilson, Jr.

In Partial Fulfillment

of the Requirements for the Degree

Master of Science

in the School of Nuclear Engineering

Georgia Institute of Technology

June, 1976

HEAT CONDUCTION IN HEAT-GENERATING UNIDIRECTIONAL COMPOSITES

Approved:

James H. Rust, Chairman

J. Karl Davidson

Roger W. Carlson

Date approved by Chairman: April 29, 197

ACKNOWLEDGMENTS

The author wishes to express his thanks to his thesis advisor, Dr. James H. Rust, for his never-ending encouragement. His experience and expert critical suggestions provided inspiration and incentive during the preparation of this paper.

Thanks are also due to Dr. J. Narl Davidson and Dr. Roger W. Carlson. Their critical suggestions as members of the Reading Committee were very helpful.

Finally, the author wishes to thank Mrs. Lydia S. Geeslin and Mrs. Teresa G. Mosley for their patience and support while typing this thesis and lettering the equations, respectively.

TABLE OF CONTENTS

TABLE OF CONTENTS (Concluded)

LIST OF TABLES

LIST OF ILLUSTRATIONS

LIST OF ILLUSTRATIONS (Continued)

LIST OF ILLUSTRATIONS (Concluded)

SUMMARY

Heat conduction is analyzed in composite nuclear fuels consisting of metal fibers uniformly aligned in a matrix of uranium dioxide. A unit cell consisting of a single fiber and the surrounding hexagonal matrix is approximated by concentric cylinders. A gap conductance boundary condition is assumed at the fiber-matrix interface. An exact solution to the heat conduction equation is obtained for constant thermal conductivity and an approximate solution is obtained for thermal conductivity linearly dependent on temperature. The temperature distributions are used to define the following properties: effective conductivity, heat content, and effective volumetric heat capacity.

The calculated properties and temperature distributions are evaluated in a parametric study for a range of cell dimensions, physical properties, and gap conductances. The study shows that, for constant thermal conductivity, the calculated properties approach asymptotes for both large and small length-to-radius ratios. The formula for the effective conductivity upper asymptote is the volume-weighted average of the constituent conductivities for heat generation in both phases and a gap conductance at the fiber matrix interface. Temperature distributions for large length-to-radius ratios are independent of the radial coordinate and parabolic in the axial coordinate. In addition, temperature distributions are used to derive an easily calculated, approximate formula for effective conductivities for regions slightly less than the upper asymptote.

For a linear thermal conductivity in the matrix, a first-order

perturbation solution for temperature distributions is shown to be a good approximation. Limits of applicability are presented, and calculated properties are defined. A parametric study shows that, for large length-to-radius ratios, the calculated properties do not approach asymptotes as in the constant conductivity case. However, there is a reasonably uniform, quasi-asymptotic region in which the calculated quantities may be approximated by the asymptotic formulas for large length-to-radius ratios given for the constant conductivity problem.

CHAPTER I

INTRODUCTION

Composite materials contain two or more distinguishable phases. Unidirectional composites are binary composites with a base material called the matrix and long, continuous, rod-like inclusions uniformly aligned in the matrix. The rod-like inclusions are referred to as fibers, filaments, or rods. The parallel axis refers to the coordinate axis parallel to the rods; the normal or transverse axis to the coordinate axis perpendicular to the rods.

A composite of this type consisting of tungsten fibers in a uranium dioxide matrix has been successfully fabricated by Chapman, Clark, and Hendrix [1]. The fiber density is of the order of 40 million fibers per square centimeter with a fiber diameter of less than one micron. An electron micrograph, Figure 1, shows the regular microstructure of the composite.

Nuclear reactor fuels made of the UO_2-W composite are expected to exhibit considerable improvements in conductivity. The conductivity is significantly anisotropic, being larger along the parallel axis than the normal.

To capitalize on the greatest conductivity enhancement, fuel elements should have fibers parallel to the path of greatest heat conduction. This suggests plate elements with fibers oriented perpendicular to the plate surfaces or cylindrical elements with fibers aligned radially

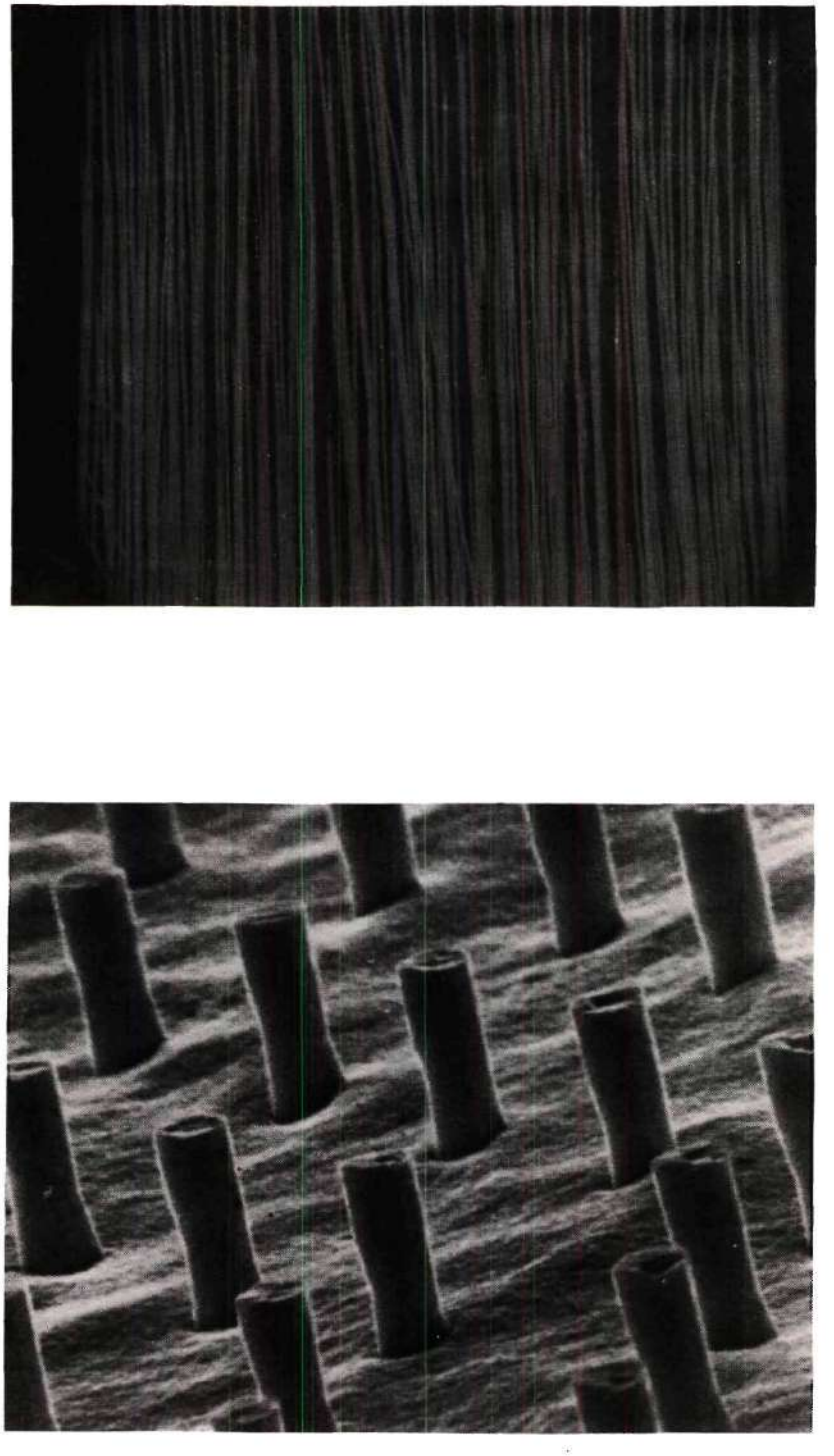

Figure 1. Tungsten-UO_2 Composites

in sectors (Figure 2).

The increased conductivity of composite fuel elements will permit reduced maximum fuel temperatures and heat content when compared to fuel elements made of pure UO_2.

The purpose of this research is to solve the heat conduction equation for a unit cell consisting of a single fiber and the surrounding matrix. The temperature distributions obtained are used to evaluate the effective conductivity along the parallel axis, fuel heat content, and the effective specific heat for a range of physical properties, cell dimensions and gap conductances at the matrix-filament interface. Formulas for asymptotic solutions and regions, in terms of the composite parameters, where the asymptotic solutions apply are presented.

History of Unidirectionally Solidified Composites

Prior to the work by Chapman, Clark, and Hendrix, directionally solidified composites were created from metallic, ceramic, or alkali-halide eutectic melts. The literature on the theory, fabrication, and physical properties of directionally solidified composites is based on the eutectic solutions.

In 1971, Hulse and Batl gave the following concise theory of unidirectional solidification:

> At a eutectic composition two or more phases solidify simultaneously from the fully liquid state to the solid state at a fixed temperature called the eutectic temperature. If a flat liquid-solid interface can be maintained as the liquid is solidified, a uniform directional composite microstructure may be obtained in which the minor phase or phases are aligned parallel to the direction of heat flux [2].

A survey of unidirectionally solidified eutectics proposed for

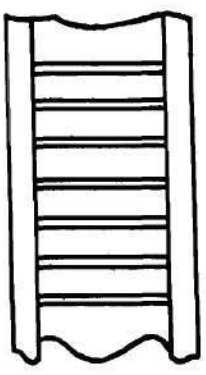

(a)

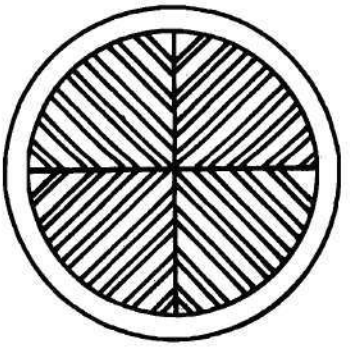

(b)

Figure 2. Proposed Fuel Elements

optical, electronic, and magnetic applications was presented by Galasso (1967) [3]. In this presentation, tables containing 44 different unidirectional composites which have been successfully fabricated are listed. Among the eutectics listed are metallic and alkali-halide systems.

Liebmann and Miller, whose InSb-Sb eutectic is included in the above survey, performed measurements of thermoelectric properties of the InSb-Sb composite [4]. Interestingly, their measurements showed that the composite thermal conductivity is lower than the conductivity of either of the constituent phases. Their studies also revealed the highly anisotropic nature of conductivity in directional composites.

Foxhall and Hellawell fabricated directionally solidified alkali-halide systems for a variety of combinations of sodium, potassium, and lithium and bromine, fluorine, and chlorine [5]. Their study reveals microstructures similar to the metallic systems.

Schmid and Viechnicki investigated unidirectional solidification for several ceramic systems [6,7]. Reference [8] compares the Bridgeman crystal growing furnace with the gradient furnace.

The method of fabrication of UO_2-W composites is a modified floating zone process termed by Chapman as Internal Centrifugal Zone Growth (ICZG) [1]. The ICZG method is described in detail in other articles by Chapman and Clark on growing single crystals of pure UO_2 [9,10].

Literature Survey

Analysis for the prediction of thermal conductivities of unidirectional composites without internal heat generation has been developed by Springer and Tsai [11]. Their method, published in 1967, predicts the

axial conductivity by the volume weighted average conductivity formula,

$$\frac{k_{eff\,11}}{k_2} = \frac{k_1}{k_2} V_1 + V_2 \qquad (1.1)$$

where

$k_{eff\ 11}$ = effective axial conductivity

k_1, k_2 = thermal conductivities of fiber and matrix, respectively

v_1, v_2 = volume fractions of fiber and matrix, respectively, and

$v_1 + v_2 = 1.0$.

Equation 1.1 is obtained by assuming the filament and matrix are connected in parallel, an assumption not justified for heat-generating composites. In a heat generating composite, temperature functions become dependent on the radial position around a fiber which complicates the averaging of the conductivities of fiber and matrix. Perhaps recognizing this limitation, Springer and Tsai caution that Eq. 1.1 should be considered an upper bound.

In the same article, Springer and Tsai develop two methods for determining the transverse conductivity. One method draws upon an analogy with the longitudinal shear loading problem, solved numerically by Adams and Doner [12]. The second method uses a simplified thermal model. The result of the calculation is the following formula for transverse conductivity of cylindrical filaments in a square array.

$$\frac{k_{eff\perp}}{k_2} = \frac{1}{B}\left\{\pi - \frac{4}{\sqrt{1-\frac{B^2V_1}{\pi}}}\tan^{-1}\left[\frac{\sqrt{1-\frac{B^2V_1}{\pi}}}{1+\sqrt{\frac{B^2V_1}{\pi}}}\right]\right\} + 1 - 2\sqrt{\frac{V_1}{T_1}} \qquad (1.2)$$

where

$k_{eff\perp}$ = transverse conductivity

$B = 2((k_1/k_2) - 1)$

In 1970, Zinsmeister and Purohit compared the accuracy of Eq. 1.2 to a more accurate numerical calculation. Their findings show the majority of cases compare within 10% [13].

In 1968, Behrens used the method of "long waves" to derive formulas for the three principal components of conductivity for composites with orthorhombic symmetry, including unidirectional composites [14]. His method yields the same volume-weighted average formula for axial conductivity as Springer and Tsai (Eq. 1.1). Like them, he does not consider the effect of heat generation on effective conductivity.

In 1972, Donea applied variational principles to derive formulas for upper and lower bounds for transverse conductivities in unidirectional composites with fibers in square, hexagonal, and random packing. Formulas were also given for bounds for composites with uniformly and randomly dispersed spherical inclusions [15].

In 1970, D'Andrea published an article investigating experimentally and analytically "thermal conductivities of composites made of highly conductive metal fibers randomly distributed in low conductive matrices" [16].

In 1975, Rust and Boyle performed a study which is the direct predecessor of this thesis [17]. They considered unidirectional composites with heat generation in the matrix. Effective axial conductivities were calculated, and it was concluded that the conductivity approached the volume-weighted average, Eq. 1.1, for large values of fiber length-to-radius ratios. The present study extends the work by Rust and Boyle to include contact conductance at the matrix-fiber interface, heat generation in the fiber, and temperature dependent conductivity.

A literature survey on the theories of thermoelastic properties of composites, including thermal conductivities, has been compiled by Charnis and Sendeckyz [18]. Their study is reasonably complete for work published before 1968. Included in it are many of the references cited in this section.

CHAPTER II

PROBLEM FORMULATION

The stated objective of this study is to find a general mathematical solution to the heat conduction equation in unidirectional composites. The major assumptions are as follows:

a) Filament and matrix are locally isotropic and homogeneous.

b) A unit cell consisting of a single filament at the center of a hexagonal prism of matrix material may be approximated by concentric cylinders of equal volume (Wigner-Seitz method).

c) A contact conductance exists at filament matrix interface.

d) Uniform heat generation in filament and matrix.

e) Steady state.

f) Fiber thermal conductivity is constant. Matrix thermal conductivity is constant or linearly dependent on temperature. The linearly dependent conductivity case is solved using first order perturbation theory.

With regard to assumption (b), the Wigner-Seitz method states that in general a complex polyhedral unit cell may be replaced by a simpler geometry such as sphere, cylinder, or ellipsoid without substantially changing the function of interest. The usual reflective boundary condition on the surface of the polyhedron

$$\left.\frac{\partial \phi}{\partial n}\right|_{S_p} = 0 \qquad (2.1)$$

where

ϕ = function of interest

S_p = surface of polyhedron

$\frac{\partial \phi}{\partial n}$ = normal derivative

is replaced by the corresponding reflective boundary condition in the simpler geometry.

$$\left.\frac{\partial \phi}{\partial r}\right|_{S_s} = 0 \tag{2.2}$$

where S_s = surface of Wigner-Seitz cell

This type of approximation is used for calculating energy bonds in crystalline solids [19]. It is also commonly used in neutron diffusion around a fuel rod [20]. Behrens [14] and Donea [15] applied the approximation in calculating effective conductivities in composites. Cohen discusses the Wigner-Seitz method for the problem of neutron diffusion in a square array of fuel rods [21]. He concludes that the method does not introduce significant error.

Electron micrographs of the UO_2-W composite reveal filaments arranged in a hexagonal lattice [1]. Figure 3 illustrates Wigner-Seitz cell superimposed on the hexagonal unit cell.

The relationship between the interfiber spacing, s, and the radius of the Wigner-Seitz cell, b, is given by,

$$s = \left(\frac{4\pi^2}{3}\right)^{1/4} b \simeq 1.9046\, b \tag{2.3}$$

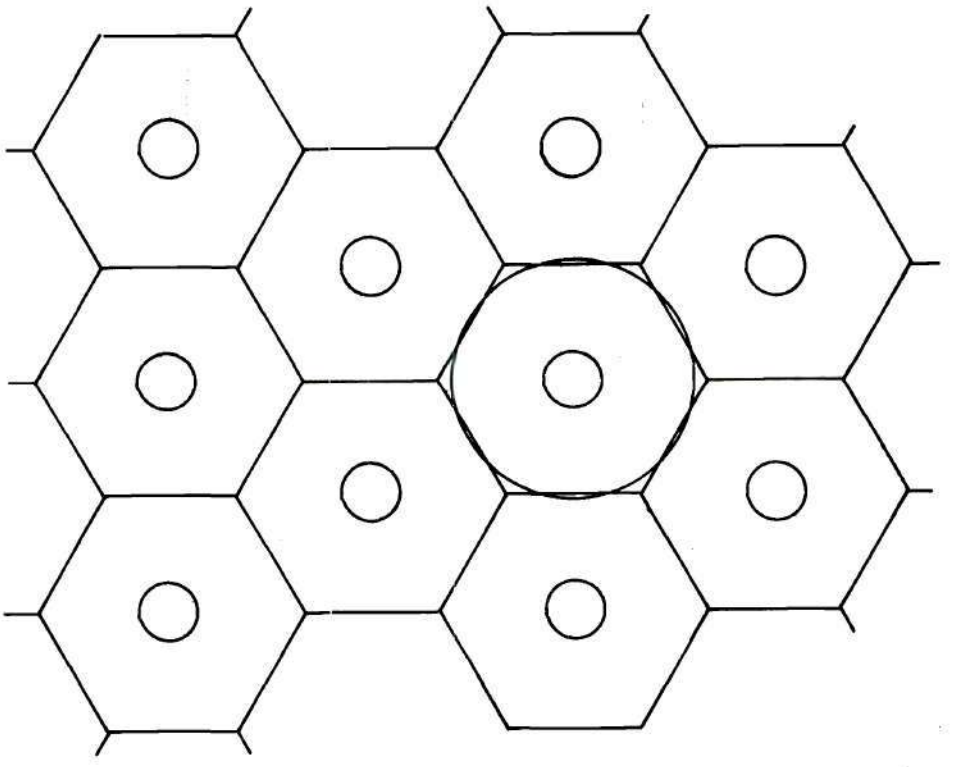

Figure 3. Wigner-Seitz Cell and Hexagonal Array

Assumption (c) involves the gap conductance at the interface. This assumption is more for the sake of mathematical generality than physical reality. For UO_2-W composites, the thermal contact would be expected to be nearly perfect, implying a very large value for the gap conductance. However, there is no theory for a quantitative evaluation. The parametric study evaluates the sensitivity of the effective conductivity to this parameter.

Differential Equations of Heat Conduction

The differential equations for the case of constant conductivity (conductivity independent of temperature) are considered along with the equations for linear conductivity (conductivity linearly dependent on temperature). This organization is necessary because the constant conductivity case is used as the zero order solution in the perturbation solution of linear conductivity and because the case of constant conductivity is of considerable interest in itself.

Constant Conductivity Equations

The differential equations and boundary conditions for heat conduction are derived and discussed in detail by Carslaw and Jaeger [22]. For the heat-generating composite shown in Figure 4, the differential equations are given by

$$\nabla^2 T_1 + \frac{q_1'''}{k_1} = 0 \qquad 0 \leq r \leq a,\ 0 \leq z \leq L \tag{2.4}$$

$$\nabla^2 T_2 + \frac{q_2'''}{k_2} = 0 \qquad a \leq r \leq b,\ 0 \leq z \leq L \tag{2.5}$$

where

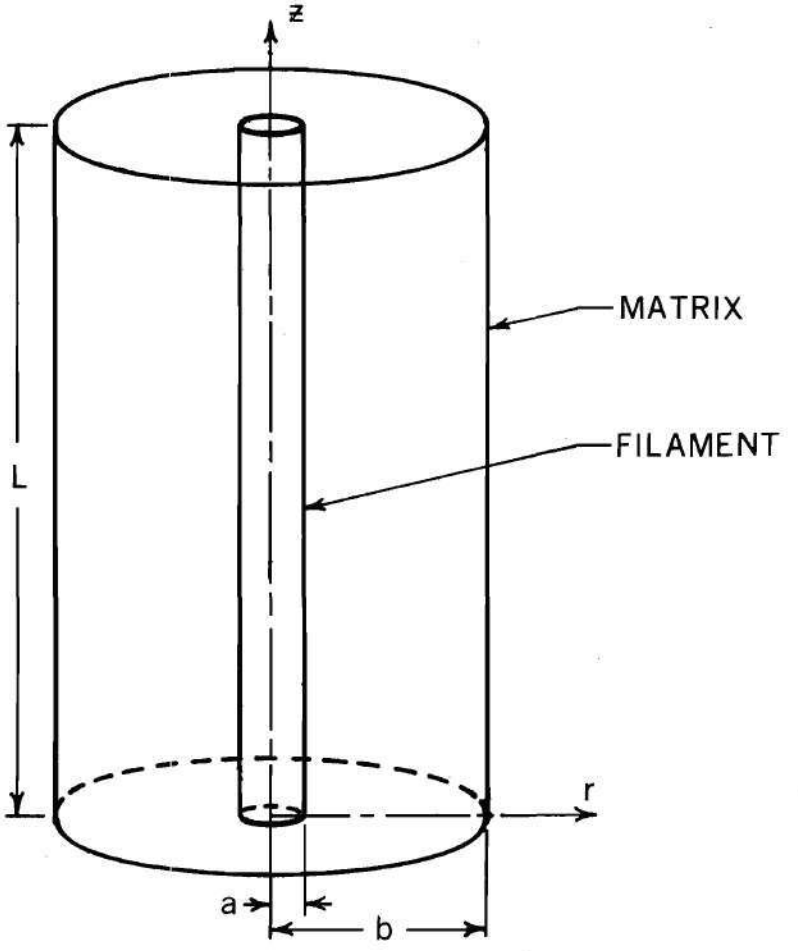

Figure 4. Concentric Cylinders Model

T = temperature

q_i''' = volumetric heat generation rate

k_i = thermal conductivity

$$\nabla^2 = \frac{1}{r}\frac{\partial}{\partial r}\left(r\frac{\partial}{\partial r}\right) + \frac{\partial^2}{\partial z^2}$$

r,z = radial and axial coordinates

a,b,L = filament radius, matrix radius, axial length of cell

The boundary conditions are as follows:

At $z = 0$, $0 \leqq r \leqq a$

$$\frac{\partial T_1}{\partial z} = 0 \tag{2.6}$$

At $z = 0$, $a \leqq r \leqq b$

$$\frac{\partial T_2}{\partial z} = 0 \tag{2.7}$$

At $z = L$, $0 \leqq r \leqq a$

$$T_1 = T_s \tag{2.8}$$

At $z = L$, $a \leqq r \leqq b$

$$T_2 = T_s \tag{2.9}$$

At $r = 0$, $0 \leqq z \leqq L$

$$\frac{\partial T_1}{\partial r} = 0 \tag{2.10}$$

At $r = a$, $0 \leqq z \leqq L$

$$k_1\frac{\partial T_1}{\partial r} = k_2\frac{\partial T_2}{\partial r} \tag{2.11}$$

At $r = a$, $0 \leqq z \leqq L$

$$-k_1\frac{\partial T_1}{\partial r} = h_c(T_1 - T_2) \tag{2.12}$$

At $r = b$, $0 \leq z \leq L$

$$\frac{\partial T_2}{\partial r} = 0 \tag{2.13}$$

Linear Conductivity Equations

A linear thermal conductivity is written in the following form:

$$k_2(T) = k_2^0(1+\epsilon_T T) \tag{2.14}$$

The differential equations for the linear conductivity problem are given by:

$$\nabla^2 T_1 + \frac{q_1'''}{k_1} = 0 \tag{2.15}$$

$$\nabla\cdot(1+\epsilon_T T)\nabla T + \frac{q_2'''}{k_2^0} = 0 \tag{2.16}$$

The boundary conditions remain the same as Eq. 2.16 - 2.13 except that the following is substituted for Eq. 2.11.

At $r = a$, $0 \leq z \leq L$

$$k_1 \frac{\partial T_1}{\partial r} = k_2^0 (1 + \epsilon_T T_2) \frac{\partial T_2}{\partial r} \tag{2.17}$$

Dimensionless Equations

The mathematical solutions can be made more concise by putting the equations in dimensionless form. Tables 1 and 2 list substitutions to make the heat conduction equations dimensionless.

Table 1. Dimensionless Variables for Constant Conductivity Equations

$\rho = \frac{r}{b}$	$q_0''' = \frac{1}{b^2}\left[q_{r_1}''' a^2 + q_{r_2}'''(b^2 - a^2)\right]$
$\zeta = \frac{z}{b}$	$p_1 = \frac{q_{r_1}'''}{q_0'''}$
$\gamma = \frac{k_1}{k_2}$	$p_2 = \frac{q_{r_2}'''}{q_0'''}$
$\delta = \frac{a}{b}$	$\eta = \frac{q_{r_1}'''}{q_{r_2}'''}$
$\xi = \frac{L}{b}$	$\beta = \frac{C_{p1}\rho_1}{C_{p2}\rho_2}$
$H_L = \frac{h_c b}{k_1}$	$\theta_i(\rho, \zeta) = \frac{f k_2}{q_0''' b^2}\left[T_i(r, z) - T_s\right]$

Table 2. Dimensionless Variables for Linear Conductivity Equations

$\rho = \frac{r}{b}$	$q_0''' = \frac{1}{b^2}[q_1''' a^2 + q_2''' (b^2 - a^2)]$
$\zeta = \frac{z}{b}$	$p_1 = \frac{q_1'''}{q_0'''}$
$\gamma = \frac{k_1}{k_2^0(1+\epsilon_T T_s)}$	$p_2 = \frac{q_2'''}{q_0'''}$
$\delta = \frac{a}{b}$	
$\xi = \frac{L}{b}$	$\beta = \frac{cp_1 \rho_1}{cp_2 \rho_2}$
$H_c = \frac{h_c b}{k_1}$	$\theta_i(\rho, \zeta) = \frac{fk_2^0(1+\epsilon T_s)}{q''' b^2}[T_i(r,z) - T_s]$
$\epsilon_\theta = \frac{\epsilon_T q_0''' b^2}{fk_2^0(1+\epsilon_T T_s}$	

The dimensionless equations for constant conductivity are

$$\nabla^2_{\rho,\zeta}\,\theta_1(\rho,\zeta) + \frac{f p_1}{\gamma} = 0 \tag{2.18}$$

$$\nabla^2_{\rho,\zeta}\,\theta_2(\rho,\zeta) + f p_2 = 0 \tag{2.19}$$

The boundary conditions are

At $\zeta = 0,\ 0 \le \rho \le \delta$

$$\frac{\partial \theta_1}{\partial \zeta} = 0 \tag{2.20}$$

At $\zeta = 0,\ \delta \le \rho \le 1.0$

$$\frac{\partial \theta_2}{\partial \zeta} = 0 \tag{2.21}$$

At $\zeta = \xi,\ 0 \le \rho \le \delta$

$$\theta_1 = 0 \tag{2.22}$$

At $\zeta = \xi,\ \delta \le \rho \le 1.0$

$$\theta_2 = 0 \tag{2.23}$$

At $\rho = 0,\ 0 \le \zeta \le L$

$$\frac{\partial \theta_1}{\partial \rho} = 0 \tag{2.24}$$

At $\rho = \delta,\ 0 \le \zeta \le L$

$$\gamma \frac{\partial \theta_1}{\partial \rho} = \frac{\partial \theta_2}{\partial \rho} \tag{2.25}$$

$$-\frac{\partial \theta_1}{\partial \rho} = H_R(\theta_1 - \theta_2) \tag{2.26}$$

At $\rho = 1, 0 \leq \zeta \leq L$

$$\frac{\partial \theta_2}{\partial \rho} = 0 \tag{2.27}$$

The dimensionless linear conductivity is given by

$$\frac{k_2(\theta_2)}{k_2^0} = (1 + \epsilon_\theta \theta_2) \tag{2.28}$$

For the linear conductivity equations, the following changes are made to Eq. 2.18 - 2.25.

Substitute the following differential equation for Eq. 2.19.

$$\nabla \cdot [(1 + \epsilon_\theta \theta_2) \nabla \theta_2] + f_{p_2} = 0 \tag{2.29}$$

Substitute the following boundary condition for Eq. 2.25.

At $\rho = \delta, 0 \leq \zeta \leq \xi$

$$\gamma \frac{\partial \theta_1}{\partial \rho} = (1 + \epsilon_\theta \theta_2) \frac{\partial \theta_2}{\partial \rho} \tag{2.30}$$

The parameters p_1 and p_2 depend only on the ratios q_1'''/q_2''' and a/b.

$$p_2 = \frac{q_2''' b^2}{q_1''' a^2 + q_2'''(b^2 - a^2)} \tag{2.31}$$

$$p_2 = \frac{1}{\left(\frac{q_1'''}{q_2'''}\right)\left(\frac{a}{b}\right)^2 + 1 - \left(\frac{a}{b}\right)^2} \tag{2.32}$$

The ratios q_1'''/q_2''' and a/b are defined in Tables 1 and 2 to be η

and δ, respectively. Therefore, Eq. 2.31 and 2.32 become

$$p_2 = \frac{1}{\eta\delta^2 + 1 - \delta^2} \tag{2.33}$$

Similarly, p_1 can be found

$$p_1 = \frac{\eta}{\eta\delta^2 + 1 - \delta^2} = \eta p_2 \tag{2.34}$$

It is apparent from Eq. 2.33 and 2.34 that the dimensionless heat generation functions, fp_1 and fp_2, are normalized so that the power of the unit cell is unity.

$$1.0 = \pi\xi\left[fp_1\delta^2 + fp_2(1-\delta^2)\right] \tag{2.35}$$

The dimensionless parameters δ, ξ, γ, η, ε_θ, and H_c are the parameters required to determine a temperature function. In addition, the parameter, β, which is the ratio of volumetric heat capacity, is used in calculating the heat content of a unit cell.

Estimated Parameter Values

Dimensionless equations are helpful from the mathematical viewpoint but the physical significance of various parameters is somewhat obscured. To alleviate this problem, Table 3 lists a set of physical parameters of "reasonable" magnitude for a UO_2-W nuclear fuel in a light water reactor. The numbers are not based on experimental data but are order-of-magnitude estimates drawn from a variety of sources.

Table 3. Estimates of Parameter Values

Physical Parameters	Dimensionless Parameters
$a = .66 \times 10^{-6}$ ft	$\delta = .2$
$b = 3.3 \times 10^{-6}$ ft	$\xi = 6400$
$L = .021$ ft	$\gamma = 32$
$q_1''' = 80$ Btu/hr-ft^3	$\gamma_{\epsilon_\theta} = 36$
$q_2''' = 8 \times 10^6$ Btu/hr-ft^3	$H_c = 1.5 \times 10^{-2}$
$T_s = 1000°F$	$\eta = 10^{-5}$
$k_1 = 74.01$ Btu/hr-ft-°F	$\epsilon_\theta = -1.532 \times 10^{-4}$
$k_2 = 2.3$ Btu/hr-ft-°F	$\beta = .95$
$h_c = 4000$ Btu/hr-ft^2-°F	$\rho_1 = 1204$ lb/ft^3
$\epsilon_T = -1.895 \times 10^{-4}$ °F^{-1}	$\rho_2 = 685$ lb/ft^3
$k_2^0 = 2.58$ Btu/hr-ft-°F	$c_{p_1} = .032$ Btu/lb-°F
$k_2^0(1+\epsilon_T T_s) = 2.08$ Btu/hr-ft-°F	$c_{p_2} = .059$ Btu/lb-°F

One parameter, h_c, is difficult to estimate. There are no data for its evaluation. A very large value corresponds to perfect thermal contact. Some notion of a lower bound may be obtained using correlations derived for gas-filled gaps. Ross and Stoute's [27] correlation is given by Eq. 2.36

$$h_C = h_{gap} + h_{solid} \tag{2.36}$$

where h_{solid} and h_{gap} are defined for the total interface area. The solid-to-solid conductance is given by

$$h_{solid} = \frac{k_m P}{a_0 R^{1/2} H} \tag{2.37}$$

where

k_m = harmonic mean conductivities of interface materials, $2k_1k_2/(k_1+k_2)$

P = contact pressure, psia

a_o = empirical constant, 0.0905 $ft^{\frac{1}{2}}$

R = root-mean-square of contact materials' surface roughness $[(R_1^2 + R_2^2)/2]^{\frac{1}{2}}$, ft

H = Meyer hardness of softer material, psi

The gap conductance is given by

$$h_{gap} = \frac{k_{gas}}{(2.75 - 1.7 \times 10^{-4} P)(R_1+R_2)+(g_1+g_2)} \tag{2.38}$$

where

k_{gas} = thermal conductivity of gas in gap, Btu/hr-ft-°F

R_1+R_2 = surface roughness of interface materials, ft

P = contact pressure

g_1+g_2 = increase in gap.

Ross and Stoute calculated values of (g_1+g_2) for various gases by comparing analysis with experimental data.

Equation 2.36 is evaluated by assuming a helium-filled gap of thickness equal to the radius of a tungsten fiber with no contact pressure.

For helium at 1000°F

$$k_g = .167 \text{ Btu/hr-ft-°F}$$

$$g_1+g_2 = 3.28 \times 10^{-5} \text{ ft}$$

Assuming

$$R_1+R_2 = 3.3 \times 10^{-6} \text{ ft}$$

$$P = 0$$

The contact conductance is calculated to be

$$h_c = 4.0 \times 10^{3} \text{ Btu/hr-ft}^2\text{-°F}$$

The parametric study showing the dependence of effective conductivity, heat content, and effective specific heat on the dimensionless parameters will be performed over the range of values given in Table 4. The ranges are not chosen to agree closely with the estimated values but to cover the range of values in which the significant features of parametric dependence can be shown.

Table 4. Ranges of Dimensionless Parameters

$\delta = 0.1 - 0.35$	$H_c = 10^{-4} - 10^{1}$
$\xi = 0.1 - 10{,}000$	$\eta = 0 - 25$
$\gamma = 10 - 70$	$\epsilon_\theta = 0 - 3 \times 10^{-4}$
$\gamma_{\epsilon_\theta} = 10 - 70$	$\beta = 0.3 - 1.0$

$$\nabla^2\theta_{1L} = 0 \tag{3.5}$$

$$\nabla^2\theta_{2L} = 0 \tag{3.6}$$

Since the functions θ_{1p} and θ_{2p} are constructed to satisfy the boundary conditions at $\zeta = 0$ and $\zeta = \xi$, the boundary conditions are easily obtained for θ_{1L} and θ_{2L}.

At $\zeta = 0,\ 0 \le \rho \le \delta$

$$\frac{\partial\theta_{1L}}{\partial\zeta} = 0 \tag{3.7}$$

At $\zeta = 0,\ \delta \le \rho \le 1.0$

$$\frac{\partial\theta_{2L}}{\partial\zeta} = 0 \tag{3.8}$$

At $\zeta = \xi,\ 0 \le \rho \le \delta$

$$\theta_{1L} = 0 \tag{3.9}$$

At $\zeta = \xi,\ \delta \le \rho \le 1.0$

$$\theta_{2L} = 0 \tag{3.10}$$

At $\rho = 0,\ 0 \le \zeta \le \xi$

$$\frac{\partial\theta_{1L}}{\partial\rho} = 0 \tag{3.11}$$

At $\rho=\delta, 0\leq\zeta\leq\xi$

$$\gamma\frac{\partial\theta_{1L}}{\partial\rho}=\frac{\partial\theta_{2L}}{\partial\rho} \tag{3.12}$$

and

$$\frac{-\partial\theta_{1L}}{\partial\rho}=H_c\left[\theta_{1L}-\theta_{2L}+\frac{1}{2}\left(\frac{fp_1}{\gamma}-fp_2\right)(\xi^2-\zeta^2)\right] \tag{3.13}$$

At $\rho=1.0, 0\leq\zeta\leq\xi$

$$\frac{\partial\theta_{2L}}{\partial\rho}=0 \tag{3.14}$$

The solution of this system is obtained using the separation of variables technique. A solution of the form

$$\theta_{1L}(\rho,\zeta)=R_1(\rho)Z_1(\zeta) \tag{3.15}$$

$$\theta_{2L}(\rho,\zeta)=R_2(\rho)Z_2(\zeta) \tag{3.16}$$

is assumed to exist. After substituting into the differential equations, the spatial dependence is separated into two parts

$$\frac{1}{\rho R_i}\frac{d}{d\rho}\left[\rho\frac{dR_i}{d\rho}\right]=-\frac{1}{Z_i}\frac{d^2Z_i}{d\zeta^2} \tag{3.17}$$

where i = 1,2 denotes filament and matrix, respectively.

By the usual arguments, the two parts must be equal to a constant.

$$\frac{1}{Z_i}\frac{d^2 Z_i}{d\zeta} = -\lambda_i^2 \tag{3.18}$$

$$\frac{1}{\rho R_i}\frac{d}{d\rho}\left[\rho\frac{d(\rho R_i)}{d\rho}\right] = \lambda_i^2 \tag{3.19}$$

The boundary conditions for the axial functions, Z_i, are as follows:

At $\zeta = 0$

$$\frac{dZ_i}{d\zeta} = 0 \tag{3.20}$$

and

$$\frac{dZ_2}{d\zeta} = 0 \tag{3.21}$$

At $\zeta = \xi$

$$Z_1 = 0 \tag{3.22}$$

and

$$Z_2 = 0 \tag{3.23}$$

The solution to Eqs. 3.18 - 3.23 is a set of eigenfunctions

$$Z_{1j}(\zeta) = \cos(\lambda_{ij}\zeta) \tag{3.24}$$

$$Z_{2j}(\zeta) = \cos(\lambda_{2j}\zeta) \tag{3.25}$$

whose eigenvalues are

$$\lambda_{1j} = \frac{2j-1}{2}\frac{\pi}{\xi} \tag{3.26}$$

$$\lambda_{2j} = \frac{2j-1}{2}\frac{\pi}{\xi} \tag{3.27}$$

where j = 1,2,3, ...

Since the solutions for Z_1 and Z_2 are identical, the subscript indicating filament or matrix can be omitted.

$$Z_j(\zeta) = Z_{1j}(\zeta) = Z_{2j}(\zeta) \tag{3.28}$$

and

$$\lambda_j = \lambda_{1j} = \lambda_{2j} \tag{3.29}$$

The preceding solution for the axial functions suggests a general solution of the form

$$\theta_{1L}(\rho,\zeta) = \sum_{j=1}^{\infty} R_{1j}(\rho) Z_j(\zeta) \tag{3.30}$$

$$\theta_{2L}(\rho,\zeta) = \sum_{j=1}^{\infty} R_{2j}(\rho) Z_j(\zeta) \tag{3.31}$$

The boundary conditions for the radial functions are as follows:

At $\rho = 0$

$$\frac{dR_1}{d\rho} = 0 \tag{3.32}$$

At $\rho = 1.0$

$$\frac{dR_2}{d\rho} = 0 \tag{3.33}$$

The boundary conditions at the interface, $\rho = \delta$, require some mathematical ingenuity. Substituting Eqs. 3.30 and 3.31 into Eq. 3.12 yields the following:

$$\sum_{j=1}^{\infty} \gamma \frac{dR_{1j}(\delta)}{d\rho} \cdot Z_{1j}(\zeta) = \sum_{j=1}^{\infty} \frac{dR_{2j}(\delta)}{d\rho} \cdot Z_{2j}(\zeta) \tag{3.34}$$

The elements of the summation must agree term by term, therefore

$$\gamma \frac{dR_{1j}(\delta)}{d\rho} = \frac{dR_{2j}(\delta)}{d\rho} \tag{3.35}$$

The remaining boundary condition, Eq. 3.13 is separated by noting that the parabolic term

$$\theta_{1p} - \theta_{2p} = \frac{1}{2}\left(\frac{fp_1}{\gamma} - fp_2\right)(\xi^2 - \zeta^2) \tag{3.36}$$

can be written in terms of the axial functions using Fourier series expansion.

$$\frac{1}{2}(\xi^2 - \zeta^2) = \sum_{j=1}^{\infty} L_j \cos(\lambda_j \zeta) \tag{3.37}$$

where

$$L_j = \frac{2}{\xi} \frac{(-1)^{j-1}}{\lambda_j^3} \tag{3.38}$$

Equation 3.13 is expressed in terms of R_{ij}, Z_j, and L_j by Eq. 3.39

$$-\sum_{j=1}^{\infty} \frac{dR_{ij}(\delta)}{d\rho} \cdot Z_j(\zeta) = H_c \left\{ \sum_{j=1}^{\infty} [R_{1j}(\delta) - R_{2j}(\delta)] Z_j(\zeta) + \left(\frac{fp_1}{\gamma} - fp_2 \right) \sum_{j=1}^{\infty} L_j Z_j(\zeta) \right\} \tag{3.39}$$

As with Eq. 3.34, the elements of the summations must be equal term by term

$$-\frac{dR_{1j}(\delta)}{d\rho} = H_c \left[R_{1j}(\delta) - R_{2j}(\delta) + \left(\frac{fp_1}{\gamma} - fp_2 \right) L_j \right] \tag{3.40}$$

The differential equations and boundary conditions for the radial functions are summarized as follows:

$$\frac{1}{\rho} \frac{d}{d\rho} \left[\rho \frac{dR_{1j}}{d\rho} \right] - \lambda_j^2 R_{1j} = 0 \tag{3.41}$$

$$\frac{1}{\rho} \frac{d}{d\rho} \left[\rho \frac{dR_{2j}}{d\rho} \right] - \lambda_j^2 R_{2j} = 0 \tag{3.42}$$

At $\rho = 0$

$$\frac{dR_{1j}}{d\rho} = 0 \tag{3.43}$$

At $\rho = \delta$

$$\gamma \frac{dR_{1j}}{d\rho} = \frac{dR_{2j}}{d\rho} \tag{3.44}$$

and

$$-\frac{dR_{1j}}{d\rho} = H_C\left[R_{1j} - R_{2j} + \left(\frac{fp_1}{\gamma} - fp_2\right)L_j\right] \tag{3.45}$$

At $\rho = 1.0$

$$\frac{dR_{2j}}{d\rho} = 0 \tag{3.46}$$

The general solutions for Eqs. 3.41 and 3.42 are modified Bessel functions

$$R_{1j}(\rho) = A_j I_0(\lambda_j \rho) + B_j K_0(\lambda_j \rho) \tag{3.47}$$

$$R_{2j}(\rho) = C_j I_0(\lambda_j \rho) + D_j K_0(\lambda_j \rho) \tag{3.48}$$

Inserting the general solutions into the four boundary conditions, Eqs. 3.43 - 3.46, yields a system of four linear equations in four unknowns. The linear equations are not all homogeneous, so the unknowns, A_j, B_j, C_j, and D_j, can be uniquely evaluated.

The system of equations can be written in the following fashion:

$$A_j t_1 + B_j t_2 = 0 \tag{3.49}$$

$$A_j q_1 + B_j q_2 + C_j q_3 + D_j q_4 = 0 \tag{3.50}$$

$$A_j r_1 + B_j r_2 + C_j r_3 + D_j r_4 = r_5 \tag{3.51}$$

$$C_j s_1 + D_j s_2 = 0 \tag{3.52}$$

where

$$\left.\begin{aligned}
t_1 &= I_1(0) = 0 \\
t_2 &= -K_1(0) \to \infty \\
q_{r1} &= \gamma I_1(\lambda_j \delta) \\
q_{r2} &= -\gamma K_1(\lambda_j \delta) \\
q_{r3} &= -I_1(\lambda_j \delta) \\
q_{r4} &= K_1(\lambda_j \delta) \\
r_1 &= -\lambda_j I_1(\lambda_j \delta) - H_c I_0(\lambda_j \delta) \\
r_2 &= \lambda_j K_1(\lambda_j \delta) - H_c K_0(\lambda_j \delta) \\
r_3 &= H_c I_0(\lambda_j \delta) \\
r_4 &= H_c K_0(\lambda_j \delta) \\
r_5 &= H_c \left(\frac{fp_1}{\gamma} - fp_2\right) L_j \\
s_1 &= I_1(\lambda_j) \\
s_2 &= -K_1(\lambda_j)
\end{aligned}\right\} \tag{3.53}$$

Equation 3.49 can be used to show that all of the coefficients, B_j, must vanish. Straightforward algebraic steps determine A_j, C_j, and D_j from the remaining equations.

$$C_j = r_5 \Big/ \left\{ -r_1 \left[\frac{q_{r3}}{q_{r1}} - \frac{q_{r4} s_1}{q_{r1} s_2} \right] + \left[r_3 - \frac{r_4 s_1}{s_2} \right] \right\} \tag{3.54}$$

$$D_j = -C_j \frac{s_1}{s_2} \tag{3.55}$$

$$A_j = -C_j \left[\frac{q_{r3}}{q_{r1}} - \frac{q_{r4}}{q_{r1}} \cdot \frac{s_1}{s_2} \right] \tag{3.56}$$

Collecting terms, the dimensionless temperature functions are summarized as follows:

$$\Theta_1(\rho,\zeta) = \sum_{j=1}^{\infty} A_j I_0(\lambda_j \rho)\cos(\lambda_j \zeta) + \frac{f_{p_1}}{2\gamma}(\xi^2 - \zeta^2) \tag{3.57}$$

$$\Theta_2(\rho,\zeta) = \sum_{j=1}^{\infty} \left[C_j I_0(\lambda_j \rho) + D_j K_0(\lambda_j \rho)\right]\cos(\lambda_j \zeta) + \frac{f_{p_2}}{2}(\xi^2 - \zeta^2) \tag{3.58}$$

where the coefficients and eigenvalues are

$$C_j = -H_c\left(\frac{f_{p_1}}{\gamma} - f_{p_2}\right)\left(\frac{L_j}{G_j}\right) \tag{3.59}$$

$$A_j = \frac{C_j}{\gamma}\left[1 - \frac{I_1(\lambda_j)K_1(\lambda_j\delta)}{K_1(\lambda_j)I_1(\lambda_j\delta)}\right] \tag{3.60}$$

$$D_j = C_j \frac{I_1(\lambda_j)}{K_1(\lambda_j)} \tag{3.61}$$

$$L_j = \frac{2}{\xi}\frac{(-1)^{j-1}}{\lambda_j^3} \tag{3.62}$$

$$G = \frac{1}{\gamma}\left[1 - \frac{I_1(\lambda_j)K_1(\lambda_j\delta)}{K_1(\lambda_j)I_1(\lambda_j\delta)}\right]\left[\lambda_j I_1(\lambda_j\delta) + H_c I_0(\lambda_j\delta)\right] - H_c\left[I_0(\lambda_j\delta) + \frac{I_1(\lambda_j)}{K_1(\lambda_j)}K_0(\lambda_j\delta)\right] \tag{3.63}$$

$$\lambda_j = \left(\frac{2j-1}{2}\right)\left(\frac{\pi}{\xi}\right) \tag{3.64}$$

Equations 3.57 and 3.58 contain infinite series of eigenfunctions; however, the series converges, and accuracy within a desired error can be attained by taking a sufficient number of terms.

One generalization might be added to this solution. The source functions, fp_1 and fp_2, may be functions of the axial coordinate, ζ,

$$fp_1 = fp_1(\zeta) \tag{3.65}$$

$$fp_2 = fp_2(\zeta) \tag{3.66}$$

The limitations for suitable functions are that they must be normalized, they may not have a radial dependence, and their Fourier series expansions must exist.

Perturbation Solution to Linear Conductivity Problem

A perturbation solution is an approximate solution which uses the exact solution to a similar problem. Park describes perturbation theory in the context of wave functions [25]. Aizen developed a general procedure for finding the first-order perturbation solution to the heat conduction problem in multi-layered slabs, cylinders, and spheres with linear conductivities, heat generation, and contact conductances at the interfaces [26]. However, his method applies only to simpler, one-dimensional problems.

The problem to be solved is given by differential equations, Eqs. 2.18 and 2.29, and boundary conditions, Eqs. 2.20 - 2.24, 2.26, 2.27, and 2.30. The differential operator for Eq. 2.29 is rewritten as

$$\nabla^2\theta_2 + \epsilon_\theta \nabla\cdot(\theta_2 \nabla\, \theta_2) + f p_2 = 0 \tag{3.67}$$

The zero-order equation is obtained when the factor, ϵ_θ, is vanishingly small.

$$\nabla^2\theta_2^0 + f p_2 = 0 \tag{3.68}$$

Hence, the zero-order solution is the constant conductivity problem solved in the previous section.

As Park suggests, it is plausible to assume that θ_1 and θ_2 may be expanded in powers of ϵ_θ.

$$\theta_1 = \theta_1^0 + \epsilon_\theta \theta_1^1 + \epsilon_\theta^2 \theta_1^2 + \ldots \tag{3.69}$$

$$\theta_2 = \theta_2^0 + \epsilon_\theta \theta_2^1 + \epsilon_\theta^2 \theta_2^2 + \ldots \tag{3.70}$$

where θ_1^i, θ_2^i are the i^{th} order perturbation functions.

Substituting Eqs. 3.69 and 3.70 into Eqs. 2.18 and 2.29 yields the following set of equations:

$$\epsilon_\theta^0 \begin{cases} \nabla^2\theta_1^0 + \dfrac{f p_1}{\gamma} = 0 \\ \nabla^2\theta_2^0 + f p_2 = 0 \end{cases} \tag{3.71}$$

$$\epsilon_\theta^1 \begin{cases} \nabla^2 \theta_1^1 = 0 \\ \nabla^2 \theta_2^1 + \frac{1}{2} \nabla^2 [\theta_2^0]^2 = 0 \end{cases} \tag{3.72}$$

$$\epsilon_\theta^2 \begin{cases} \nabla^2 \theta_1^2 = 0 \\ \nabla^2 \theta_2^2 + \nabla^2 (\theta_2^0 \theta_2^1) = 0 \end{cases} \tag{3.73}$$

$$\vdots$$

First-order perturbation considers only terms of zero and first order in ϵ_θ.

$$\theta_1 \sim \tilde{\theta}_1 = \theta_1^0 + \epsilon_\theta \theta_1^1 \tag{3.74}$$

$$\theta_2 \sim \tilde{\theta}_2 = \theta_2^0 + \epsilon_\theta \theta_2^1 \tag{3.75}$$

where $\tilde{\theta}_i$ is the first-order perturbation solution.

The zero-order functions have been derived previously. The first-order functions are obtained by solving the differential equations given by Eq. 3.72 and boundary conditions obtained by substituting Eqs. 3.69 and 3.70 into Eqs. 2.20 - 2.24, 2.26, 2.27, and 2.30 and equating coefficients of first power in ϵ_θ. Equations 3.76 - 3.83 list the boundary conditions.

At $\zeta = 0$, $0 \leq \rho \leq \delta$

$$\frac{\partial \theta_1^1}{\partial \rho} = 0 \tag{3.76}$$

At $\zeta = 0, \delta \leq \rho \leq 1.0$

$$\frac{\partial \theta_2^1}{\partial \rho} = 0 \tag{3.77}$$

At $\zeta = \xi, \delta \leq \rho \leq 1.0$

$$\theta_1^1 = 0 \tag{3.78}$$

At $\zeta = \xi, 0 \leq \rho \leq \delta$

$$\theta_2^1 = 0 \tag{3.79}$$

At $\rho = 0, 0 \leq \zeta \leq \xi$

$$\frac{\partial \theta_1^1}{\partial \rho} = 0 \tag{3.80}$$

At $\rho = \delta, 0 \leq \zeta \leq \xi$

$$\gamma \frac{\partial \theta_1^1}{\partial \rho} = \frac{\partial \theta_2^1}{\partial \rho} + \theta_2^0 \frac{\partial \theta_2^0}{\partial \rho} \tag{3.81}$$

and

$$-\frac{\partial \theta_1^1}{\partial \rho} = H_c(\theta_1^1 - \theta_2^1) \tag{3.82}$$

At $\rho = 1.0, 0 \leq \zeta \leq \xi$

$$\frac{\partial \theta_2^1}{\partial \rho} = 0 \tag{3.83}$$

Equation 3.71 is reduced to Laplace's equation by the following substitution:

$$\theta_2^1 = \theta_{2L}^1 - \frac{[\theta_2^0]^2}{2} \tag{3.84}$$

Equations involving θ_2^1 are restated in terms of θ_{2L}^1 giving the following:

$$\nabla^2 \theta_{2L}^1 = 0 \tag{3.85}$$

At $\zeta = 0, \delta \leq \rho \leq 1.0$

$$\frac{\partial \theta_{2L}^1}{\partial \rho} = 0 \tag{3.86}$$

At $\zeta = \xi, \delta \leq \rho \leq 1.0$

$$\theta_{2L}^1 = 0 \tag{3.87}$$

At $\rho = \delta, 0 \leq \zeta \leq \xi$

$$\gamma \frac{\partial \theta_1^1}{\partial \rho} = \frac{\partial \theta_{2L}^1}{\partial \rho} \tag{3.88}$$

and

$$-\frac{\partial \theta_1^1}{\partial \rho} = H_c \left[\theta_1^1 - \theta_{2L}^1 + \frac{(\theta_2^0)^2}{2} \right] \tag{3.89}$$

At $\rho = 1.0, 0 \leq \zeta \leq \xi$

$$\frac{\partial \theta_{2L}^1}{\partial \rho} = 0 \tag{3.90}$$

The equations for the perturbation solution have the same form as Eqs. 3.5 - 3.14. If the Fourier series for $[\theta_2^0]^2$ exists at $\rho = \delta$, then the solution found previously can be applied. Appendix A verifies that such a series exists. The solution is taken directly from Eqs. 3.57 - 3.64.

$$\theta_1^1 = \sum_{j=1}^{\infty} U_j I_0(\lambda_j \rho)\cos(\lambda_j \zeta) \tag{3.91}$$

$$\theta_2^1 = \sum_{j=1}^{\infty} V_j\left[I_0(\lambda_j \rho) + \frac{I_1(\lambda_j)}{K_1(\lambda_j)} K_0(\lambda_j)\right]\cos(\lambda_j \zeta) - \frac{[\theta_2^0]^2}{2} \tag{3.92}$$

where

$$V_j = \frac{-F_j}{G_j} \tag{3.93}$$

$$U_j = \frac{V_j}{\gamma}\left[1 - \frac{I_1(\lambda_j) K_1(\lambda_j \delta)}{K_1(\lambda_j) I_1(\lambda_j \delta)}\right] \tag{3.94}$$

$$G_j = \frac{1}{\gamma}\left[1 - \frac{I_1(\lambda_j) K_1(\lambda_j \delta)}{K_1(\lambda_j) I_1(\lambda_j \delta)}\right]\left[\lambda_j I_1(\lambda_j \delta) + H_c I_0(\lambda_j \delta)\right] - H_c\left[I_0(\lambda_j \delta) + \frac{I_1(\lambda_j)}{K_1(\lambda_j)} K_0(\lambda_j \delta)\right] \tag{3.95}$$

F_j = Fourier coefficients of $[\theta_2^0]^2/2$ (evaluated in Appendix A). $\left.\dfrac{[\theta_2^0]^2}{2}\right|_{\rho=\delta} = \sum_{j=1}^{\infty} F_j \cos \lambda_j \zeta$ (3.96)

This series solution converges and accuracy within a given error can be obtained by taking a sufficient number of terms.

Temperature Functions for Solid Matrix

For purposes of comparing advantages of composite fuels relative to conventional fuels, the temperature functions in a solid cylindrical matrix cell with insulated boundaries at one end and along its side and a uniform temperature at the other end are calculated. In terms of dimensionless variables, the heat conduction equations are given by the following:

Constant Conductivity

$$\frac{d^2\theta_{SM}}{d\zeta^2} + \frac{1}{\pi\xi} = 0 \tag{3.97}$$

Linear Conductivity

$$\frac{d}{d\zeta}\left[(1+\epsilon_\theta\theta_{SM})\frac{d\theta_{SM}}{d\zeta}\right] + \frac{1}{\pi\xi} = 0 \tag{3.98}$$

where θ_{SM} is the dimensionless temperature function in the solid matrix.

The boundary conditions for Eqs. 3.97 and 3.98 are

At $\zeta = 0$,

$$\frac{d\theta_{SM}}{d\zeta} = 0 \tag{3.99}$$

At $\zeta = \xi$,

$$\theta_{SM} = 0 \tag{3.100}$$

The heat generation term, $\frac{1}{\pi\xi}$, is normalized so that

$$1.0 = 2\pi \int_{\zeta=0}^{\xi} \int_{\rho=0}^{1.0} \frac{1}{\pi\xi} \rho \, d\rho \, d\zeta \tag{3.101}$$

which corresponds to the same heat generation as in the composite cell.

The constant conductivity solution is given by

$$\theta_{SM}(\zeta) = \frac{1}{2\pi\xi}(\xi^2 - \zeta^2) \tag{3.102}$$

The linear conductivity problem can be solved explicitly by integrating twice, avoiding the need for perturbation theory. The solution is

$$\theta_{SM}(\zeta) = \frac{1}{\epsilon_\theta}\left[-1 + \sqrt{1 + \frac{\epsilon_\theta}{\pi\xi}(\xi^2 - \zeta^2)}\right] \tag{3.103}$$

Interestingly, Eq. 3.103 illustrates a limiting case for linear conductivity. If ϵ_θ is negative, the temperature function does not exist unless

$$\frac{\epsilon_\theta \xi}{\pi} \geq -1 \tag{3.104}$$

The condition has a physical interpretation. The conductivity must be greater than zero. For negative ϵ_θ, the minimum conductivity occurs where the temperature is a maximum, at $\zeta = 0$; therefore,

$$\left(1 + \epsilon_\theta \theta_{SM}\right)_{min.} = \left[1 + \epsilon_\theta \left(\theta_{SM}\right)_{max}\right] \tag{3.105}$$

or

$$(1+\epsilon_\theta\theta_{SM})_{min.} = \left(1+\frac{\epsilon_\theta\xi}{\pi}\right)^{1/2} \tag{3.106}$$

Equation 3.106 shows that the minimum conductivity is zero when

$$\frac{\epsilon_\theta\xi}{\pi} = -1 \tag{3.107}$$

For ξ outside the range defined by Eq. 3.104, the linear conductivity problem has no physical meaning.

Validity of Linear Conductivity Solution

There are two considerations in evaluating the linear conductivity solution. First, can the actual conductivity be adequately modeled by a linear function, and, second, is the first-order perturbation solution reasonably close to the exact solution? Both points are discussed in this section.

Linear Conductivity

If the matrix material is uranium dioxide, the conductivity may be described by the following formula [27]:

$$k(T) = \frac{1}{a+bT} + c(T+d)^3 \tag{3.108}$$

Bianchieria [27] empirically fitted Eq. 3.108 to experimental data for mixed oxide fuel, $(UO_2)_{.8}$-$(PuO_2)_{.2}$, 95 percent theoretically dense. His results, shown in Table 5, probably are not accurate for a single-crystal UO_2 in a melt-grown UO_2-W composite, but perhaps are indicative

of general trends for temperature dependent conductivities.

Table 5. Conductivity Parameters

	For k $\left(\frac{W}{cm-°K}\right)$ and T(°K)	For k $\left(\frac{Btu}{hr-ft-°F}\right)$ and T(°F)
a	3.11	.1739
b	.0272	2.614×10^{-4}
c	5.39×10^{-13}	5.344×10^{-12}
d	0	459.69

The linear conductivity approximation is based on the existence of a straight line that best approximates the function, k(T), between any two temperatures, T_1 and T_2. The best straight line in the least squares sense is determined by evaluating k_0 and ϵ_T such that the following integral is a minimum:

$$\overline{\Delta k^2} = \int_{T_1}^{T_2} \left[k_0(1 + \epsilon_T T) - k(T)\right]^2 dT \qquad (3.109)$$

Appendix C shows the minimization calculation for the conductivity k(T) given by Eq. 3.108. The parameters k_0 and ϵ_T for (T_1, T_2) of (1000, 2000°F) and (1000, 3000°F) are presented in Table 6.

Table 6. Linear Conductivity Parameters

T_1, T_2	$k_0 \left(\frac{\text{Btu}}{\text{hr-ft-°F}}\right)$	ϵ_T
(1000, 2000°F)	3.013	-2.59×10^{-4}
(1000, 3000°F)	2.58	-1.895×10^{-4}

Figure 5 shows the linear conductivity approximation superimposed on Bianchieria's conductivity function. Observation of Figure 5 shows that over a temperature range of 1000°F to 3000°F the conductivity decreases a maximum of 50 percent. This suggests the following criterion for acceptability

$$\frac{1}{2} < \frac{1+\epsilon_T T_{max}}{1+\epsilon_T T_S} < 1.0 \tag{3.110}$$

or, in dimensionless variables

$$\frac{1}{2} < 1 + \epsilon_\theta \theta_{max} < 1.0 \tag{3.111}$$

The acceptability criterion for the linear conductivity is based on the model being within the physically reasonable range of temperatures rather than on a defect in the model.

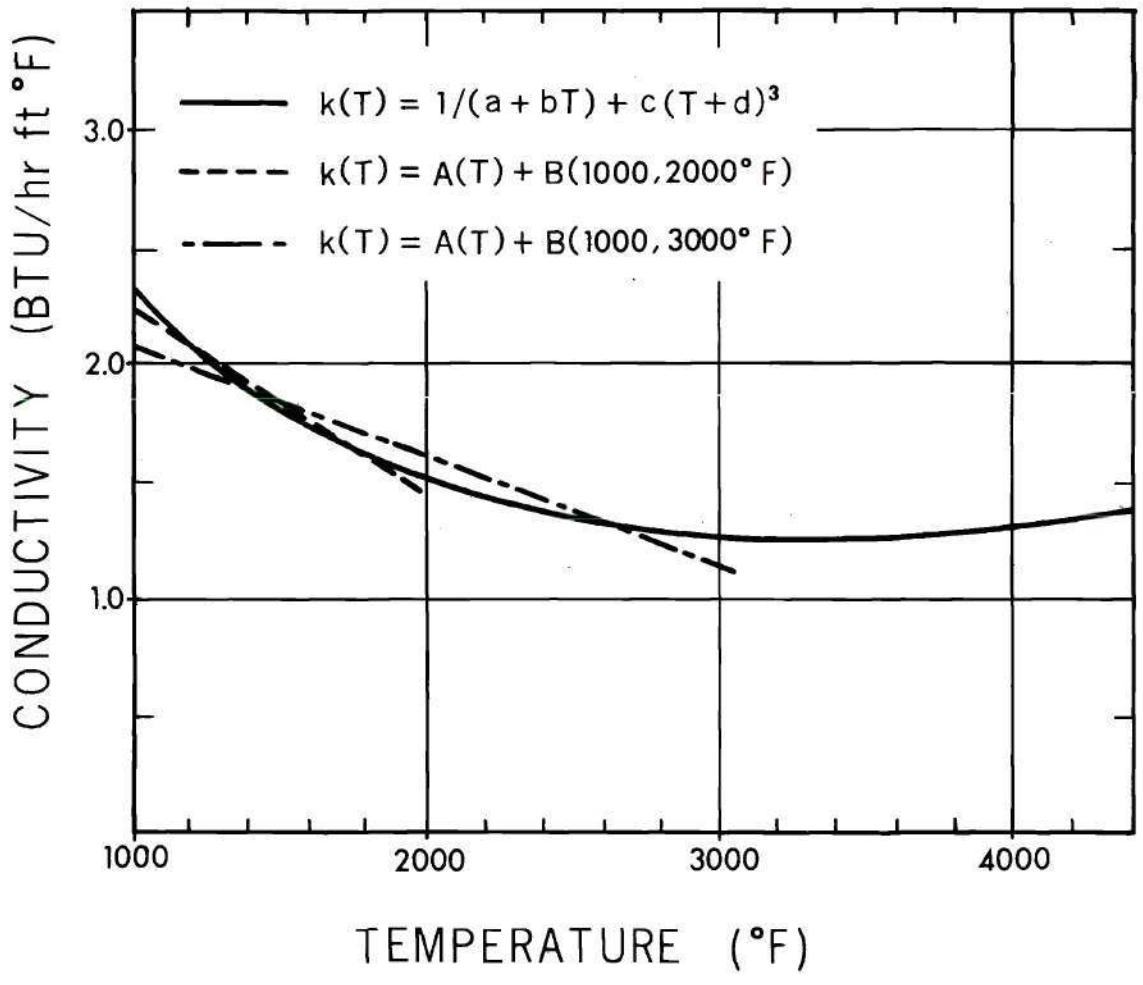

Figure 5. Conductivity of UO_2

Perturbation Solution

The deviation of the first-order perturbation solution from the exact solution cannot be assessed directly since an exact solution is not known. However, some insight into the accuracy of the method can be obtained from some related problems for which both exact and perturbation solutions exist, such as, the solid matrix material problem discussed in the previous section.

The exact solution given by Eq. 3.103 is

$$\Theta(\zeta) = \frac{1}{\epsilon_\Theta}\left[-1 + \sqrt{1 + \frac{\epsilon_\Theta}{\pi\xi}(\xi^2 - \zeta^2)}\right]$$

The zero-order function for the perturbation solution is the constant conductivity equation, Eq. 3.102

$$\Theta^0(\zeta) = \frac{1}{2\pi\xi}\left[\xi^2 - \zeta^2\right]$$

The equation for the first-order function is similar to Eq. 3.72.

$$\frac{d^2\Theta^1}{d\zeta^2} + \frac{1}{2}\frac{d^2[\Theta^0]^2}{d\zeta^2} = 0 \qquad (3.112)$$

The solution is apparent from inspection

$$\Theta^1(\zeta) = -\frac{1}{2}[\Theta^0]^2 + a\zeta + b \qquad (3.113)$$

The undetermined coefficients are evaluated from the boundary

conditions, Eqs. 3.98 and 3.99.

$$a = b = 0 \tag{3.114}$$

The perturbation solution, $\tilde{\theta}$, is given by

$$\tilde{\theta}(\zeta) = \theta^0(\zeta) + \epsilon_\theta \theta^1(\zeta) \tag{3.115}$$

$$= \frac{1}{2\pi\xi}\left[\xi^2 - \zeta^2\right] \cdot \left[1 - \frac{\epsilon_\theta}{4\pi\xi}(\xi^2 - \zeta^2)\right]$$

The maximum deviation between the two solutions occurs at the point where both attain maximum values, at $\xi = 0$. Table 7 compares the perturbation and exact solutions over a range of values of ϵ_θ.

Table 7. Comparison of Exact and Perturbation Solutions for One-Dimensional Linear Conductivity Problems

ϵ_θ	ξ	θ_{Max}	$\tilde{\theta}_{Max}$	$\frac{\Delta\theta}{\theta_{Max}} \cdot 100\%$	$1 + \epsilon_\theta \theta_{Max}$
-0.0025	1000	219.23	190.82	12.96	.44
-0.002	1000	198.59	184.49	7.10	.60
-0.001	1000	174.35	171.82	1.45	.83
-0.0001	1000	160.44	160.42	.01	.98
0.0	1000	159.15	159.15	0.0	1.0
0.0001	1000	157.91	157.89	.01	1.02
0.001	1000	148.18	146.89	1.14	1.15
0.002	1000	139.65	133.82	4.17	1.28
0.003	1000	132.73	121.16	8.72	1.40

One can see that the perturbation solution systematically underestimates temperatures. The error increases as the conductivity term, $(1 + \epsilon_\theta \theta)$, varies above and below one. In the previous section, a reasonable range for conductivities was suggested as

$$\frac{1}{2} < 1 + \epsilon_\theta \theta_{max} < 1.0 \tag{3.116}$$

Within this range, the perturbation solution error is within approximately 10 percent. On the basis of the preceding discussion it is concluded that the linear conductivity problem solved by perturbation analysis is acceptable when

$$.5 < 1 + \epsilon_\theta \theta_{max} < 1.5 \tag{3.117}$$

Calculated Properties

While temperature functions are the basis for most heat conduction analysis, they give little insight into the physical properties of composites. Calculated properties, such as effective conductivity, heat content, and effective volumetric heat capacity, must be defined using the temperature functions to show the dependence of these properties on input parameters.

Effective Conductivity

The definition of thermal conductivity comes from Fourier's heat conduction law given by Eq. 3.118

$$q'' = -k \frac{\partial T}{\partial n} \tag{3.118}$$

where q'' = heat flux through surface

$\frac{\partial T}{\partial n}$ = component of temperature gradient along line normal to surface

k = thermal conductivity.

An effective conductivity for composites can be derived using Eq. 3.118

$$k^* = \frac{\overline{q''}_{L/2}}{\frac{T_{max} - T_s}{L}} \tag{3.119}$$

where

$\overline{q}''_{L/2}$ = average heat flux through a surface halfway between ends of cylinder = $q'''_o \frac{L}{2}$

T_{Max} = maximum temperature of composite (occurs at $(r,z) = (b,0)$ for $\frac{q'''_1}{k_1} < \frac{q'''_2}{k_2}$

T_s = surface temperature at $z = L$.

This choice is designed so that, when applied to solid matrix material, it gives the actual conductivity of the matrix

$$k_2 = \frac{\overline{q''}_{L/2}}{\frac{[T_{SM}]_{max} - T_s}{L}} \tag{3.120}$$

The effective conductivity ratio is then given by

$$\frac{k^*}{k_2} = \frac{[T_{SM}]_{max} - T_s}{[T_{COMP}]_{max} - T_s} = \frac{[\theta_{SM}]_{max}}{[\theta_{COMP}]_{max}} = \frac{\xi}{2\pi} \frac{1}{[\theta_{COMP}]_{max}} \tag{3.121}$$

Heat Content

The amount of energy stored in nuclear fuels is an important parameter in reactor safety analysis; therefore, it is of interest to determine how much the composite stored energy is reduced in comparison to that of the solid matrix with the same total heat generation.

The heat content of a cell, E, is defined as

$$E = \int_V C \cdot (T - T_s)\, dV \tag{3.122}$$

where C = volumetric heat capacity = τC_p

τ = density

C_p = specific heat

V = cell volume

T = temperature function

T_s = surface temperature at $z = L$.

The reference state implied in Eq. 3.122 is that the heat content of a cell uniformly at $T = T_s$ is zero.

Assuming that the volumetric heat capacities for fiber and matrix, C_1 and C_2, are constants in each region, the composite cell heat content is

$$E = C_1 \int_{V_1} (T_1 - T_s)\, dV + C_2 \int_{V_2} (T_2 - T_s)\, dV \tag{3.123}$$

where V_1, V_2 = volumes of fiber and matrix.

The heat content of the corresponding cell with no fiber is

$$E_{SM} = C_2 \int_V (T_{SM} - T_s)\, dV \tag{3.124}$$

Thus, the heat content ratio is given by

$$\frac{E}{E_{SM}} = \frac{C_1 \int_{V_1} (T_1 - T_s)\, dV + C_2 \int_{V_2} (T_2 - T_s)\, dV}{C_2 \int_V (T_{SM} - T_s)\, dV} \tag{3.125}$$

or, in dimensionless variables

$$\frac{E}{E_{SM}} = \frac{\beta \int_0^{\xi} \int_0^{\delta} \theta_1 \rho\, d\rho\, d\zeta + \int_0^{\xi} \int_{\delta}^{1.0} \theta_2 \rho\, d\rho\, d\zeta}{\int_0^{\xi} \int_0^{1.0} \theta_{SM} \rho\, d\rho\, d\zeta} \tag{3.126}$$

where β = ratio of volumetric heat capacities = C_1/C_2.

The integrations for θ_1, θ_2, and θ_{SM} used in Eq. 3.126 are performed in Appendix B.

Effective Volumetric Heat Capacity

An effective volumetric heat capacity can be defined in a way consistent with the effective conductivity and heat content. Let us postulate an equivalent homogenecus material whose conductivity is equal to the effective conductivity of the composite. At the same average heat generation, the maximum temperatures of the equivalent material, and the composite are equal. By requiring the heat content of the two systems to be equal also, the effective specific heat is determined.

The temperature function of the equivalent material with constant conductivity is

$$T_{EM} - T_S = \frac{q_0'''}{2k^*}(L^2 - Z^2), \tag{3.127}$$

and the heat content is

$$E_{EM} = C^* 2\pi \int_{z=0}^{L} \int_{r=0}^{b} (T_{EM} - T_S) r\,dr\,dz \tag{3.128}$$

where C* is the effective volumetric heat capacity.

Solving Eq. 3.128 for C* yields

$$C^* = \frac{3k^* E_{EM}}{\pi q_0''' L^3 b^2} \tag{3.129}$$

The volumetric heat capacity for the solid matrix cell written the same way is

$$C_2 = \frac{3k_2 E_{SM}}{\pi q_0''' L^3 b^2} \tag{3.130}$$

After setting $E_{EM} = E$, the effective specific heat ratio is

$$\frac{C^*}{C_2} = \frac{E}{E_{SM}} \frac{k^*}{k_2} \tag{3.131}$$

The effective volumetric heat capacity for constant conductivity can be written in terms of θ_1 and θ_2 using Eqs. 3.121 and 3.126. The solutions for $[\theta_{SM}]_{Max}$ and E_{SM} for constant conductivity can be substituted

for these terms. Thus, the effective volumetric heat capacity becomes

$$\frac{C^*}{C_2} = \frac{3}{\xi}\frac{\left[\int_0^{\xi}\int_0^{\delta}\theta_1\rho d\rho d\zeta + \int_0^{\xi}\int_{\delta}^{1.0}\theta_2\rho d\rho d\zeta\right]}{\left[\theta_{COMP}\right]_{max}} \tag{3.132}$$

Effective Conductivity and Effective Specific Heat for Linear Conductivity

The definition of effective conductivity given for constant conductivity, Eq. 3.121, can be used for the linear conductivity case also.

$$\frac{k^*}{k_2} = \frac{\left[\theta_{SM}\right]_{max}}{\left[\theta_{COMP}\right]_{max}} \tag{3.133}$$

or

$$= \frac{\frac{1}{\epsilon_\theta}\left[1+\sqrt{1+\frac{\epsilon_\theta \xi}{\pi}}\right]}{\left[\theta_{COMP}\right]_{max}} \tag{3.134}$$

However, the physical meaning of the quantity is vague because the linear dependence of the conductivity on temperature is not accounted for. It is more reasonable to define an effective linear conductivity of the following form:

$$k^*(\theta) = k^{0*}(1+\epsilon_\theta\theta) \tag{3.135}$$

where ϵ_θ = linear conductivity coefficient of the matrix.

The factor, k^{0*}, is determined by requiring that the maximum temperature of an equivalent material with conductivity given by Eq. 3.135 be equal to the maximum temperature of the composite. The temperature function of the equivalent material can be obtained exactly or by the first-order perturbation method. Since the perturbation method is used to obtain the temperature function of the composite, it is consistent to use the perturbation solution for the equivalent material. In dimensionless form the temperature function for the equivalent material is given by the following:

$$\tilde{\theta}_{EM} = \left(\frac{1}{2\pi\xi}\right)\left(\frac{k_2^0}{k^{0*}}\right)\left[\xi^2-\zeta^2\right]\left[1-\left(\frac{\epsilon_\theta}{4\pi\xi}\right)\left(\frac{k_2^0}{k^{0*}}\right)(\xi^2-\zeta^2)\right] \qquad (3.136)$$

Setting $[\tilde{\theta}_{EM}]_{Max} = [\tilde{\theta}_{comp}]_{Max}$ and solving for $\frac{k^{0*}}{k_2^0}$ yields the following formula:

$$\frac{k^{0*}}{k_2^0} = \frac{\xi}{4\pi}\,\frac{\left[1+\sqrt{1-2\epsilon_\theta\left[\tilde{\theta}_{comp}\right]_{max}}\right]}{\left[\tilde{\theta}_{comp}\right]_{max}} \qquad (3.137)$$

It is worth noting that, for $\epsilon_\theta = 0$, Eq. 3.137 reduces to the formula for constant conductivity.

The effective specific heat for the linear conductivity case is obtained by equating the heat contents of the equivalent material and the composite, $E_{EM} = E_{comp}$, and solving for $\frac{C^*}{C_2}$

$$E_{EM} = \frac{C^*}{C_2} \int_{\zeta=0}^{\xi} \int_{\rho=0}^{1.0} \tilde{\Theta}_{EM}\, \rho d\rho d\zeta \tag{3.138}$$

$$E_{COMP} = \beta \int_{\zeta=0}^{\xi} \int_{\rho=0}^{\delta} \Theta_1\, \rho d\rho d\zeta + \int_{\zeta=0}^{\xi} \int_{\rho=\delta}^{1.0} \Theta_2 \rho d\rho d\zeta \tag{3.139}$$

The integrations in Eqs. 3.138 and 3.139 are performed in Appendix B. The result is given by Eq. 3.140.

$$\frac{C^*}{C_2} = \frac{k^{0*}}{k_2^0} \frac{6\pi E_{COMP}}{\xi^2 \left[1 - \frac{\epsilon_\theta \xi k_2^0}{5\pi k^{0*}}\right]} \tag{3.140}$$

Asymptotic Solutions

The calculated properties tend to asymptotes for large values of ξ (constant conductivity only). Asymptotic values of these parameters are given by volume-weighted averages.

$$\frac{k^*}{k_2} \longrightarrow \gamma\delta^2 + 1 - \delta^2 \tag{3.141}$$

$$\frac{E_{COMP}}{E_{SM}} \longrightarrow \frac{\beta\delta^2 + 1 - \delta^2}{\gamma\delta^2 + 1 - \delta^2} \tag{3.142}$$

$$\frac{C^*}{C_2} \longrightarrow \left[\beta\delta^2 + 1 - \delta^2\right] \tag{3.143}$$

This effect, noted by Rust and Boyle [17], occurs as isotherm surfaces approach flat transverse planes. In this section, we shall verify by mathematical proof that the volume-weighted average conductivity is indeed an upper bound and that it is approached asymptotically for large values of ξ. By logical extension, similar proofs could be made for heat content and effective specific heat.

To verify that the volume-weighted formula is an upper bound, the following hypothesis must be tested:

$$\frac{k^*}{k_2} \overset{?}{\leq} (\gamma-1)\delta^2+1 \tag{3.145}$$

For steady state, all of the heat generated between a transverse plane A, at $\zeta = \zeta_1$ and the insulated boundary at $\zeta = 0$ must pass through A_1. Since the total heat generated in the composite cell has been normalized to one, the heat crossing A_1 is given by

$$\frac{\zeta_1}{\xi} = 2\pi \int_{\rho=0}^{1.0} q''(\rho,\zeta_1)\rho d\rho \tag{3.146}$$

where $q''(\rho,\zeta)$ = normalized heat flux parallel to the cell axis.

The heat flux is given by

$$q''(\rho,\zeta) = \begin{cases} -\gamma \dfrac{\partial\theta_1(\rho,\zeta)}{\partial\zeta} & 0 \leq \rho \delta \\ -\dfrac{\partial\theta_2(\rho,\zeta)}{\partial\zeta} & \delta < \rho \leq 1.0 \end{cases} \tag{3.147}$$

Substituting Eq. 3.147 into Eq. 3.146 yields Eq. 3.148

$$\frac{\zeta}{\xi} = -2\pi \left[\int_0^{\delta} \gamma \frac{\partial \theta_1}{\partial \zeta} \rho d\rho + \int_{\delta}^{1.0} \frac{\partial \theta_2}{\partial \zeta} \rho d\rho \right] \qquad (3.148)$$

Integrating both sides of Eq. 3.148 with respect to ζ over the length of the cell gives

$$\int_{\zeta=0}^{\xi} \frac{\zeta}{\xi} d\zeta = -2\pi \int_{\zeta=0}^{\xi} \left[\int_{\rho=0}^{\delta} \gamma \frac{\partial \theta_1}{\partial \zeta} \rho d\rho + \int_{\rho=\delta}^{1.0} \frac{\partial \theta_2}{\partial \zeta} \rho d\rho \right] d\zeta \qquad (3.149)$$

The ζ-integration in Eq. 3.149 is accomplished by interchanging the order of integration on the right and using boundary conditions, Eqs. 2.22 and 2.23.

$$\frac{\xi}{2} = 2\pi \left[\int_{\rho=0}^{\delta} \gamma \theta_1(\rho,0) \rho d\rho + \int_{\delta}^{1.0} \theta_2(\rho,0) \rho d\rho \right] \qquad (3.150)$$

The factors $2\pi\gamma\rho$ and $2\pi\rho$ may be considered a weighting function which is normalized by dividing both sides of Eq. 3.150 by the following term:

$$2\pi \left[\int_0^{\delta} \gamma \rho d\rho + \int_{\delta}^{1.0} \rho d\rho \right] = \pi \left[(\gamma - 1)\delta^2 + 1 \right] \qquad (3.151)$$

Thus, Eq. 3.149 becomes

$$\frac{\xi}{2\pi[(\gamma-1)\delta^2+1]} = \int_0^{\delta} \theta_1(\rho,0)\frac{2\gamma\rho}{[(\gamma-1)\delta^2+1]}\rho d\rho + \int_{\delta}^{1.0} \theta_2(\rho,0)\frac{2\rho}{[(\gamma-1)\delta^2+1]}\rho d\rho \tag{3.152}$$

The quantity on the right can be considered an average temperature, $\bar{\theta}_{comp}$, along the insulated boundary ($\zeta = 0$, $0 \leq \rho \leq 1.0$).

$$\bar{\theta}_{COMP} = \frac{\xi}{2\pi}\frac{1}{(\gamma-1)\delta^2+1} \tag{3.153}$$

or

$$(\gamma-1)\delta^2+1 = \frac{\xi}{2\pi}\frac{1}{\theta_{COMP}} \tag{3.154}$$

Clearly, the average temperature along the boundary is less than or equal to the maximum temperature.

$$\bar{\theta}_{COMP} \leq [\theta_{COMP}]_{max} \tag{3.155}$$

Thus, combining Eqs. 3.121, 3.154, and 3.155, the volume-weighted average conductivity is shown to be an upper limit

$$\frac{k^*}{k_2} = \frac{\xi}{2\pi}\frac{1}{[\theta_{COMP}]_{max}} \leq \frac{\xi}{2\pi}\frac{1}{\bar{\theta}_{COMP}} = (\gamma-1)\delta^2+1 \tag{3.156}$$

Asymptotic Approach as $\xi \to \infty$

To verify that the effective conductivity approaches the volume-weighted formula as ξ goes to infinity, the following hypothesis must be

evaluated:

$$\lim_{\xi\to\infty} \frac{k^*}{k_2} \stackrel{?}{=} (\gamma-1)\delta^2+1 \tag{3.157}$$

or, an equivalent hypothesis

$$\lim_{\xi\to\infty} \frac{[\theta_{COMP}]_{max}}{\xi/2\pi} \stackrel{?}{=} \frac{1}{(\gamma-1)\delta^2+1} \tag{3.158}$$

The composite maximum temperature occurs at $(\rho,\zeta) = (1,0)$ if $\frac{fp_1}{\gamma} \leqq fp_2$. Therefore,

$$\frac{2\pi}{\xi}[\theta_{COMP}]_{max} = \frac{2\pi}{\xi}\left\{\sum_{j=1}^{\infty} C_j\left[I_0(\lambda_j)+\frac{I_1(\lambda_j)}{K_1(\lambda_j)}K_0(\lambda_j)\right]+\frac{fp_2\,\xi^2}{2}\right\} \tag{3.159}$$

The following identities, which follow from the definition of parameters in Table 1 and from the solution of the heat conduction equation, Eqs. 3.59 - 3.64, are used to simplify the dependence on ξ in Eq. 3.159.

$$\mathcal{L}_j = \frac{2L_j}{\xi^2} = \frac{32(-1)^{j-1}}{[(2_j-1)\pi^3} \tag{3.160}$$

[Note that $\sum_{j=1}^{\infty} \mathcal{L}_j = 1$]

$$\left[fp_1 - \frac{fp_2}{\gamma}\right] = \left[\frac{\eta-\gamma}{\gamma}\right]\left[\frac{1}{\pi\xi}\right]\left[\frac{1}{(\eta-1)\delta^2+1}\right] \tag{3.161}$$

$$\frac{2\pi}{\xi} C_j = -\left[\frac{H_c}{\gamma}\right] \frac{[\eta-\gamma]}{[(\eta-1)\delta^2+1]} \left[\frac{\mathcal{L}_j}{G_j}\right] \tag{3.162}$$

Thus, Eq. 3.159 can be rewritten

$$\frac{2\pi}{\xi}\theta_{max} = \frac{-(\eta-\gamma)}{\gamma[(\eta-1)\delta^2+1]} \sum_{j=1}^{\infty} \frac{\mathcal{L}_j H_c}{G_j}\left[I_0(\lambda_j) + \frac{I_1(\lambda_j)}{K_1(\lambda_j)} K_0(\lambda_j)\right] \tag{3.163}$$

$$+ \frac{1}{(\eta-1)\delta^2+1} \sum_{j=1}^{\infty} \mathcal{L}_j$$

The terms in Eq. 3.163 which depend on ξ are λ_j and G_j. The limit may be evaluated using only the portion of the expression depending on ξ,

$$\lim_{\xi\to\infty} \frac{H_c\left[I_0(\lambda_j) + \frac{I_1(\lambda_j)}{K_1(\lambda_j)} K_0(\lambda_j)\right]}{G_j} = \tag{3.164}$$

$$= \lim_{\xi\to\infty} \frac{H_c\left[I_0(\lambda_j) + \frac{I_1(\lambda_j)}{K_1(\lambda_j)} K_0(\lambda_j)\right]}{\left\{\frac{1}{\gamma}\left[1 - \frac{I_1(\lambda_j)K_1(\lambda_j\delta)}{K_1(\lambda_j)I_1(\lambda_j\delta)}\right]\left[\lambda_j I_1(\lambda_j\delta) + H_c I_0(\lambda_j\delta)\right] - H_c\left[I_0(\lambda_j\delta) + \frac{I_1(\lambda_j)}{K_1(\lambda_j)} K_0(\lambda_j)\right]\right\}}$$

Noting that as

$$\xi \to \infty \tag{3.165}$$

then,

$$\lambda_j \to 0 \tag{3.166}$$

So the limit of Eq. 3.164 may be taken directly

$$\lim_{\lambda_j \to 0} \frac{H_c\left[I_0(\lambda_j) + \frac{I_1(\lambda_j)}{K_1(\lambda_j)} K_0(\lambda_j)\right]}{G_j} = \frac{\gamma\delta^2}{\delta^2 - 1 - \gamma\delta^2} \tag{3.167}$$

Substituting Eq. 3.167 into Eq. 3.163 yields the desired limiting relation after rearranging and simplifying.

$$\lim_{\xi \to \infty} \frac{2\pi}{\xi}\left[\theta_{COMP}\right]_{max} = \frac{1}{(\gamma-1)\delta^2 + 1} \tag{3.168}$$

CHAPTER IV

RESULTS

A computer program using the mathematical solutions developed in the preceding chapter was written to determine temperature functions in the composite cell and evaluate the effective conductivity, heat content, and effective volumetric heat capacity for the range of parameter values given in Table 4. In the parametric study, the constant conductivity problem is discussed first, followed by the discussion of the linear conductivity problem.

Constant Conductivity Results

All of the figures showing k^*/k_2, E/ESM, or c^*/c_2 versus length-to-radius ratio, ξ, reveal that the properties approach asymptotes for both large and small values of ξ. Formulas for the asymptotes, which are obtained from limiting temperature functions given later in this section, are listed in Table 8. The parametric study will focus on the transition from the lower to upper asymptote evaluating bounds of the transition and noting the parametric dependence.

Figure 6 shows the effective conductivity versus ξ for several values of η. The quantity, η, which is the ratio of fiber to matrix heat generation, is expected to be small in a composite nuclear fuel since the sources of heat generation in the fiber are small compared to heat generation from fission in the matrix. The parameter, η, is conservatively

Table 8. Asymptotic Formulas

Upper Asymptotes (Large ξ)	
Effective Conductivity	$(\gamma-1)\delta^2+1$
Heat Content	$\dfrac{(\beta-1)\delta^2+1}{(\gamma-1)\delta^2+1}$
Effective Volumetric Heat Capacity	$(\beta-1)\delta^2+1$
Lower Asymptotes (Small ξ)	
Effective Conductivity	$\begin{cases}(\eta-1)\delta^2+1 & \frac{\eta}{\gamma}<1\\ \frac{\gamma}{\eta}\left[(\eta-1)\delta^2+1\right] & \frac{\eta}{\gamma}>1\\ 1-\delta^2 & \eta=0\end{cases}$
Heat Content	$\begin{cases}\dfrac{\left(\frac{\eta\beta}{\gamma}-1\right)\delta^2+1}{(\eta-1)\delta^2+1} & \eta\neq 0\\ 1 & \eta=0\end{cases}$
Effective Volumetric Heat Capacity	$\begin{cases}\left(\frac{\eta\beta}{\gamma}-1\right)\delta^2+1 & \frac{\eta}{\gamma}<1\\ \frac{\gamma}{\eta}\left[\left(\frac{\eta\beta}{\gamma}-1\right)\delta^2+1\right] & \frac{\eta}{\gamma}>1\\ 1-\delta^2 & \eta=0\end{cases}$

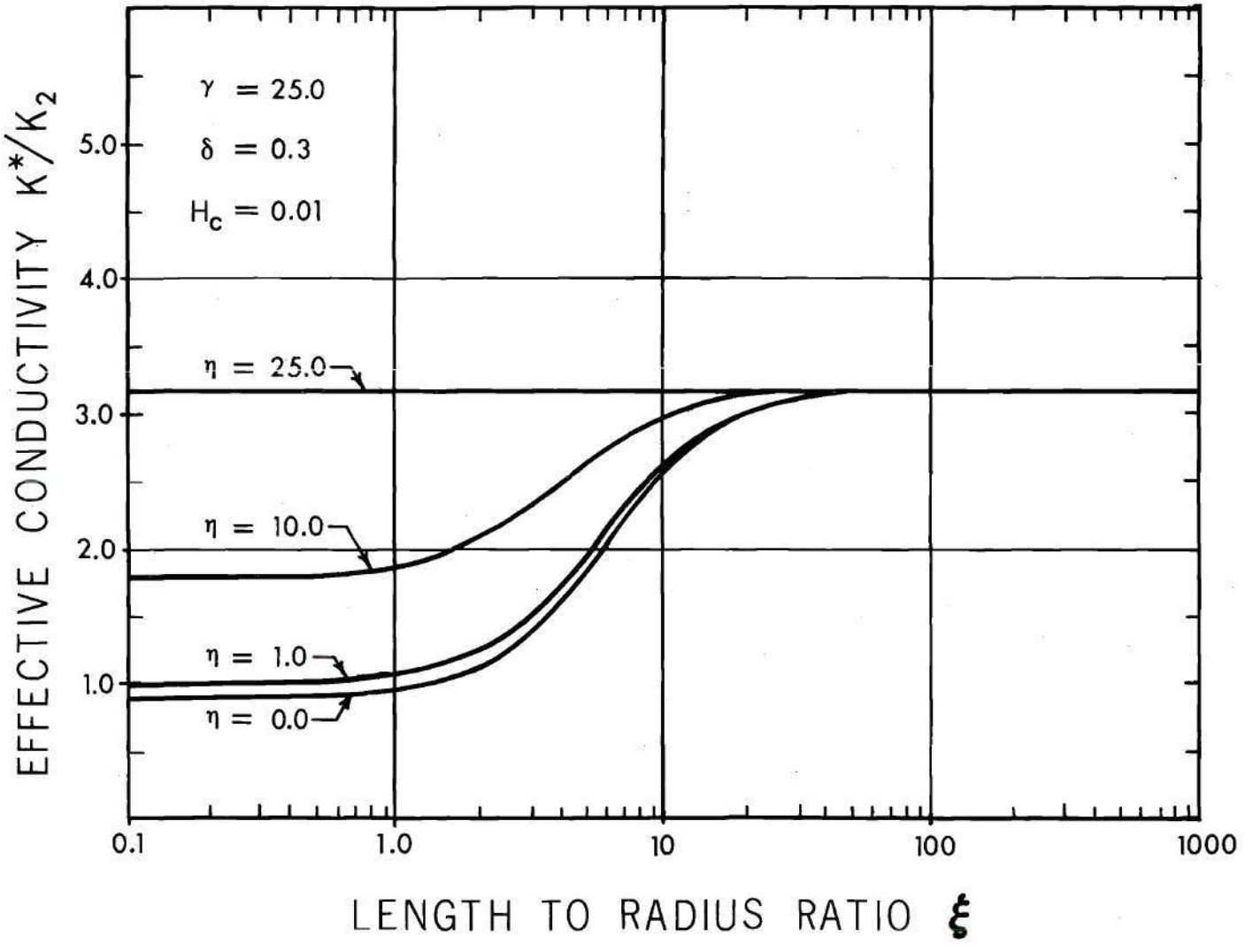

Figure 6. Effective Conductivity versus Length for Various Fiber-Matrix Heat Generation Ratios

estimated to be less than 10^{-5}. Figure 6 shows that η does not affect the upper asymptote and affects the lower noticeably only for η greater than unity. The formulas in Table 8 can be simplified by taking $\eta = 0$.

The case of $\eta = \gamma$ is of no practical significance; mathematically, however, it is the distribution of heat generation giving a temperature distribution exactly uniform in the radial direction. Figure 6 shows that, for $\eta = \gamma$, the effective conductivity is given by the upper asymptotic formula for all values of ξ.

Figures 7 through 12 show effective conductivity for various values of γ, δ, and H_c. The significant features of these illustrations are that the lower asymptotes depend only on δ and the upper on γ and δ, as the formulas in Table 8 predict. Figures 9 through 12 show decreasing values of H_c tend to shift the transition region to higher ξ without greatly changing the shape of the curve. Further calculations show that $H_c = 20$ is essentially perfect thermal contact, and all curves for $H_c \geq 20.0$ lie along the same line. In Figures 9 through 12, this case could not be shown because the difference between the curves at $H_c = 1.0$ and $H_c = 20.0$ is not distinguishable. It is well to point out that $H_c = 10^{-4}$ corresponds to an actual gap conductance of $h_c = 2000$ Btu/hr-ft^2-°F. The discussion in Chapter II suggests that this is an extraordinarily small gap conductance for a composite nuclear fuel.

Since the range over which the upper asymptotic solution applies is of considerable interest, a lower bound for the region of close approach to the upper asymptote is defined. This point will be defined as the point at which the difference between the effective conductivity and the lower asymptote is 99% of the difference between the upper

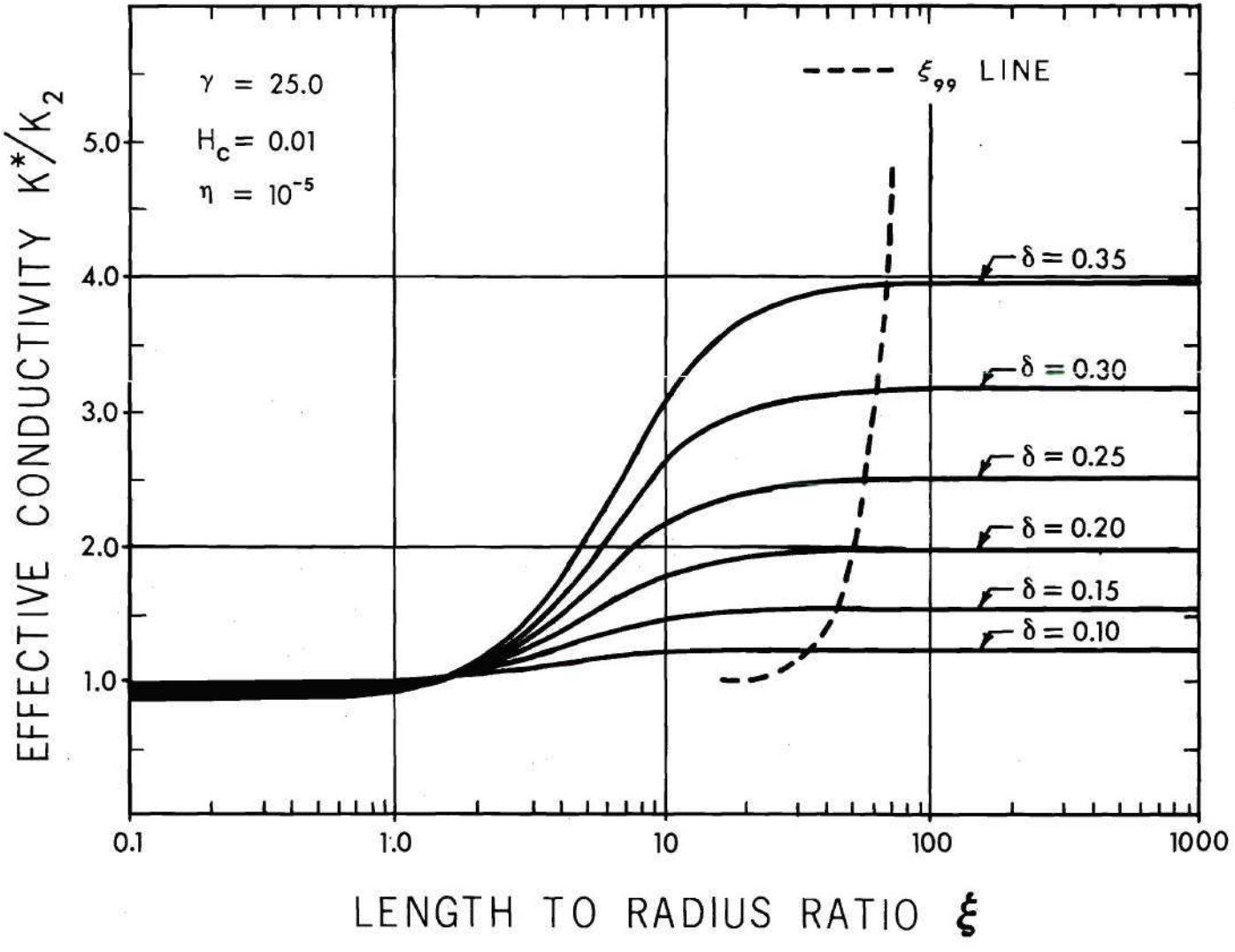

Figure 7. Effective Conductivity versus Length for Various Fiber Radii

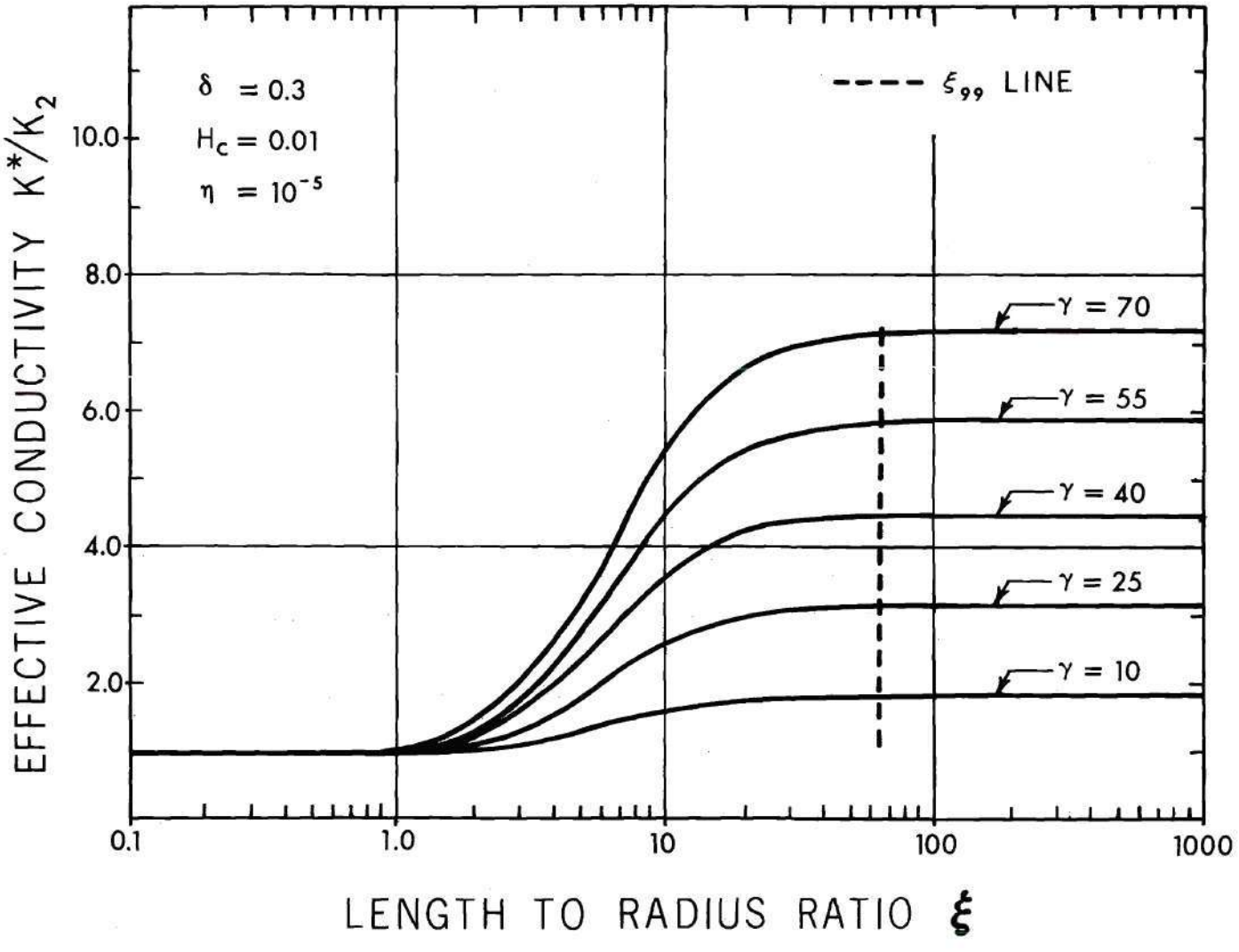

Figure 8. Effective Conductivity versus Length for Various Conductivity Ratios

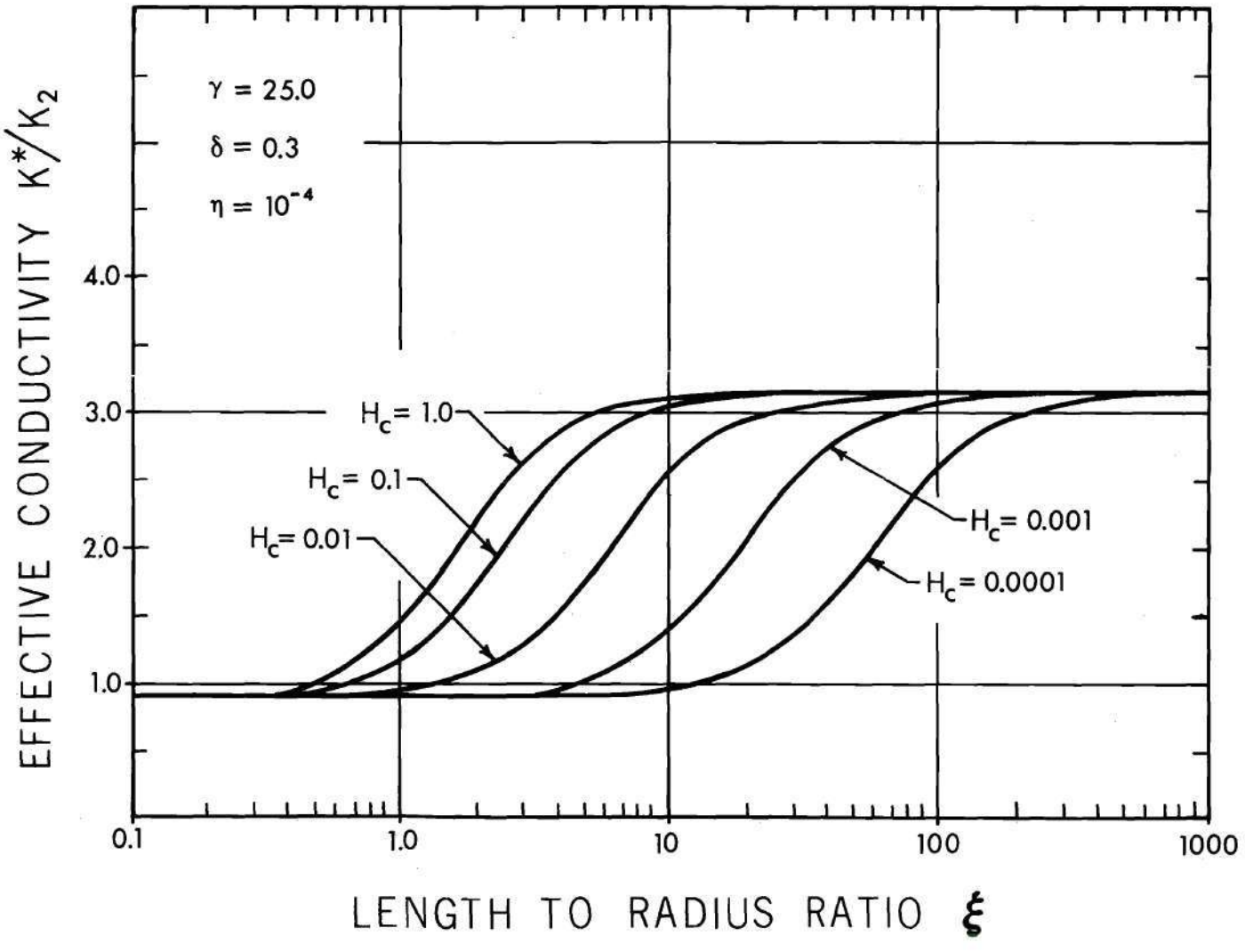

Figure 9. Effective Conductivity versus Length for Various Gap Conductances ($\gamma = 10$, $\delta = 0.1$)

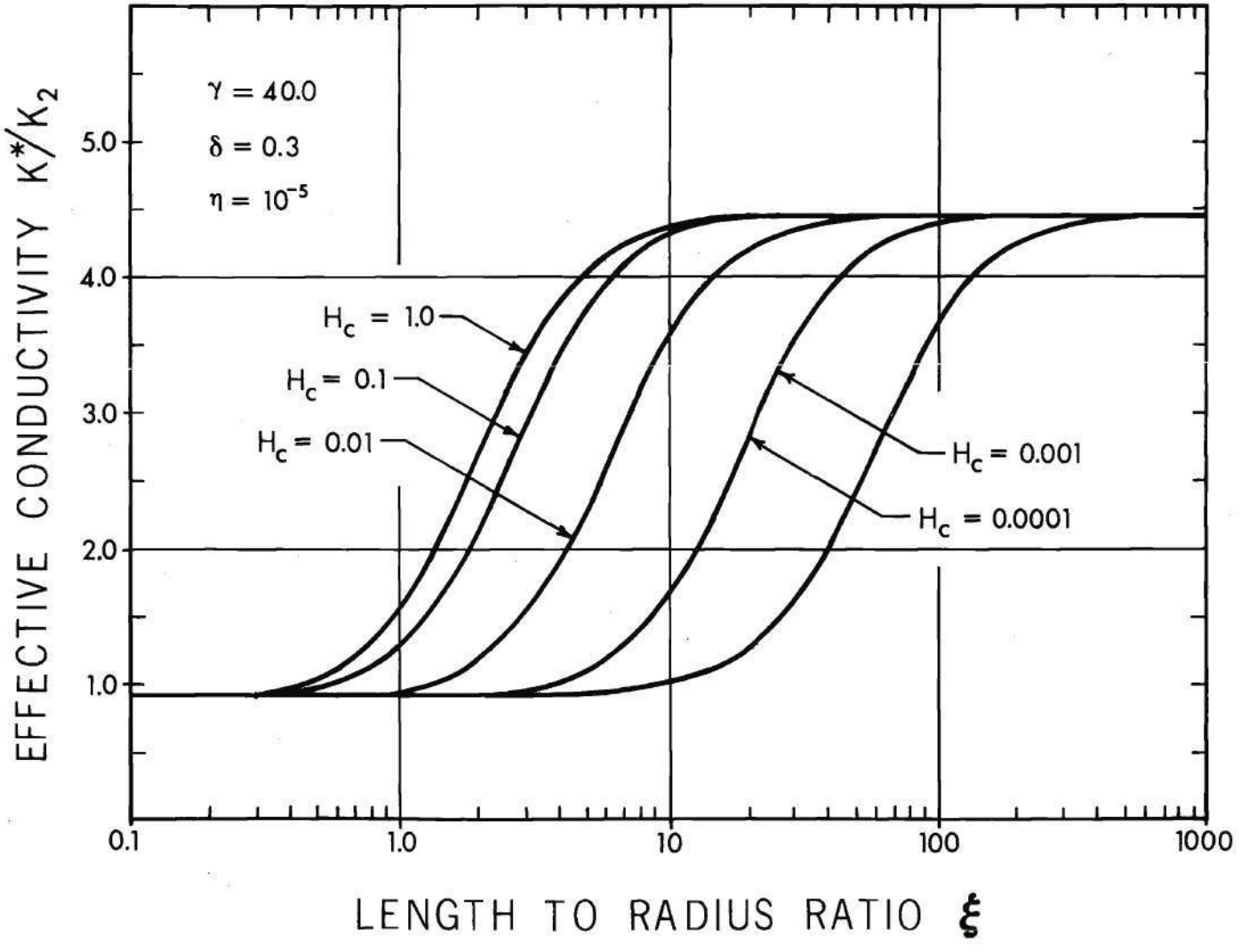

Figure 10. Effective Conductivity versus Length for Various Gap Conductances (γ = 10, δ = 0.3)

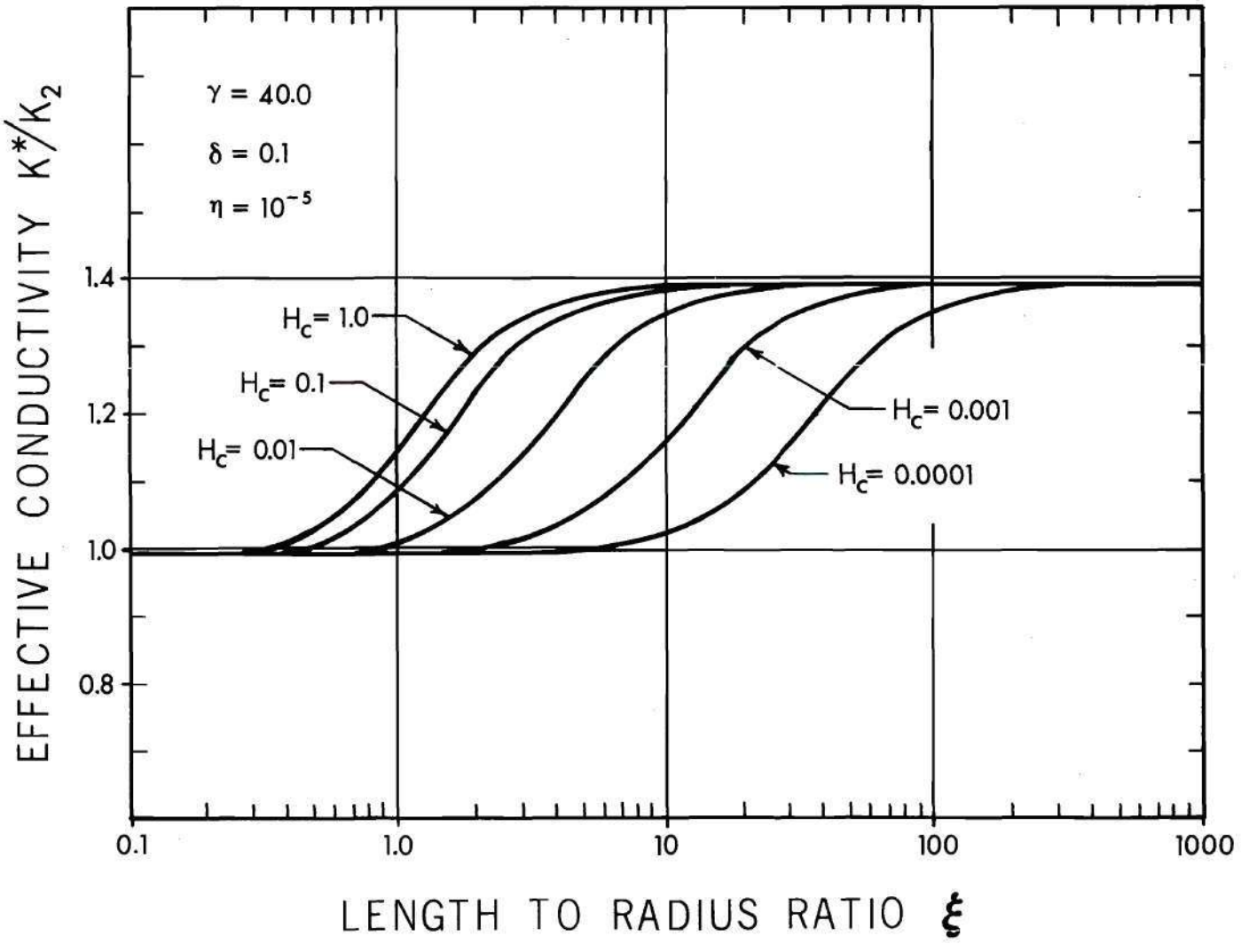

Figure 11. Effective Conductivity versus Length for Various Gap Conductances (γ = 25, δ = 0.1)

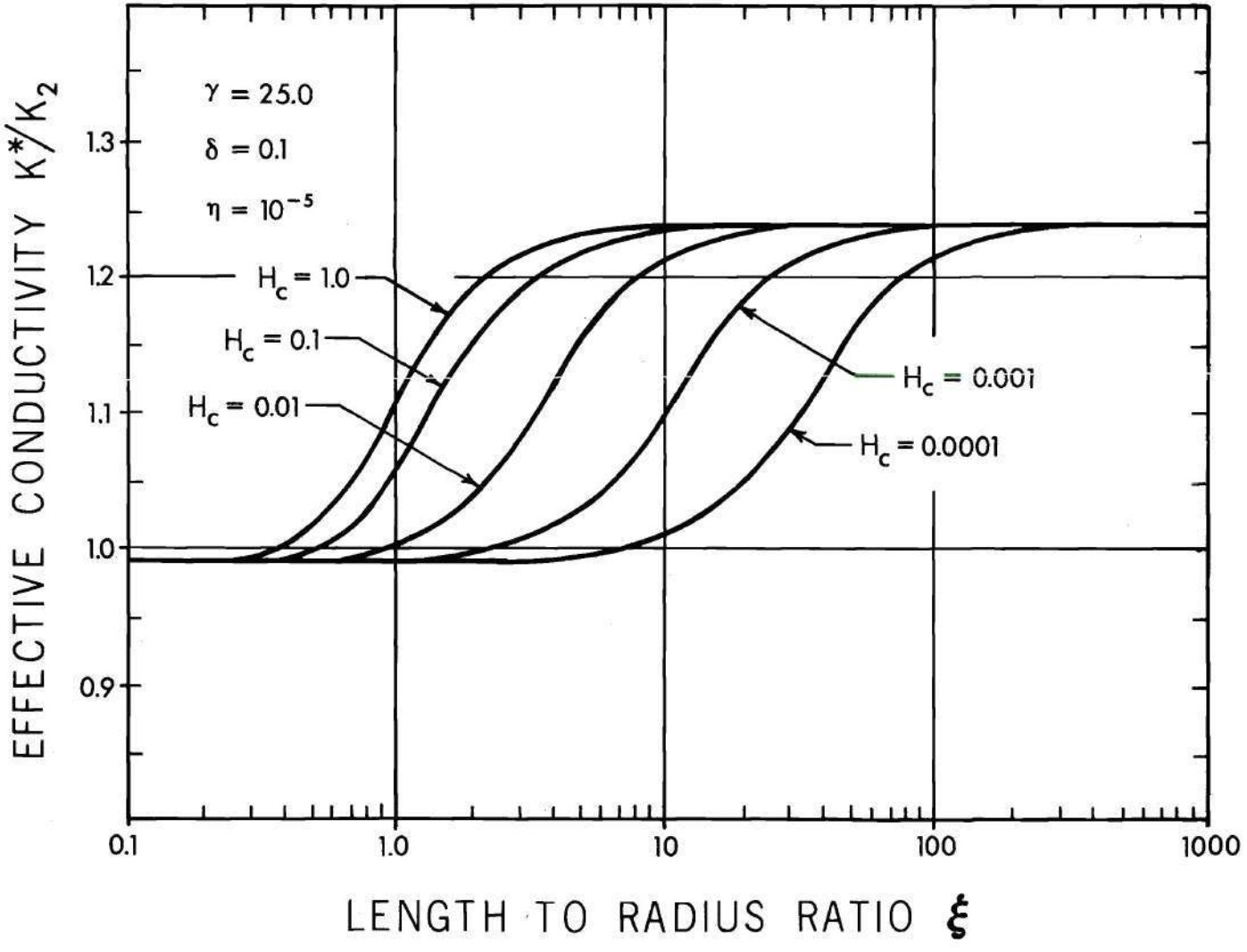

Figure 12. Effective Conductivity versus Length for Various Gap Conductances ($\gamma = 25$, $\delta = 0.3$)

asymptote and the lower. This point will be referred to as the asymptotic length or ξ_{99}. The relation defining this point is given in Eq. 4.1.

$$\frac{k^*(\xi_{99}) - k_L^*}{k_U^* - k_L^*} = 0.99 \tag{4.1}$$

where k_U^*/k_2 and k_L^*/k_2 are the upper and lower asymptotic effective conductivities.

After inserting formulas for k_U^* and k_L^* from Table 8 (at $\eta = 0$) into Eq. 4.1, the following formula is obtained:

$$\frac{k^*(\xi_{99})}{k_2} - 1 + \delta^2 - 0.99\gamma\delta^2 = 0 \tag{4.2}$$

The loci of ξ_{99} points for a family of δ curves and for a family of γ curves are shown as dashed lines in Figures 7 and 8, respectively.

It is interesting to plot ξ_{99} as a function of γ, δ, and H_c. A computer program was written to perform this calculation. Figures 13 through 15 give the results of this calculation. Figure 13 shows the dependence of ξ_{99} on H_c for several values γ. For $H_c < 0.1$, the dependence on H_c dominates the relation. Figure 14 shows the same dependence for several values of δ. The straight portion of these figures suggests that the relation for ξ_{99} reduces to an equation of the following form for $H_c < 0.1$:

$$\xi_{99}^2 = \frac{g(\delta)}{H_c} \tag{4.3}$$

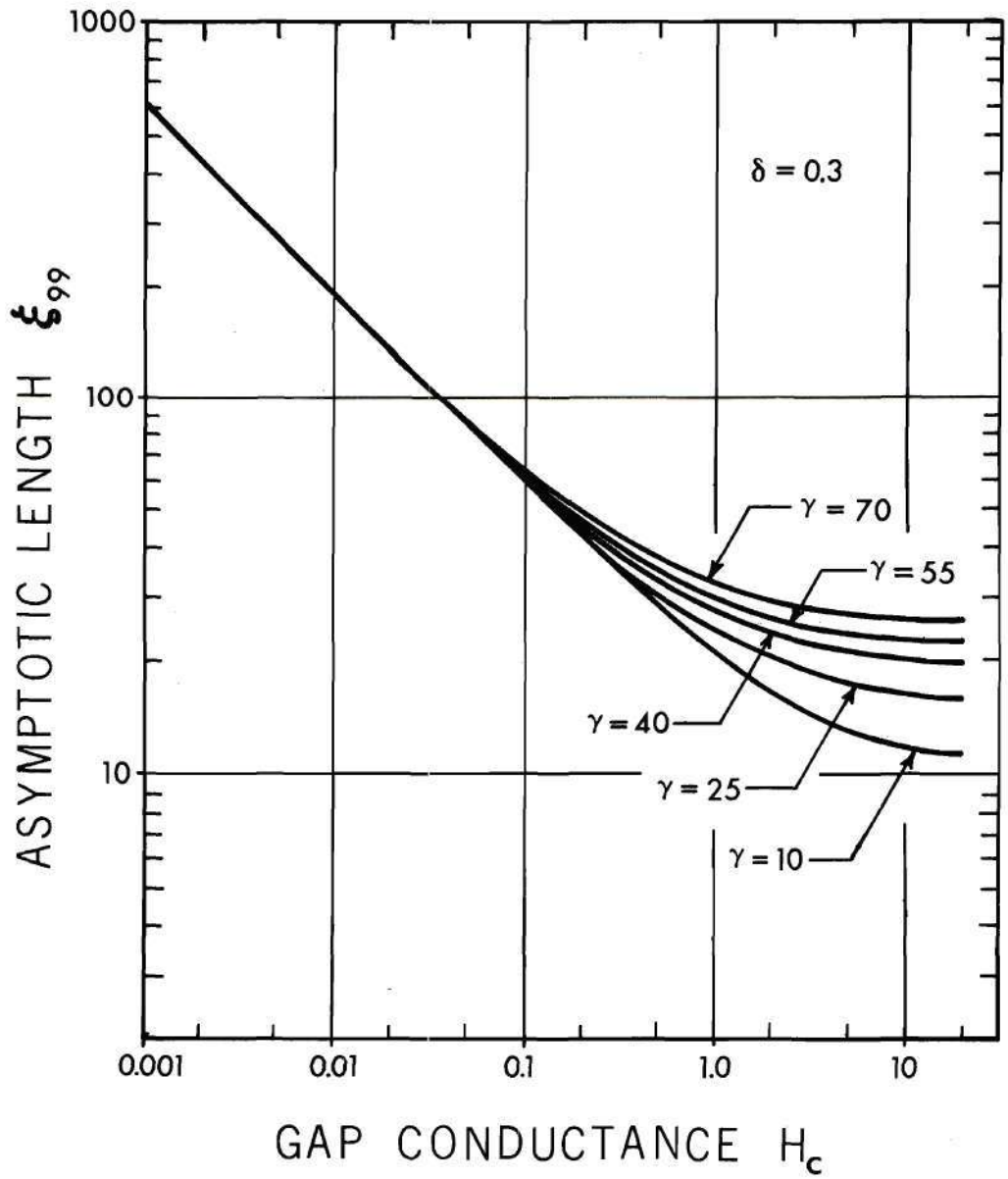

Figure 13. Asymptotic Length versus Gap Conductance for Various Conductivity Ratios

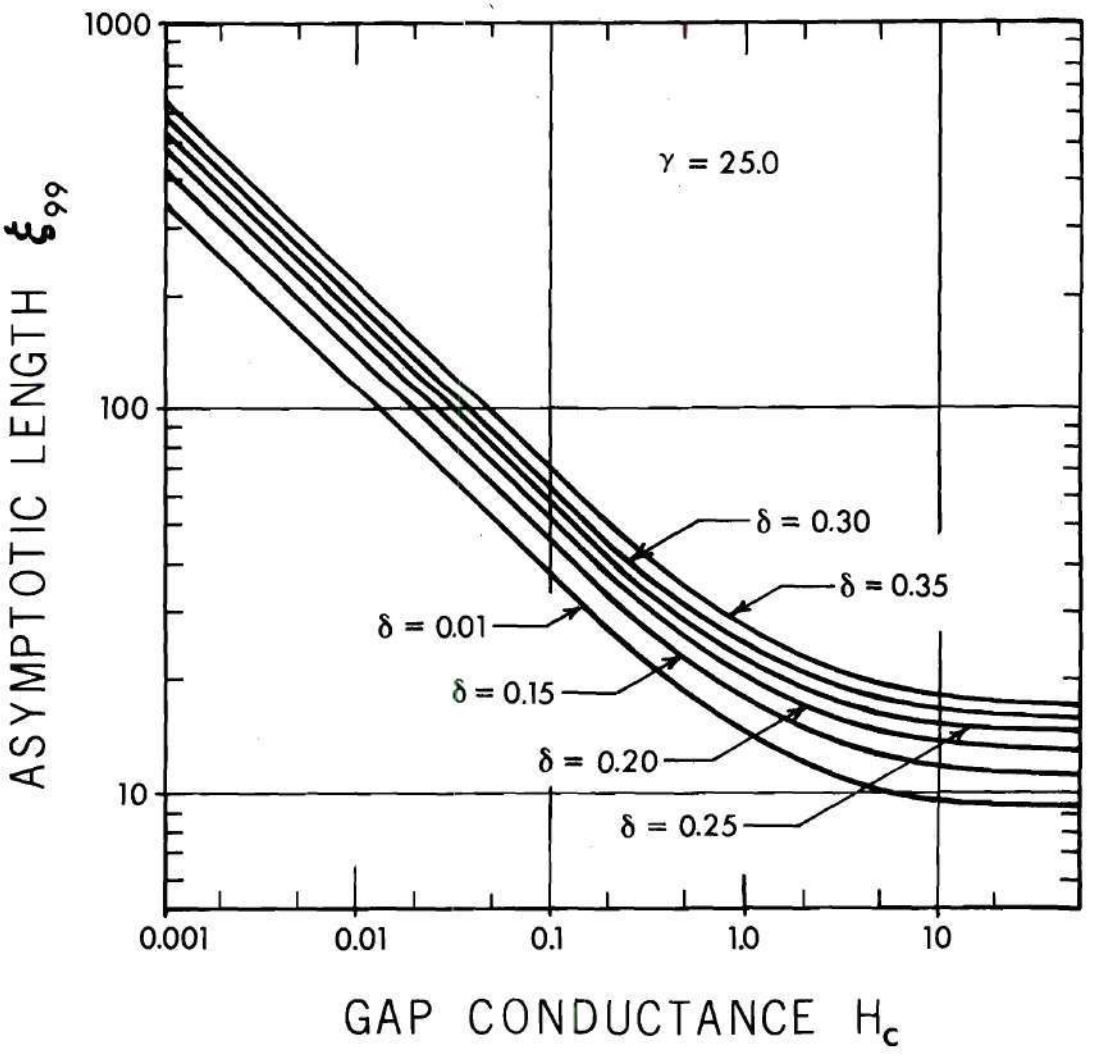

Figure 14. Asymptotic Length versus Gap Conductance for Various Fiber Radii

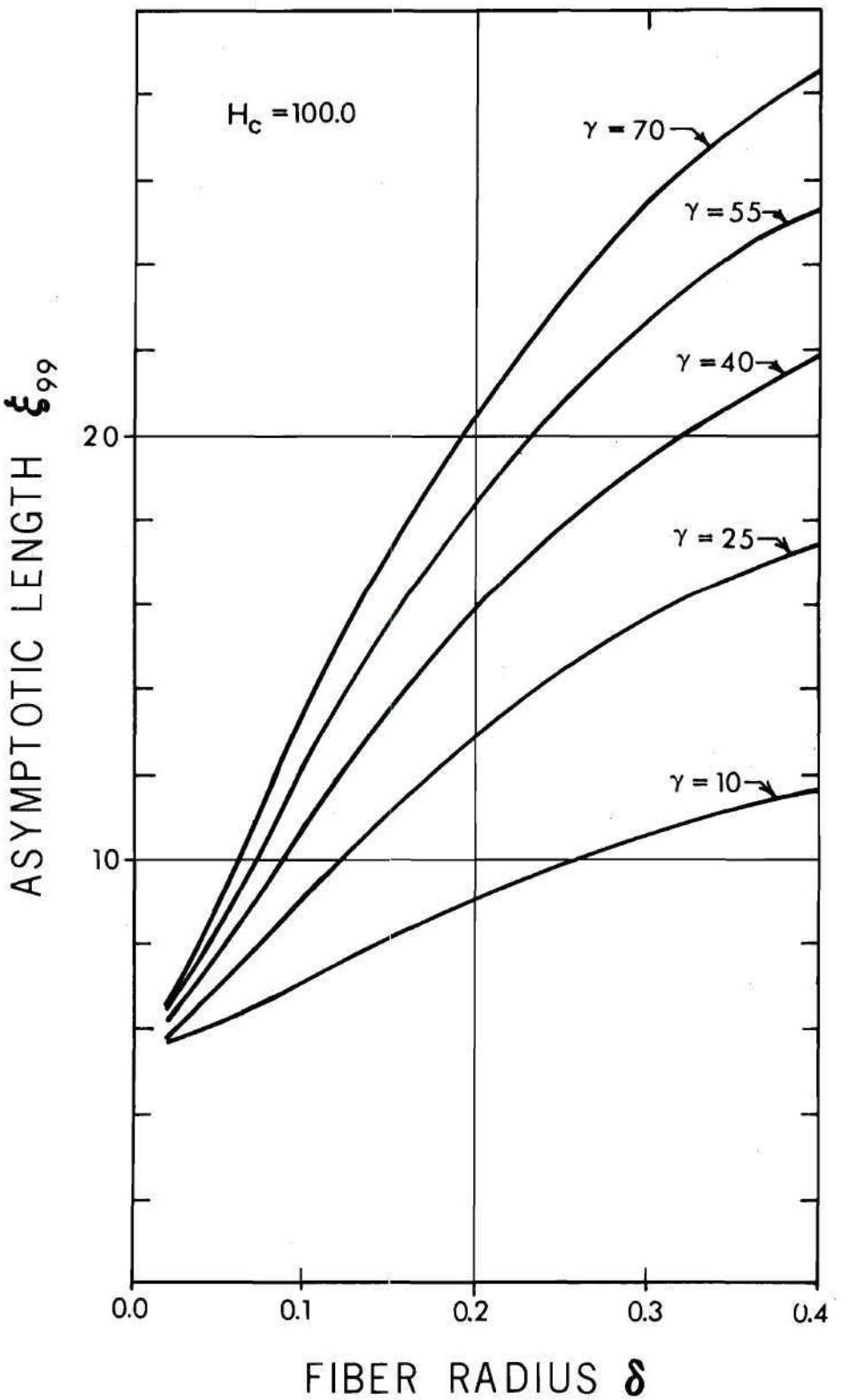

Figure 15. Asymptotic Length versus Fiber Radius for Various Conductivity Ratios

where $g(\delta)$ is an undetermined function of δ.

For $H_c > 20.0$, the dependence on H_c vanishes and the ξ_{99} relation reduces to a function depending on γ and δ. Figure 15 indicates that, in this region, ξ_{99} increases at a moderate rate for increasing γ or δ.

An important result of these calculations is that, in all cases, ξ_{99} is considerably less than the estimated value of ξ given in Table 3.

Figures 16 and 17 make a comparison between effective conductivity as a function of γ and δ^2 in the asymptotic region ($\xi = 1000$) and effective conductivity at a length slightly below the asymptotic ($\xi = 20$). The effective conductivities versus γ and δ^2 in the asymptotic region produce the straight line relations given by the formula in Table 8. Interestingly, the effective conductivity relations for $\xi = 20$ also appear as straight lines but with slightly reduced slope. This suggests that effective conductivity may be approximated reasonably well by a function of the following form

$$\frac{k^*(\xi,\gamma,\delta,H_c,\eta)}{k_2} \cong \phi(\xi,\gamma,\delta,H_c,\eta)\,\frac{k_U^*}{k_2} \tag{4.4}$$

where $\phi(\xi,\gamma,\delta,H_c,\eta)$ is a function which accounts for the reduced slope in a region near the asymptotic solutions. A function to satisfy the preceding approximation is obtained in Appendix D. The result of the derivation is the following formula:

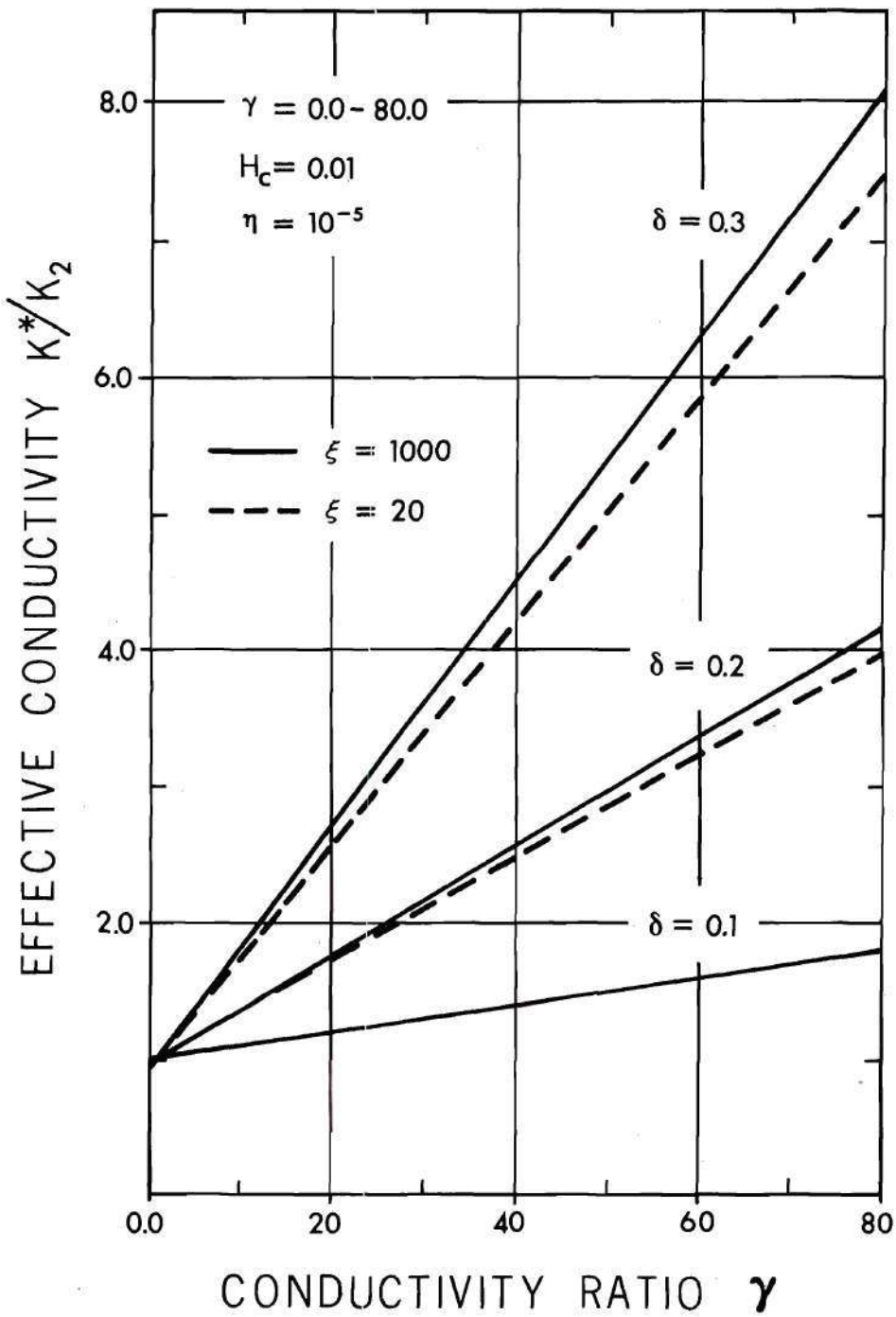

Figure 16. Effective Conductivity versus Conductivity Ratio for Various Fiber Radii (ξ = 20, 1000)

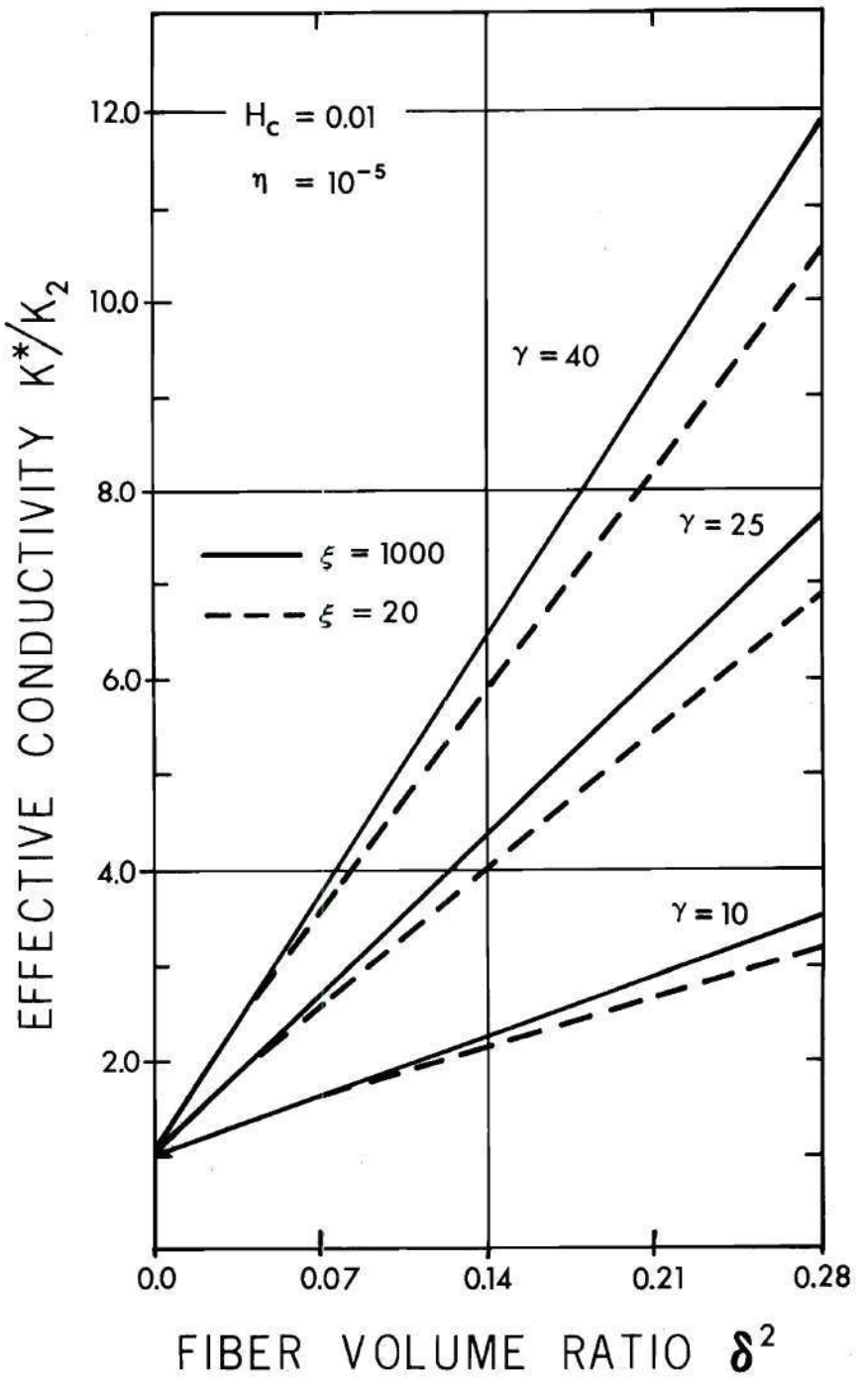

Figure 17. Effective Conductivity versus Fiber Volume Fraction for Various Conductivity Ratios (ξ = 20, 1000)

$$\phi(\xi,\gamma,\delta,H_c,\eta)=\frac{1-\left(\frac{\pi\delta}{2\xi}\right)^2\left[\frac{\gamma\ln\left(\frac{\pi\delta}{2\xi}\right)+\frac{\delta}{H_c}\left(1-\frac{1}{\delta^2}\right)}{(\gamma-1)\delta^2+1}\right]}{1-\left(\frac{\pi\delta}{2\xi}\right)^2\left[\frac{\eta\ln\left(\frac{\pi}{2\xi}\right)+\gamma\ln\delta+\frac{\delta^2}{H_c}\left(1-\frac{1}{\delta^2}\right)}{(\eta-1)\delta^2+1}\right]} \tag{4.5}$$

Equation 4.5 is based on an approximation which assumed the term, $\pi/2\xi$, is small. The formula cannot be expected to apply when this condition is unsatisfied.

Figures 18 and 19 compare the approximate formula to the exact for $H_c = 0.01$ and $H_c = 100$. These figures show the approximate formula consistently underestimates the exact value but converges to the upper asymptote at essentially the same point for large ξ. The approximate formula is somewhat closer to the exact in Figure 18. This is because the transition region occurs at a higher value of ξ. In Figure 18, it appears that the approximate formula converges to the same lower limit as the exact. Taking the limit of Eq. 4.5 as ξ goes to zero shows that this is not the case. Additional calculations for ξ smaller than those shown in Figures 18 and 19 confirm that the approximate formula diverges sharply from the lower asymptote. This failure does not detract from the major purpose of the formula, giving conservative estimates of conductivity near the upper asymptote.

The approximate formula can be substituted into the definition of asymptotic length, Eq. 4.1, to obtain an approximate relation for ξ_{99}. This derivation, performed in Appendix D, gives the following result:

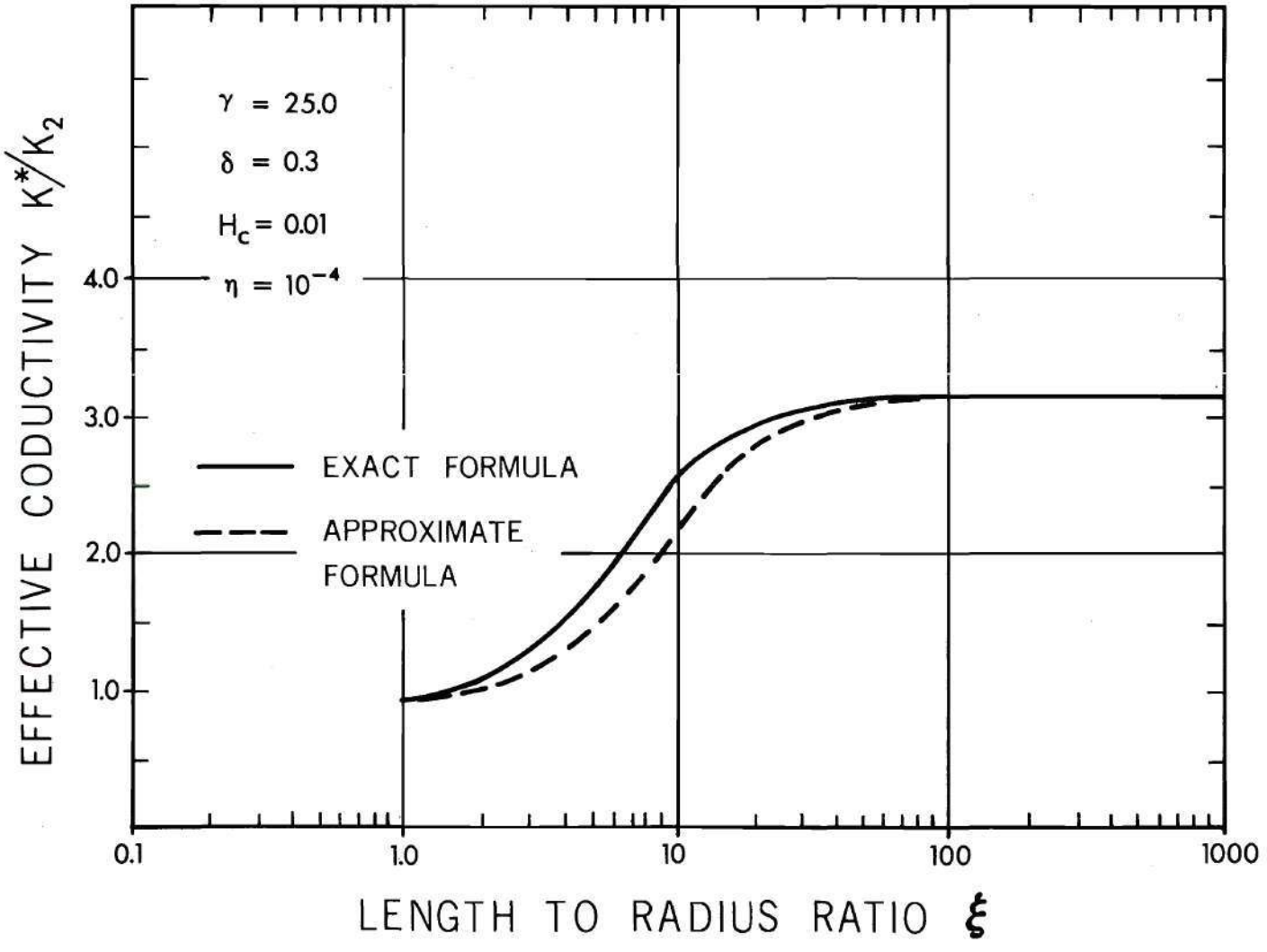

Figure 18. Effective Conductivity versus Length by Exact and Approximate Formulas (H_c = 0.01)

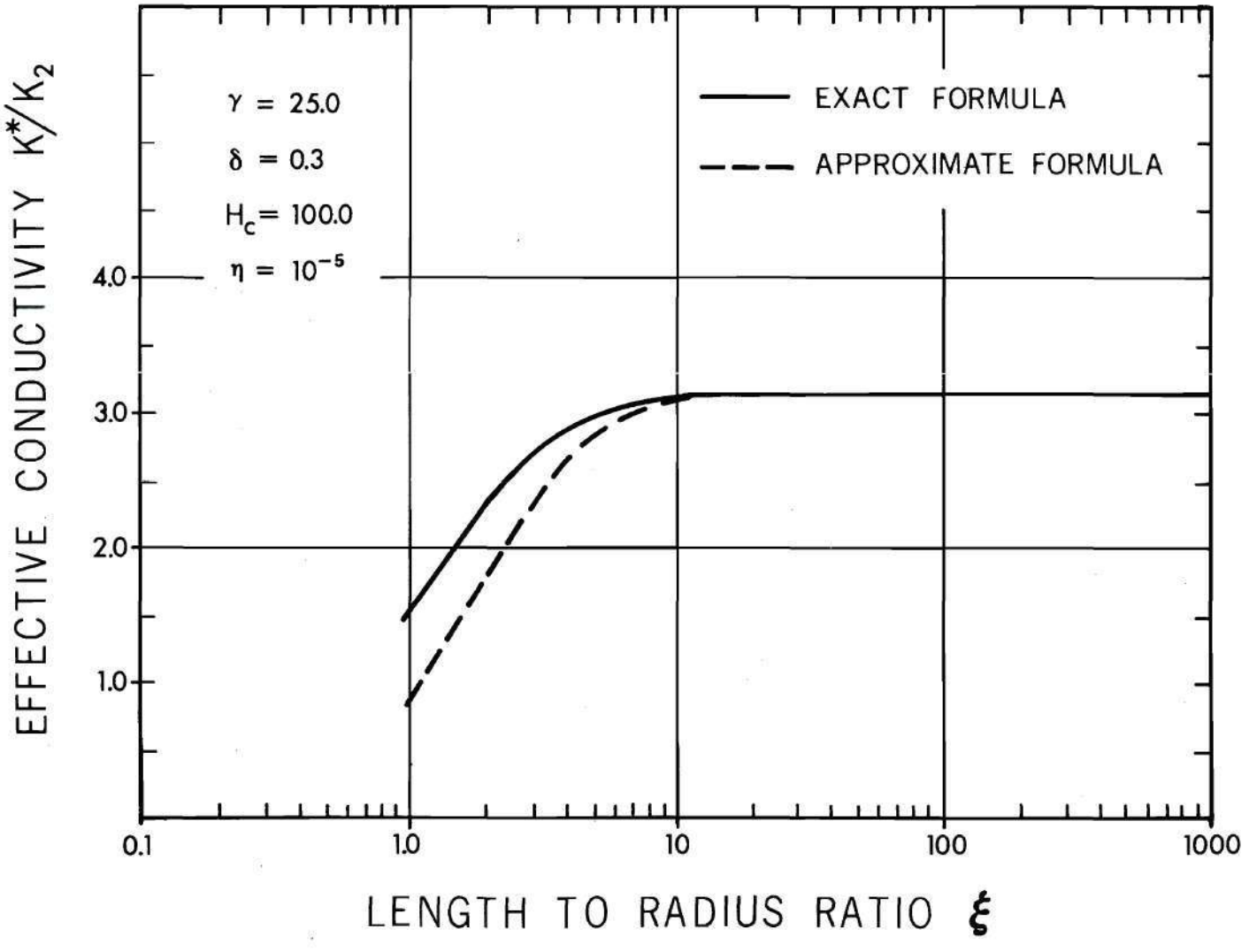

Figure 19. Effective Conductivity versus Length by Exact and Approximate Formulas (H_c = 100)

$$\frac{1-\left(\frac{\pi}{2\xi_{99}}\right)\ln\left(\frac{\pi}{2\xi_{99}}\right)}{1-\left(\frac{\pi\delta}{2\xi_{99}}\right)^2\left[\eta\ln\left(\frac{\pi}{2\xi_{99}}\right)+\gamma\ln\delta+\frac{\delta}{H_c}\left(1-\frac{1}{\delta^2}\right)\right]}=0.99 \qquad (4.6)$$

The heat content as a function of ξ is shown in Figures 20, 21, 22, and 23. The characteristic behavior of the function, decreasing from unity to a value determined by the asymptotic formula in Table 8, is generally due to the overall reduction in temperature from increased conductivity. Thus, the function is essentially reciprocal of effective conductivity. However, the heat content is a function which averages temperature over the volume of the cell, whereas the effective conductivity is determined by the temperature at a single point. For this reason, differences between the two are expected. These differences will be especially significant in discussing the effective volumetric heat capacity which is the product of heat content and effective conductivity.

Figure 20 shows the heat content for various values of the fiber-matrix volumetric heat capacity ratio, β. This parameter has little effect, primarily because the fiber volume fraction is rather small. The differences over the range $0.35 < \beta < 0.95$ are so small that the figure must be given as a single line.

Figures 21, 22, and 23 show heat content as a function of ξ for various values of γ, δ, and H_c. The transition region in these curves occurs in nearly the same range of ξ as in the corresponding effective conductivity curves. The asymptotes are seen to be correctly given by the

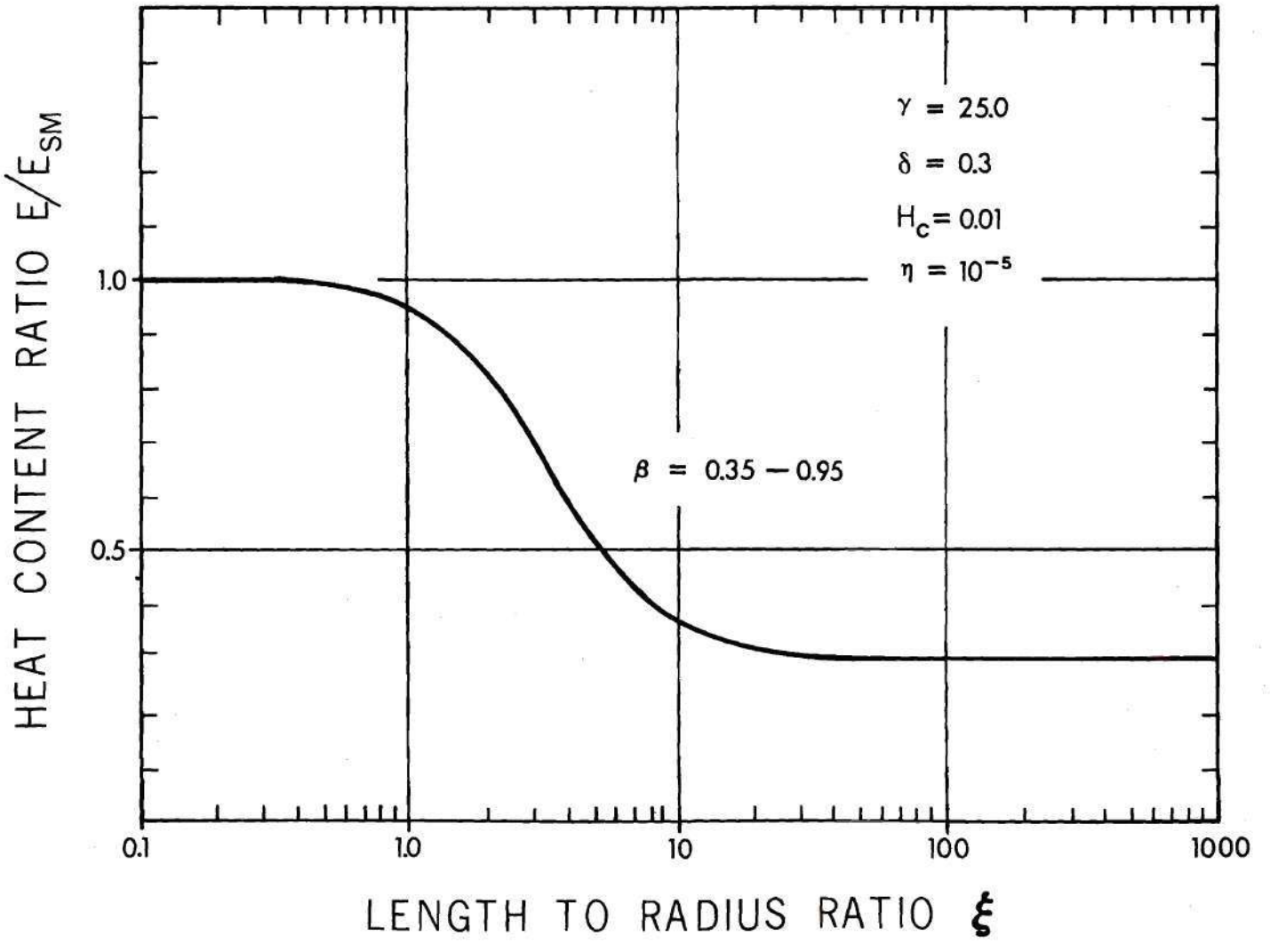

Figure 20. Heat Content versus Length for Various Volumetric Heat Capacity Ratios

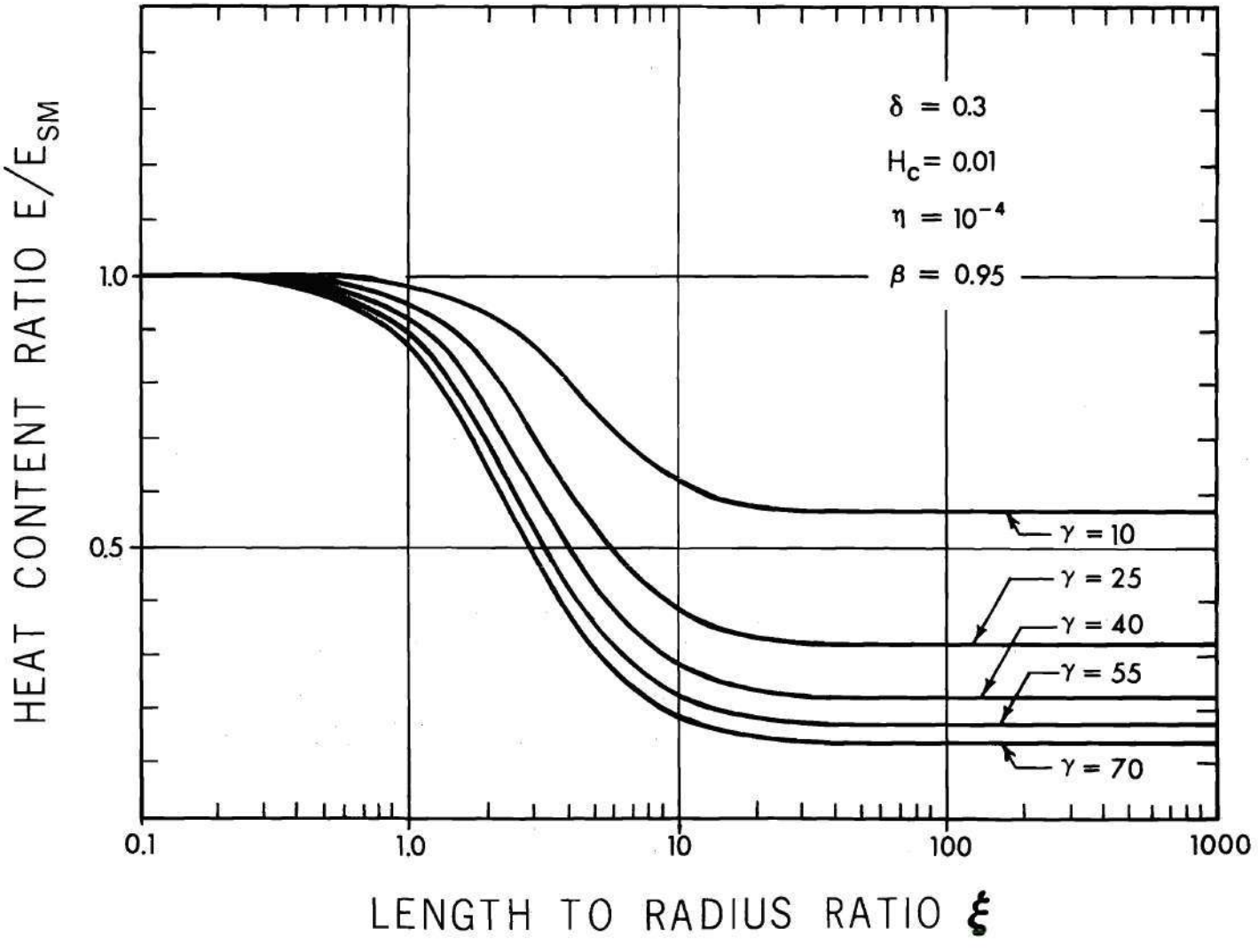

Figure 21. Heat Content versus Length for Various Conductivity Ratios

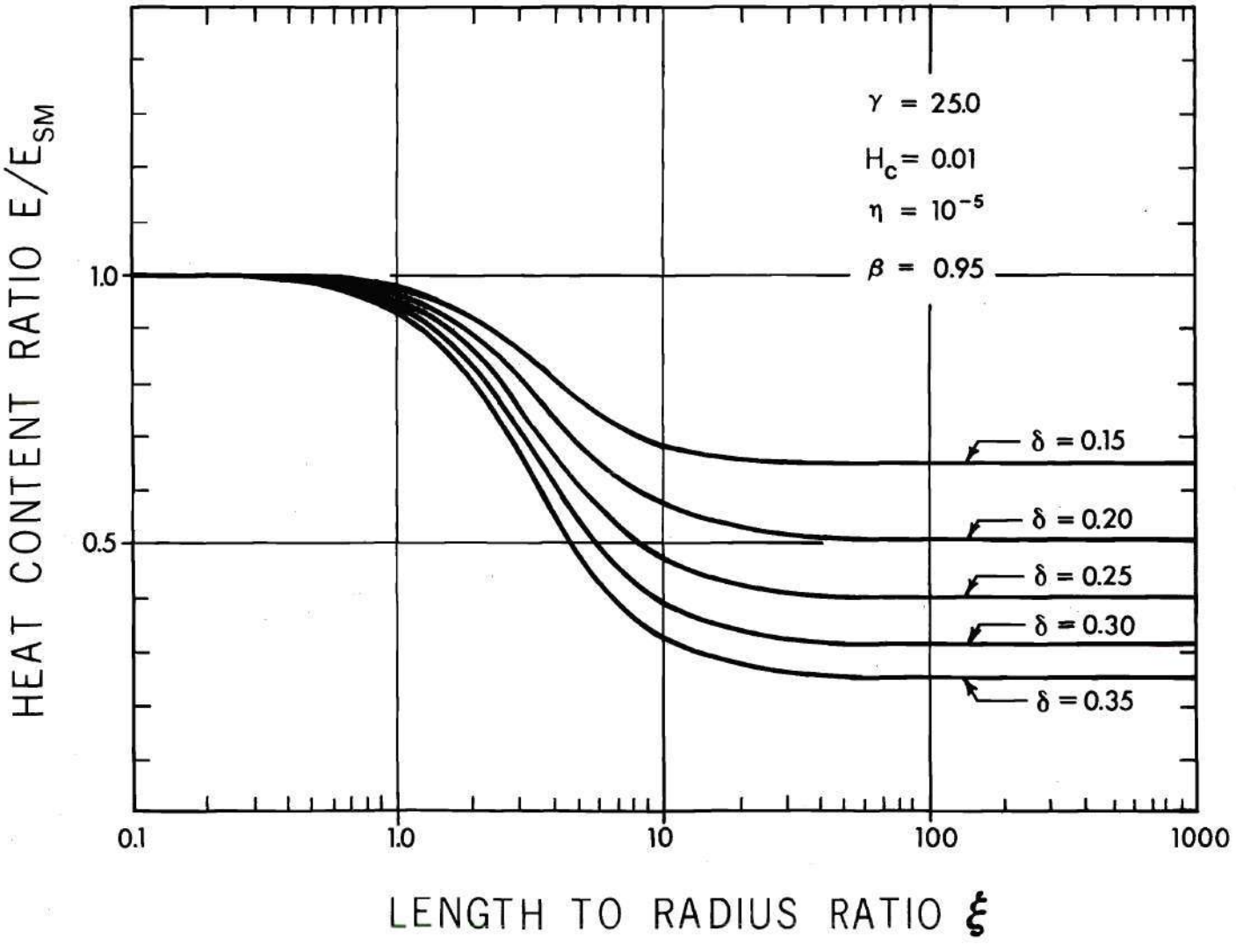

Figure 22. Heat Content versus Length for Various Fiber Radii

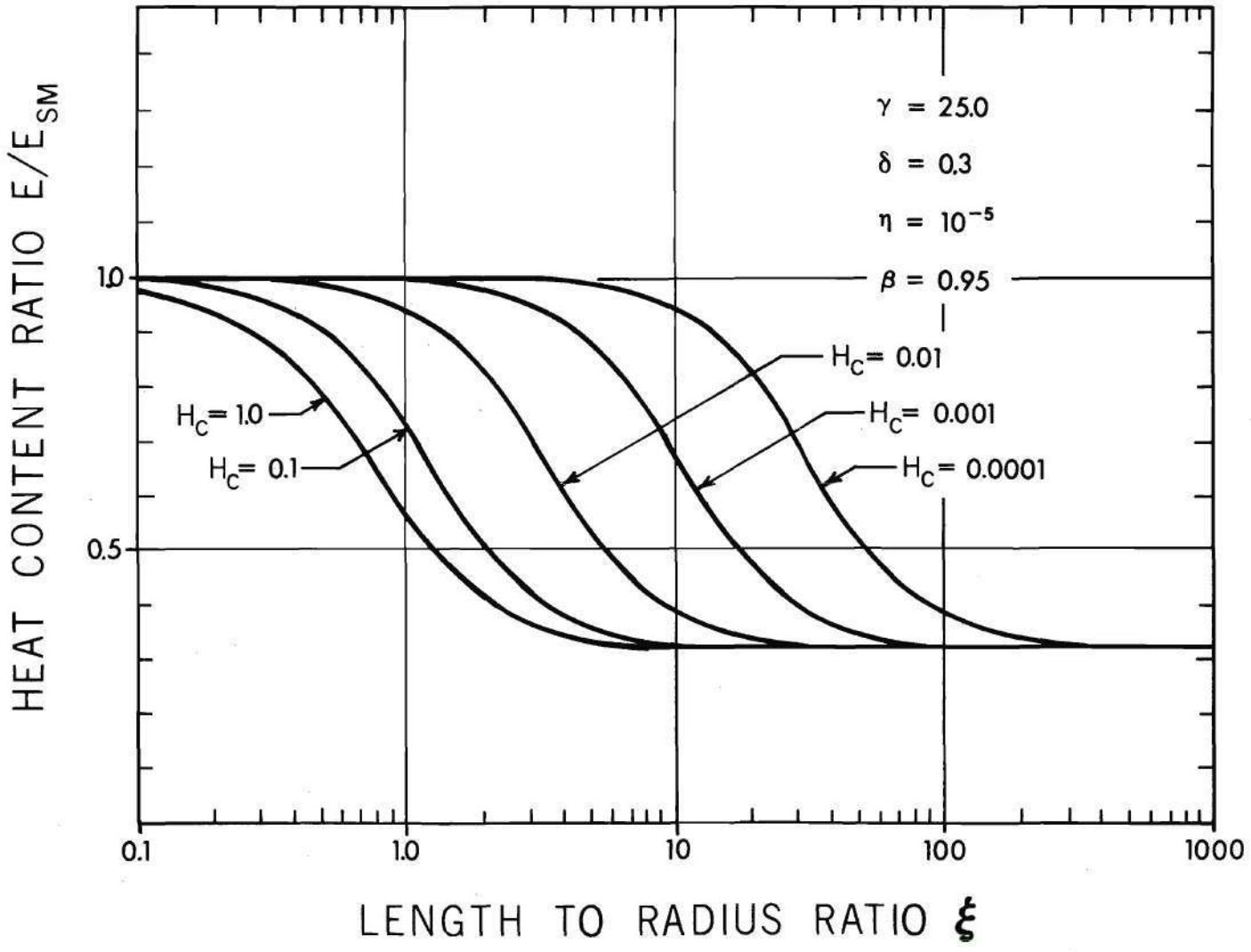

Figure 23. Heat Content versus Length for Various Gap Conductances

formulas in Table 8.

Effective volumetric heat capacities are shown in Figures 24 through 30. These curves are slightly different from those of heat content and effective conductivity in that the functions show minima and maxima within the transition region which are less than or greater than the asymptotes. Comparing Figures 24, 25, and 26, one notes that the magnitude and shape of these extremes are strongly dependent on H_c and γ. In Figure 24, the minimum at $\xi = 0.5$ is least apparent for $H_c = 0.01$ and is most apparent for $H_c = 100$. The maximum at $\xi = 20$ does not appear at all for $H_c = 100$ and is strongest for $H_c = 0.01$. Figures 25 and 26 show that the asymptotic solutions for effective volumetric heat capacities are independent of γ, but the extremes in the transition region become more pronounced as γ increases.

Figures 27 through 30 compare the dependence of effective volumetric heat capacity on δ and β for $H_c = 0.01$ and 100. As in Table 8, the lower asymptote depends on δ, and the upper asymptote on β and δ. The effect of H_c is similar to the dependence shown in Figure 24.

In all of the figures, effective volumetric heat capacities lie near unity, $0.85 < c^*/c_2 < 1.05$. This result is due primarily to the small fiber volume fraction and also to the volumetric heat capacities of the fiber and matrix being close to one another.

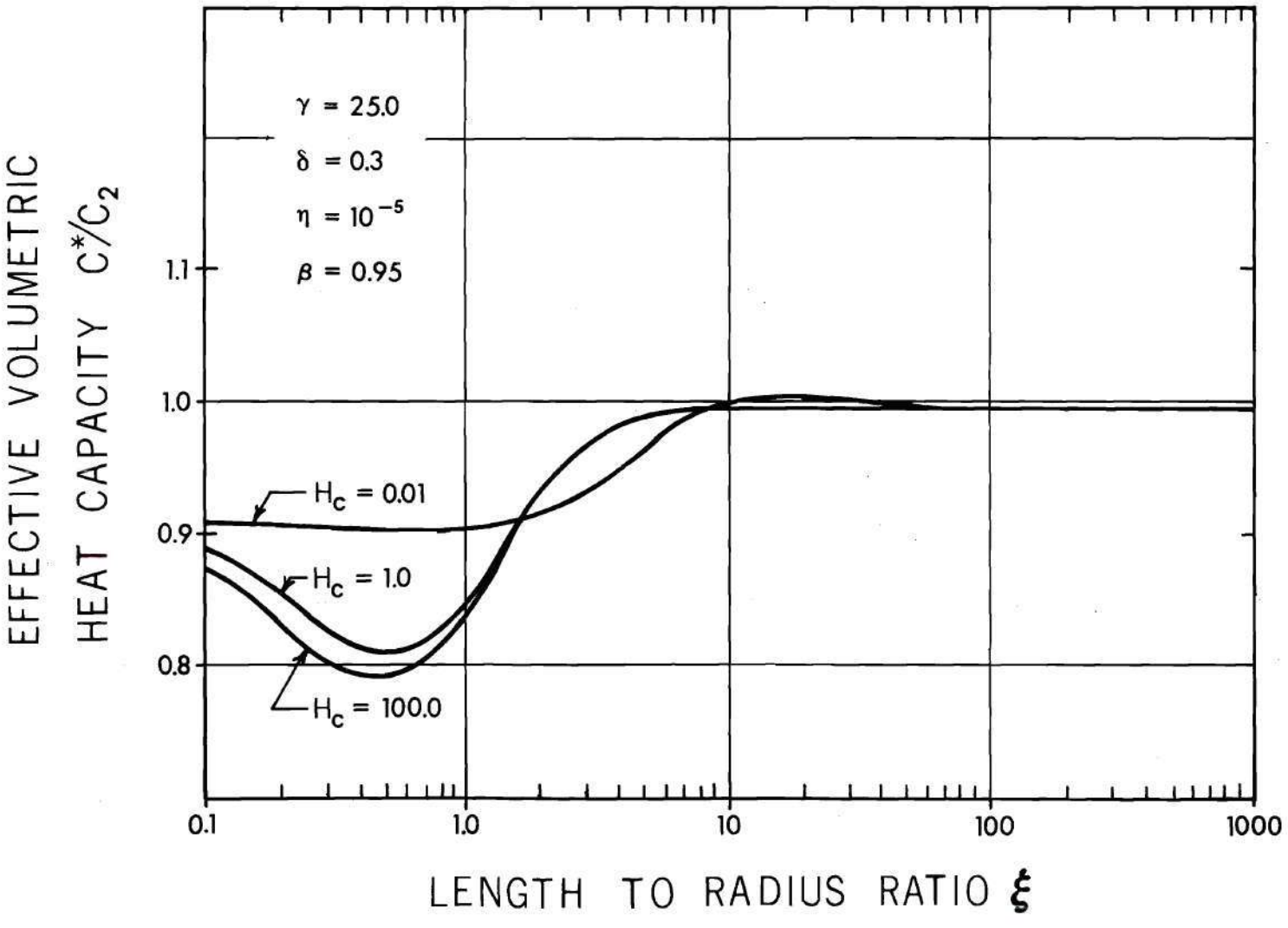

Figure 24. Effective Volumetric Heat Capacity versus Length for Various Gap Conductances

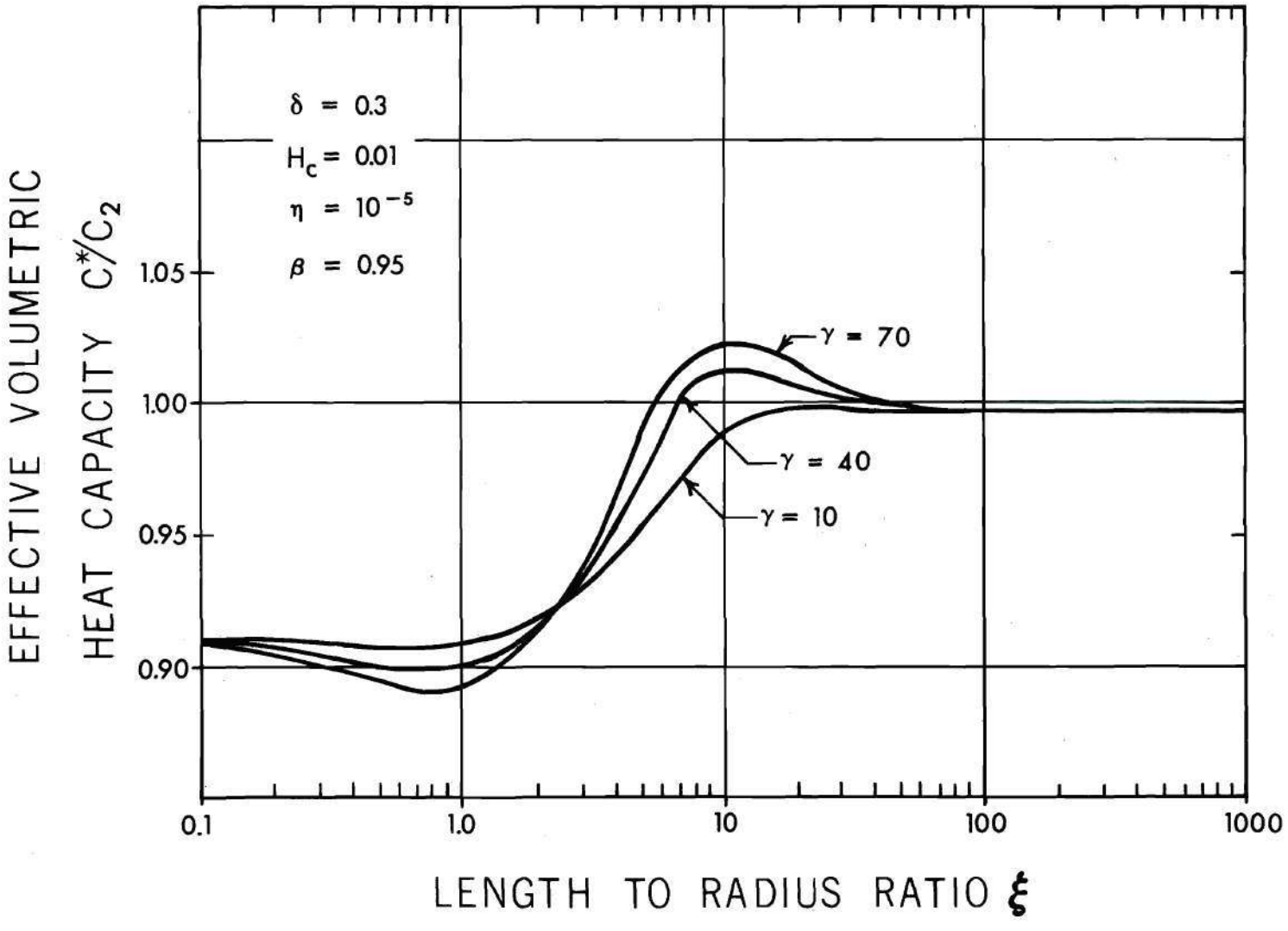

Figure 25. Effective Volumetric Heat Capacity versus Length for Various Conductivity Ratios (H_c = 0.01)

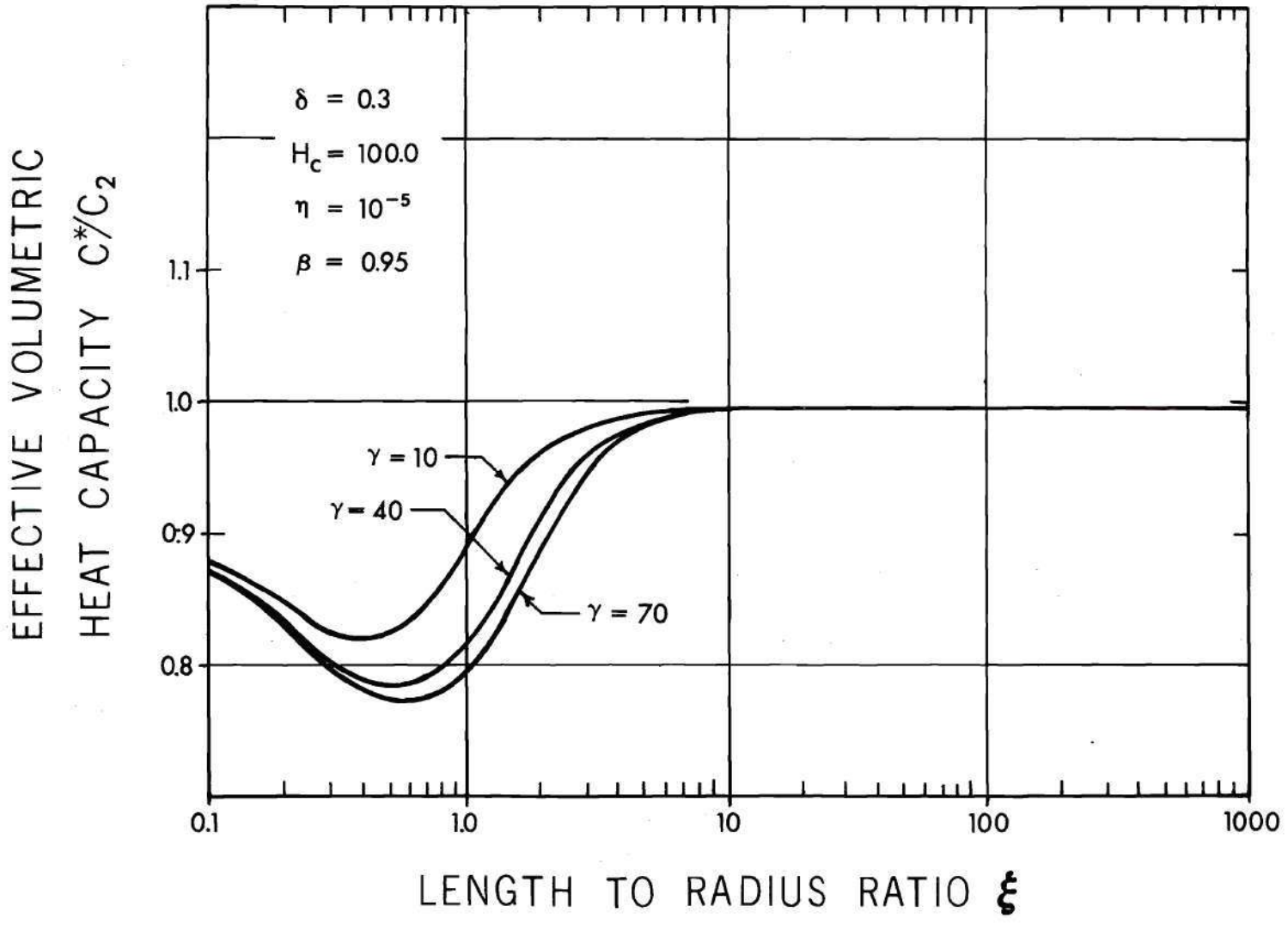

Figure 26. Effective Volumetric Heat Capacity versus Length for Various Conductivity Ratios (H_c = 100)

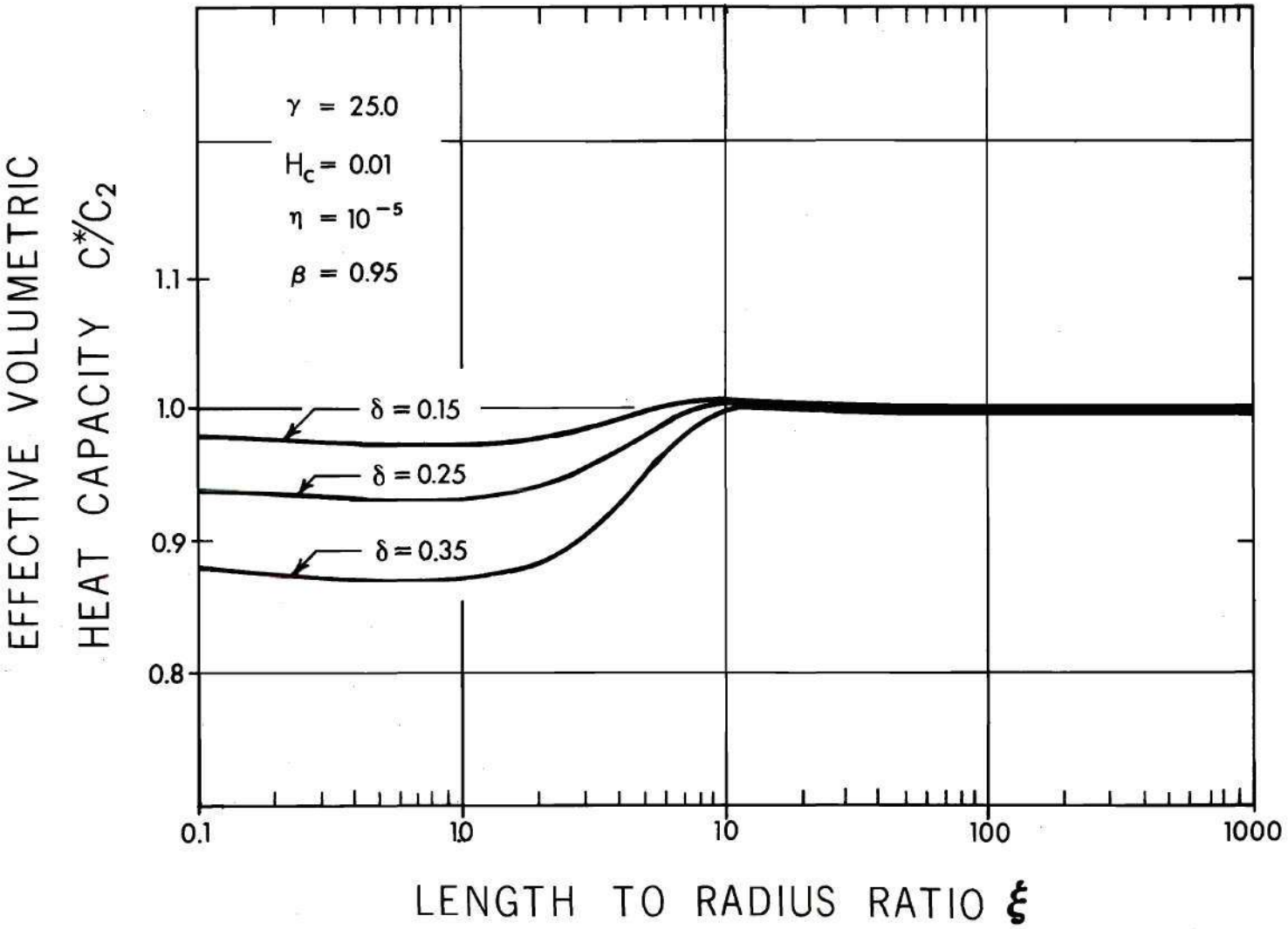

Figure 27. Effective Volumetric Heat Capacity versus Length for Various Fiber Radii (H_c = 0.01)

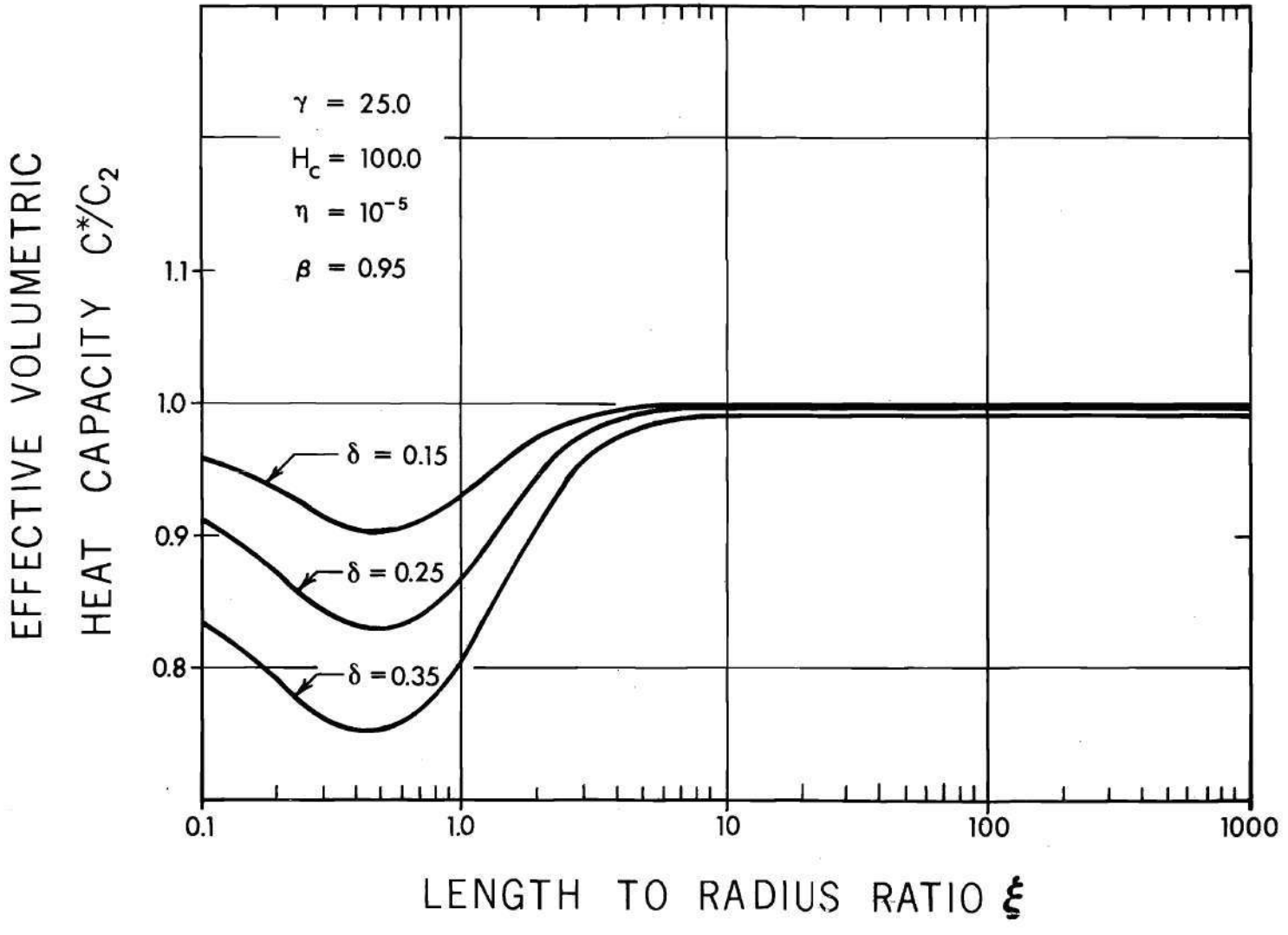

Figure 28. Effective Volumetric Heat Capacity versus Length for Various Fiber Radii (H_c = 100)

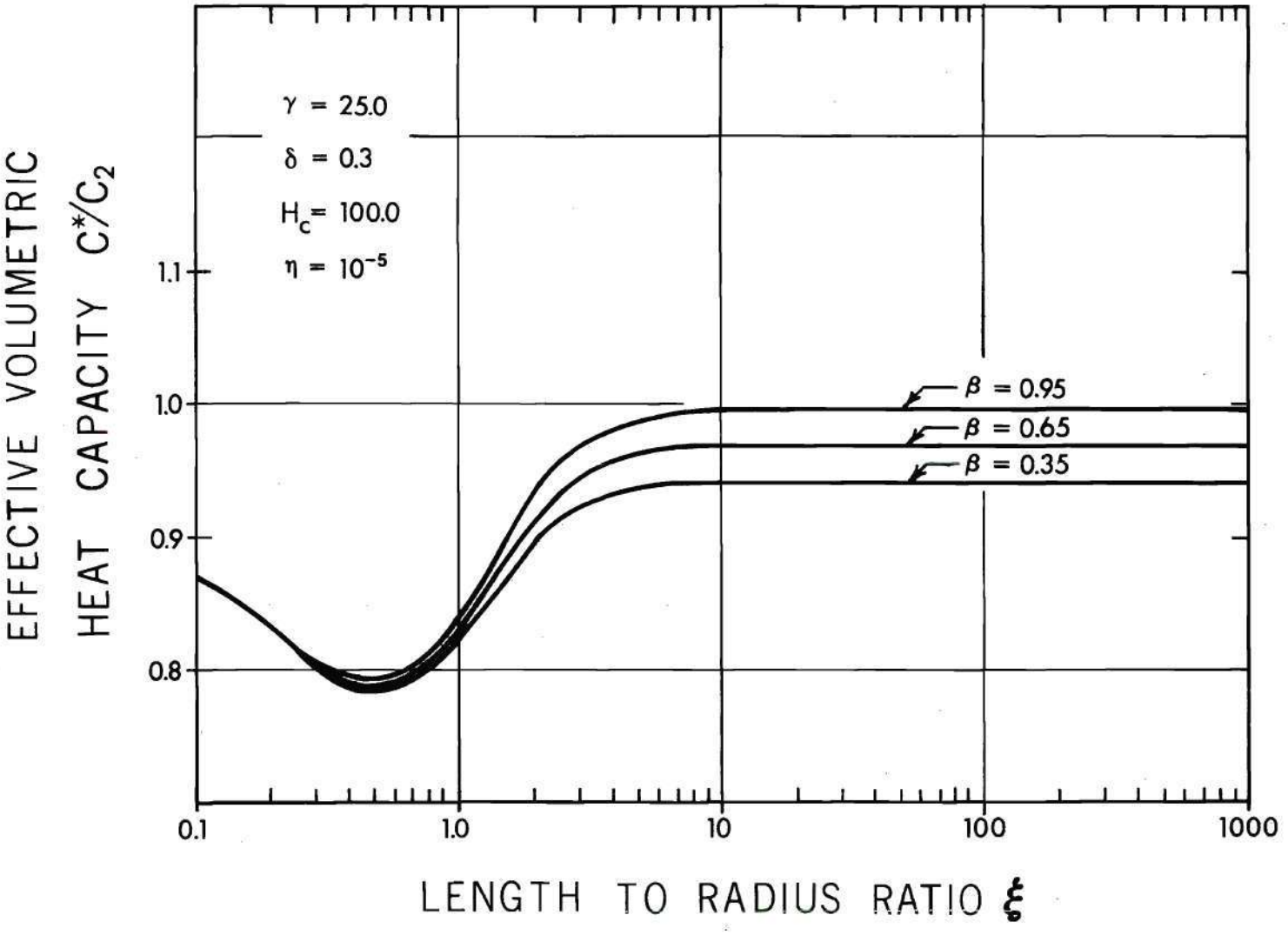

Figure 29. Effective Volumetric Heat Capacity versus Length for Various Volumetric Heat Capacity Ratios (H_c = 0.01)

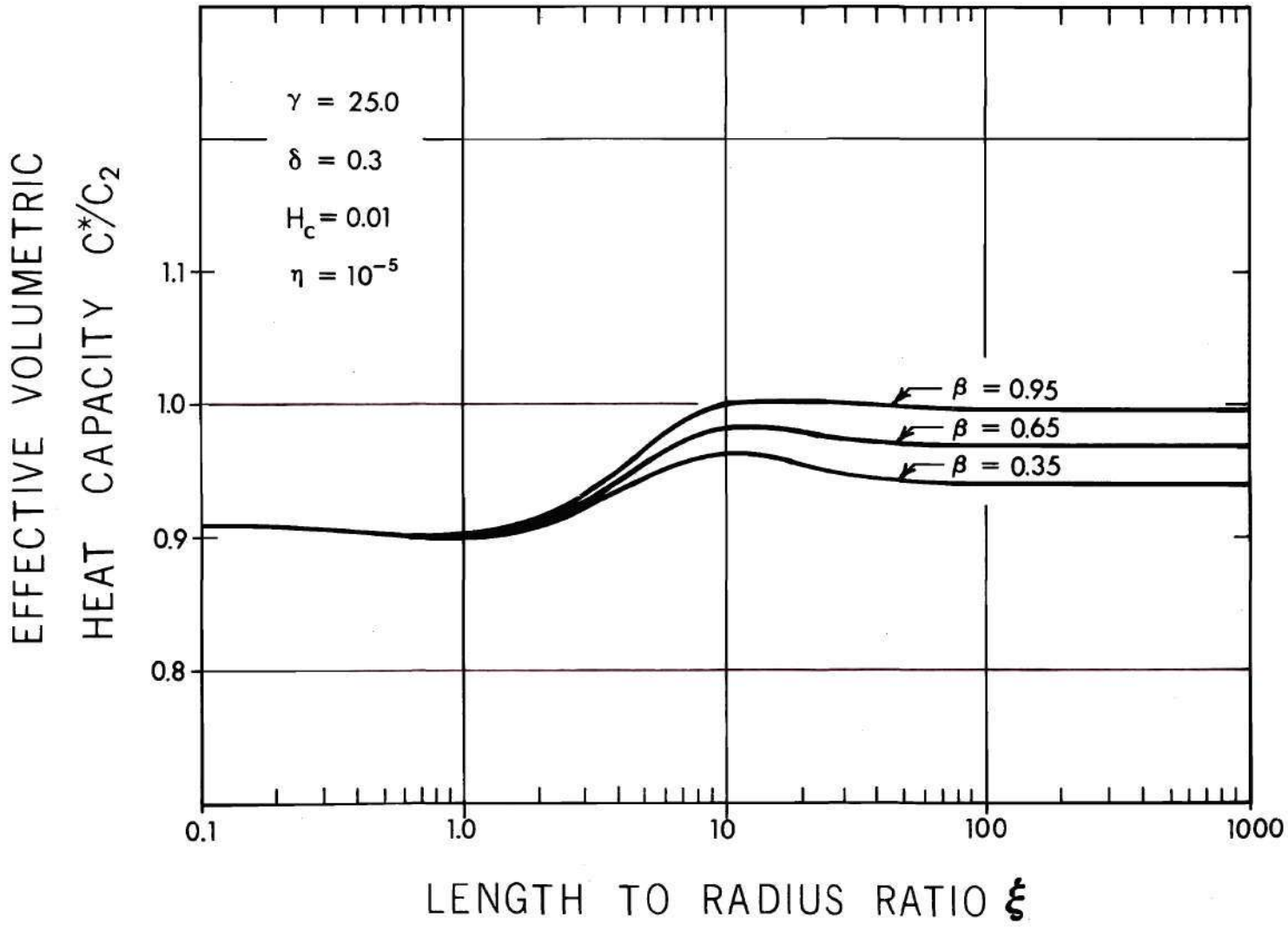

Figure 30. Effective Volumetric Heat Capacity versus Length for Various Volumetric Heat Capacity Ratios (H_c = 100)

Temperature Distributions

Constant temperature lines or isotherms are chosen to illustrate temperature distributions in composite cells. In addition, heat flux lines are shown in some figures to help visualize the direction of heat flow. Figures 31, 32, and 33 show isotherms and heat flux lines for cells in the lower asymptotic, transition, and upper asymptotic regions, respectively. The heat flux lines are actually normal to the isotherms but do not appear so in the figures because the axial scale is different from the radial scale.

In Figure 31, the isotherms bend abruptly at the fiber-matrix interface. The temperature of the fiber is almost uniformly zero. In Figure 32, the temperature of the fiber is increased. Also, one notes that the gap conductance, $H_c = 0.5$, produces a considerable temperature discontinuity across the interface. In Figure 33, the temperature is uniform in radial direction. The heat flux lines in Figures 31, 32, and 33 can be used to evaluate the effectiveness of the fiber in conducting heat. The heat flux lines intersecting the fiber-matrix interface at $\zeta = \xi$ enclose a volume in which the heat generated passes out of the cell through the fiber. Comparing this heat flux line in Figures 31, 32, and 33 shows that the volume enclosed becomes progressively larger for longer cells. The fraction of heat flowing into the fiber approaches a maximum as the temperature distribution becomes uniform in the radial direction. Hence, the heat flux in the fiber becomes "saturated." On the other hand, for small ξ, very little heat flows radially. Short cells behave as if the fiber and matrix are insulated from one another. This discussion suggests a means for evaluating the limiting temperature functions. The limiting

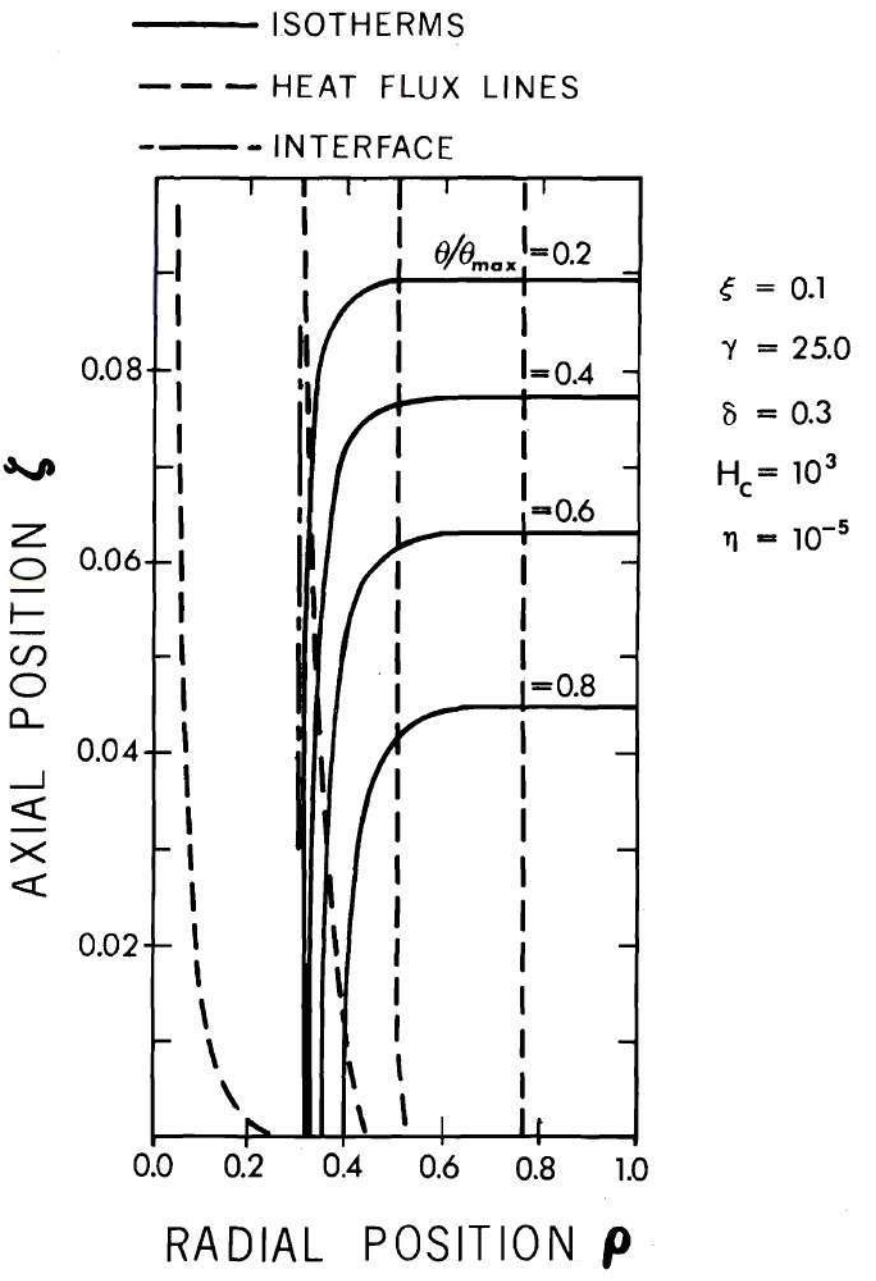

Figure 31. Isotherms and Heat Flux Lines for Small Length ($\xi = 0.1$)

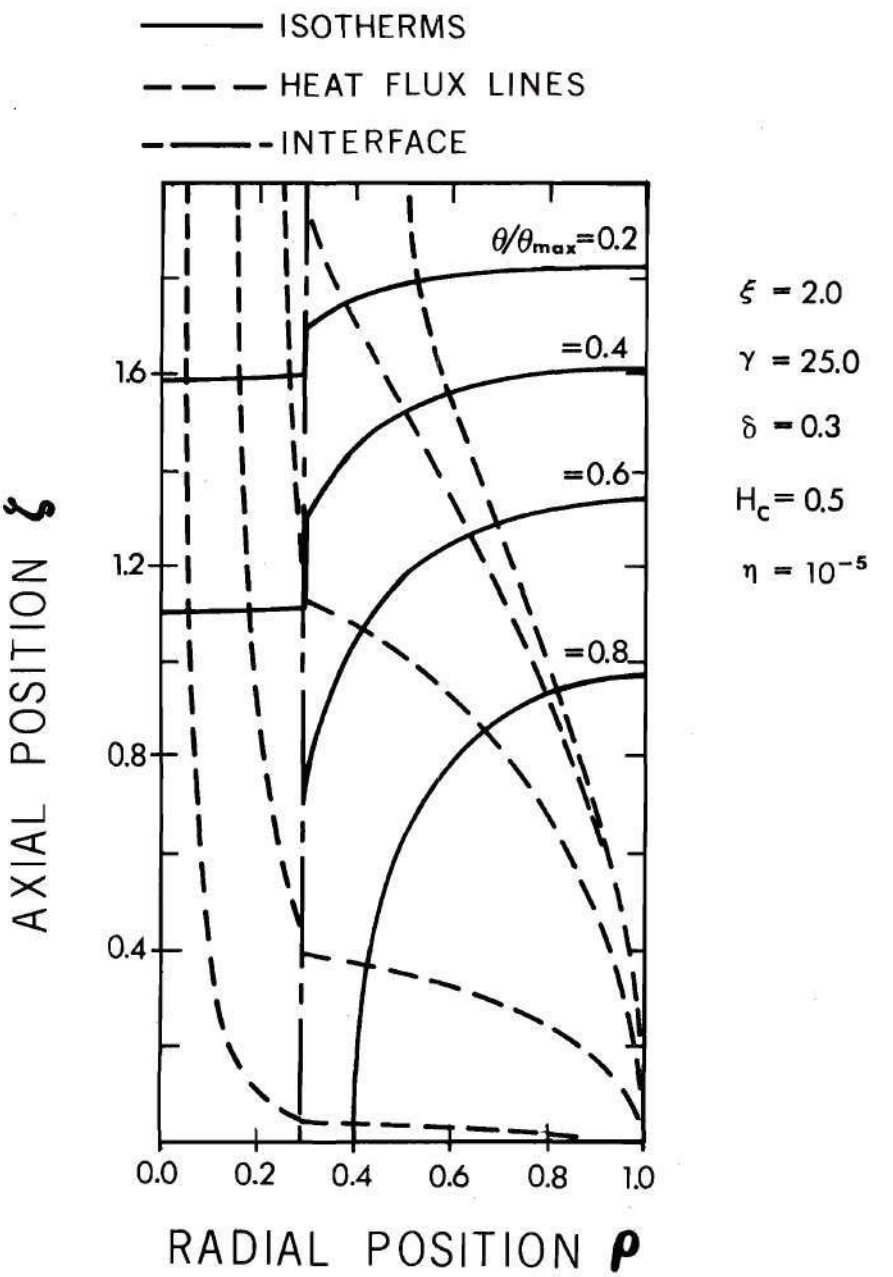

Figure 32. Isotherms and Heat Flux Lines for Intermediate Length (ξ = 2.0)

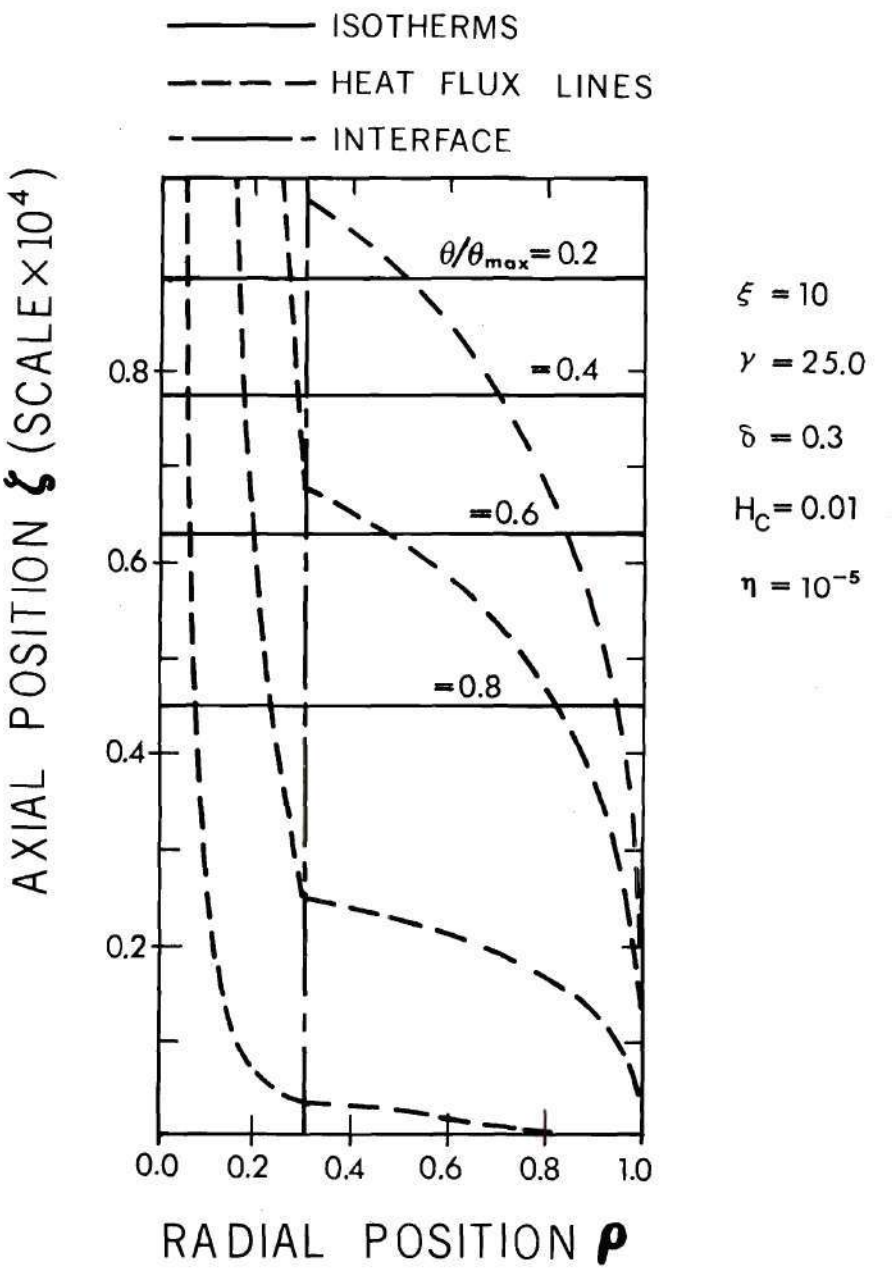

Figure 33. Isotherms and Heat Flux Lines for Large Length ($\xi = 10^4$)

temperature function for large ξ must be independent of the radial coordinate. This is achieved by artificially redistributing the heat generation in the fiber and matrix so that $\eta = \gamma$. The limiting temperature functions for large ξ are given by Eq. 4.7.

$$\text{(Large } \xi\text{)} \qquad \theta_1 = \theta_2 = \frac{1}{2\pi\xi} \frac{(\xi^2 - \zeta^2)}{[(\gamma-1)\delta^2+1]} \tag{4.7}$$

The limiting temperature function for small ξ is obtained by assuming the fiber and matrix are insulated, $H_c = 0$. The temperature functions are the following:

$$\text{(Small } \xi\text{)} \qquad \theta_1 = \frac{\eta}{2\pi\xi\gamma} \frac{(\xi^2 - \zeta^2)}{[(\gamma-1)\delta^2+1]} \tag{4.8}$$

$$\theta_2 = \frac{1}{2\pi\xi} \frac{(\xi^2 - \zeta^2)}{[(\eta-1)\delta^2+1]} \tag{4.9}$$

These limiting temperature functions are used to obtain the asymptotic formulas in Table 8.

It is well to admit that artificially changing a parameter to obtain the limiting temperature functions is not a mathematically rigorous method. However, the changes are motivated by sound reasoning, and the functions obtained are the same as those obtained by formally taking the limit as ξ goes to zero or infinity.

As stated previously, it is possible to define an equivalent homogeneous cell with conductivity equal to the effective conductivity of the corresponding composite cell. The temperature function of the equivalent

material is a parabola whose maximum is equal to the composite maximum temperature. Figure 33 verifies that, for large ξ, the composite temperature distribution is independent of the radial coordinate, as in the equivalent material. Figure 34 illustrates that the axial dependence is parabolic by showing that the normalized temperature versus the square of the normalized axial coordinate plots as a straight line. Thus, for large ξ, the temperature functions for composite and equivalent homogeneous cells become identical.

Two additional temperature distributions are given to explain the extremes in effective volumetric heat capacity. As mentioned previously, the heat content, defined in Eq. 3.126, is ratio of average temperatures of the composite to solid matrix cells. The effective conductivity, from Eq. 3.121, is the ratio of maximum temperatures of solid matrix to composite cells. Thus, the effective volumetric heat capacity is the ratio of average-to-maximum temperature in the composite divided by the ratio of average-to-maximum temperature in the solid matrix. By this interpretation, effective volumetric heat capacity of two cells can be compared by visually comparing the areas enclosed by the isotherms. Comparing Figure 35 to Figure 31, one sees that the average-to-maximum temperature is considerably less in Figure 35. This gives rise to the minimum in effective volumetric heat capacity observed at $\xi = 0.5$ in Figure 28.

Comparing Figure 36 to Figure 33 reveals that the isotherms in the matrix in Figure 36 are nearly independent of the radial coordinate to the edge of the fiber and are shifted toward the top of the cell with respect to the corresponding isotherms in Figure 33. Because of the higher relative temperatures in the matrix, the net effect is that the average-to-

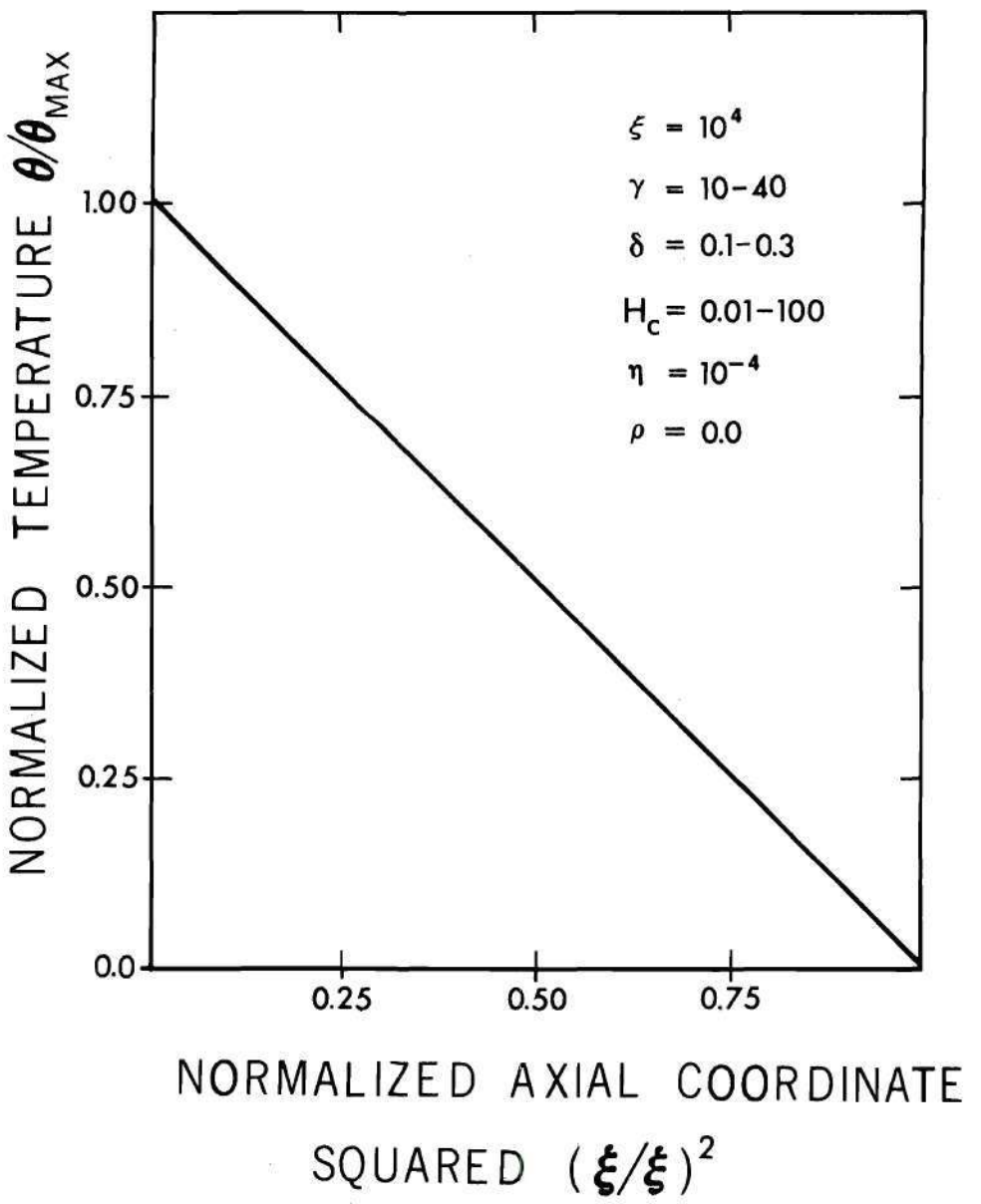

Figure 34. Normalized Temperature versus Square of Normalized Axial Coordinate

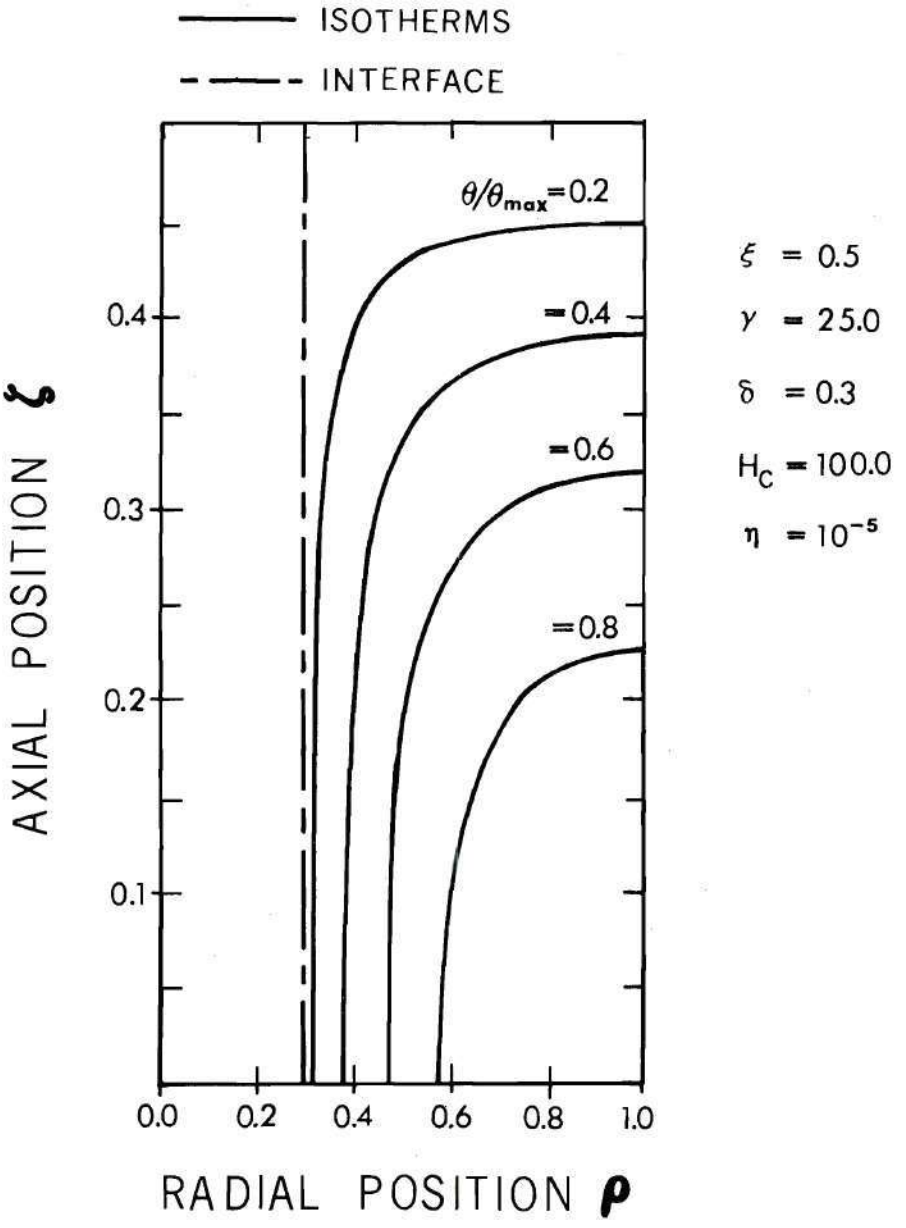

Figure 35. Isotherms for Small Length (ξ = 0.5)

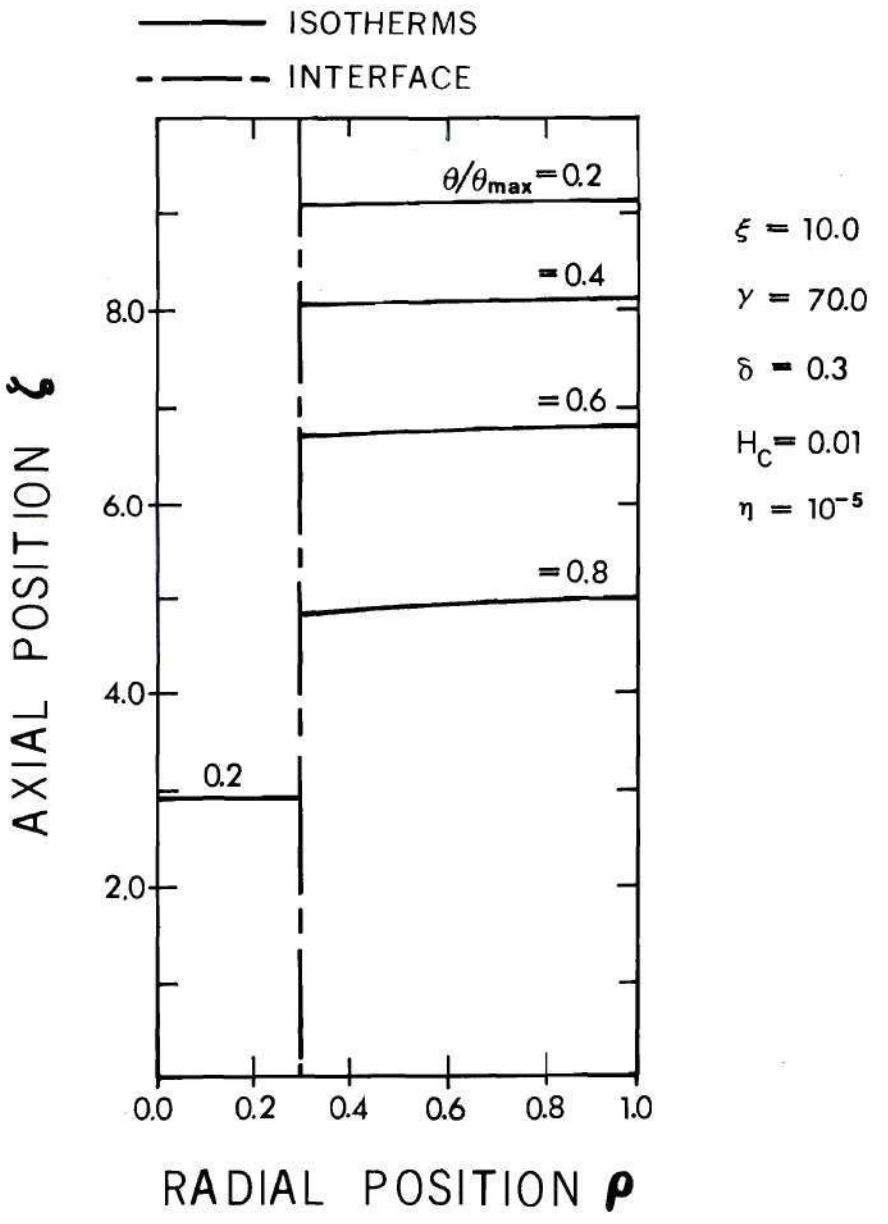

Figure 36. Isotherms for Intermediate Length (ξ = 10)

maximum temperature ratio is greater in Figure 36. This effect accounts for the maximum in the effective volumetric heat capacity that is shown at $\xi = 10$ in Figure 26.

Linear Conductivity

Two definitions for analyzing the enhancement of conductivity for the linear conductivity problem are proposed. The first, given by Eq. 3.134, is the ratio of maximum temperatures of solid matrix and composite cells. This quantity is referred to as the effective conductivity. Equation 3.137 proposed an alternate definition which accounts for the linear dependence of conductivity in the calculated quantity. This quantity is referred to as the effective linear conductivity.

Figure 37 shows the effective conductivity as a function of ξ. The sharp divergence from the constant conductivity asymptote at large ξ is due to the substantial changes in the linear conductivity term $(1 + \epsilon_\theta \theta_{SM})$ in the solid matrix cell. Table 9 lists the linear conductivity term for both the composite and solid matrix. One can see that Eq. 3.134 becomes invalid because the maximum temperature in the solid matrix exceeds the acceptability criterion for linear conductivity, Eq. 3.117, while the maximum temperature of the composite is still within the reasonable range.

This difficulty is reduced in the effective linear conductivity. Figure 38 shows that the effective linear conductivity does not produce an asymptotic solution for large ξ, but it diverges far less than the quantity shown in Figure 37.

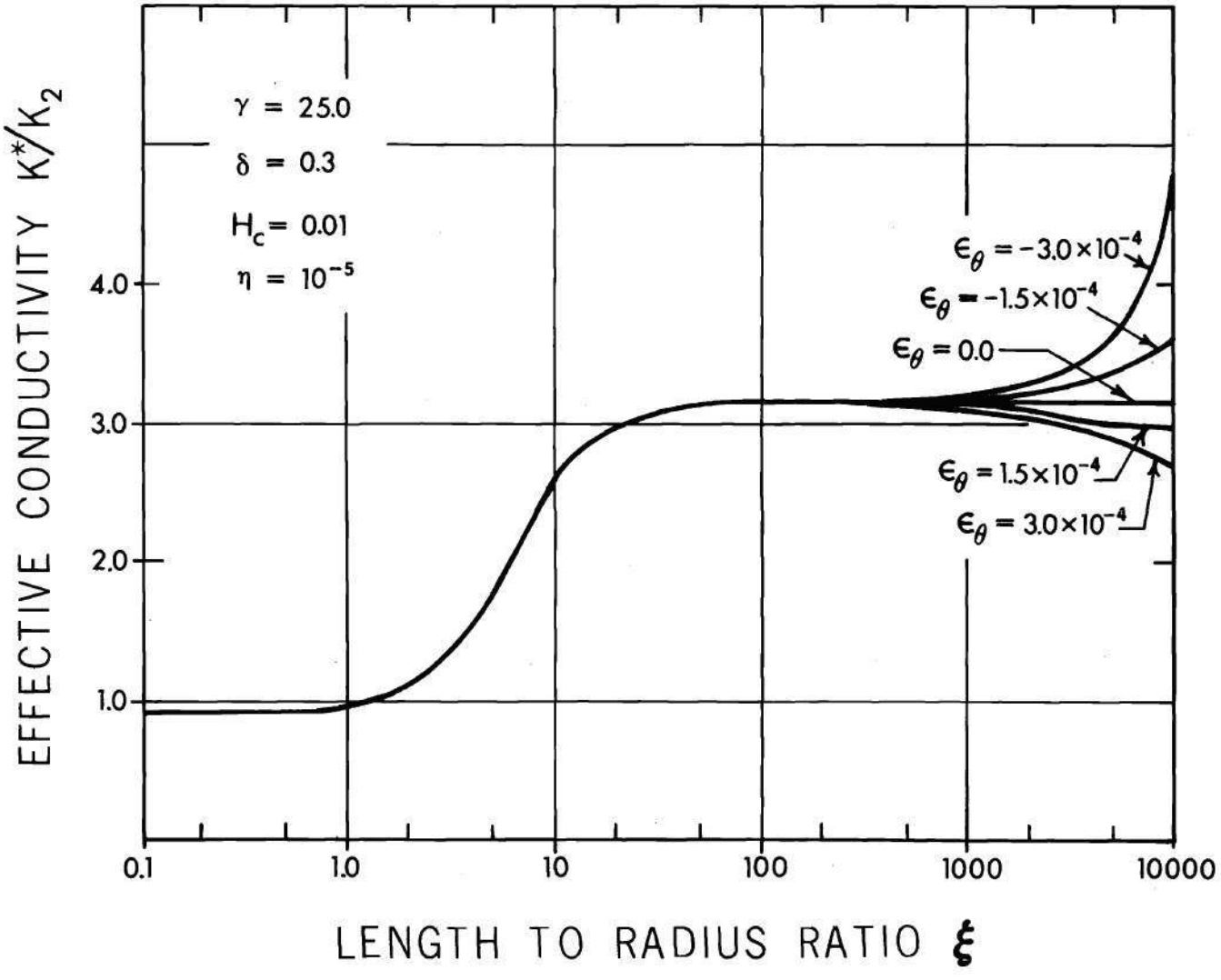

Figure 37. Effective Conductivity versus Length for Various Linear Coefficients

Table 9. Comparison of Linear Conductivity Term for Composite and Solid Matrix Cells

ξ	$[1+\epsilon_\theta\theta_{SM}]_{max}$ $\epsilon_\theta=-3.0\times10^{-4}$	$[1+\epsilon_\theta\theta_{comp}]_{max}$ $\epsilon_\theta=-3.0\times10^{-4}$	$[1+\epsilon_\theta\theta_{SM}]_{min}$ $\epsilon_\theta=3.0\times10^{-4}$	$[1+\epsilon_\theta\theta_{comp}]_{max}$ $\epsilon_\theta=3.0\times10^{-4}$
1.0	0.99995	0.99995	1.00005	1.00003
10.0	0.99952	.99982	1.00047	1.00017
100.0	0.99521	.99860	1.00476	1.00140
1000.0	0.95106	.98606	1.04666	1.0138
2000.0	0.89945	.97214	1.09132	1.0277
5000.0	0.72287	.92966	1.21551	1.06912
10000.0	0.212297	.85844	1.39818	1.13669

Composite Parameters

$\gamma = 25.0$

$\delta = 0.3$

$H_c = 0.01$

$\eta = 10^{-5}$

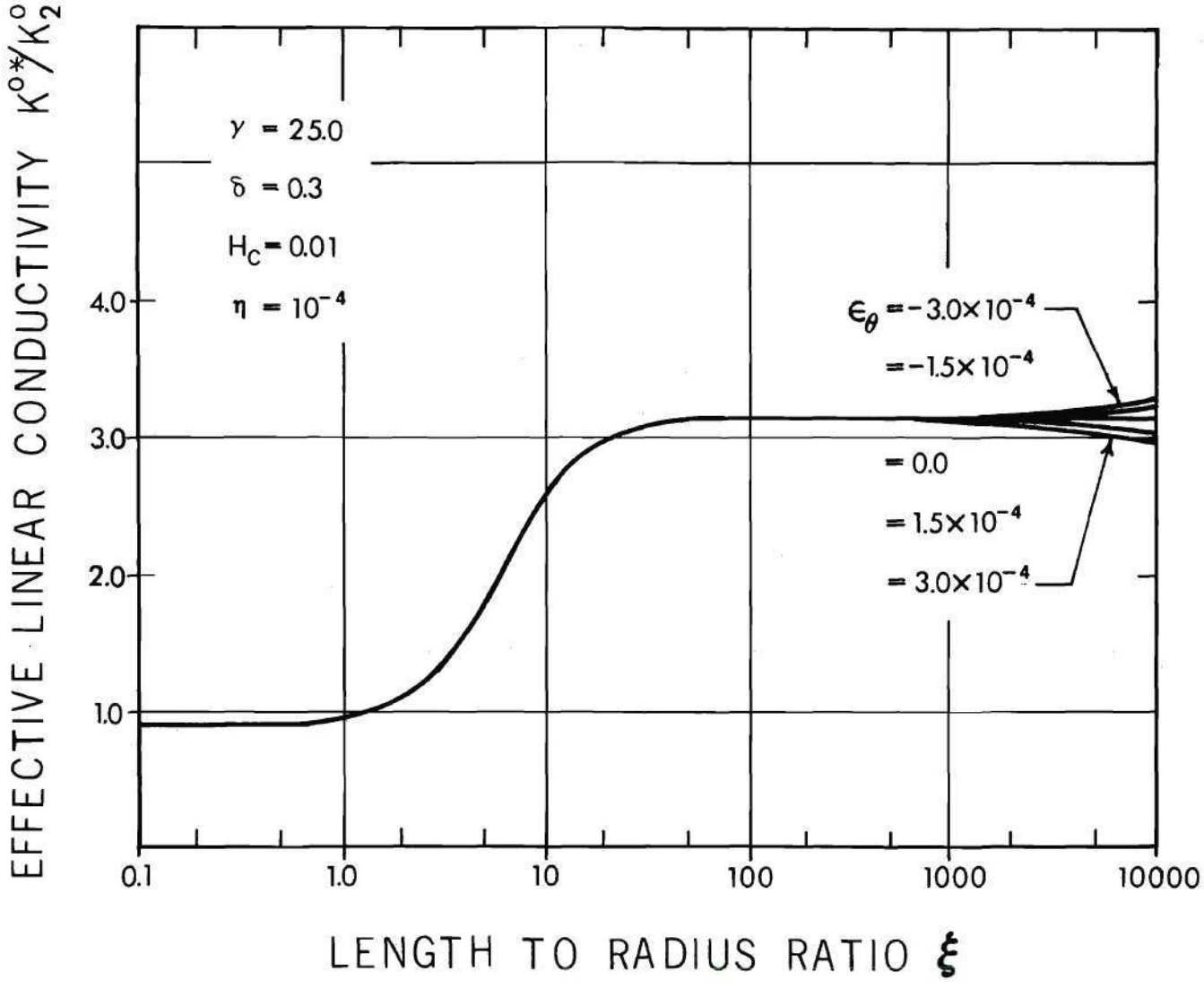

Figure 38. Effective Linear Conductivity versus Length for Various Linear Coefficients

Both of the preceding definitions reduce to the constant conductivity curve as ξ becomes small. This is because the linear conductivity term reduces to unity as ξ becomes small. Thus, the discussion with regard to the constant conductivity problem for the lower asymptote and transition region apply to the linear conductivity as well.

The acceptability criterion, defined in Eq. 3.117, is stated in terms of the maximum temperature. This relation can be converted to an expression in terms of the input parameters, by substituting the maximum temperature from the equivalent material equation, Eq. 3.136, into the acceptability criterion. After solving for ξ the following formulas are produced:

For $\epsilon_\theta < 0$

$$\xi \leq (1-\sqrt{2})\left(\frac{2\pi}{\epsilon_\theta}\frac{k^{0*}}{k_2}\right) \tag{4.10}$$

For $\epsilon_\theta > 0$

$$\xi \leq \frac{2\pi}{\epsilon_\theta}\frac{k^{0*}}{k_2} \tag{4.11}$$

Since the effective linear conductivity does not vary greatly from the volume-weighted average formula, Eqs. 4.10 and 4.11 may be approximated by the following relations:

For $\epsilon_\theta < 0$

$$\xi \leq (1-\sqrt{2})\left(\frac{2\pi}{\epsilon_\theta}\right)\left[(\gamma-1)\delta^2+1\right] \tag{4.12}$$

For $\epsilon_\theta > 0$

$$\xi \leq \left(\frac{2\pi}{\epsilon_\theta}\right)\left[(\gamma-1)\delta^2+1\right] \tag{4.13}$$

There is no upper asymptote for the effective linear conductivity and, consequently, no upper asymptotic region. However, the relatively flat region between the point defined as the asymptotic length for constant conductivity and the point defined by Eqs. 4.12 and 4.13 may be termed a quasi-asymptotic region. In this region, the temperature distributions are uniform radially and have the same axial dependence as the equivalent homogeneous material. Figure 39 shows isotherms and heat flux lines for a composite in this region.

Figure 40 shows heat content for various values of ϵ_θ. Figures 41 and 42 show effective volumetric heat capacity by the definitions in Eq. 3.132 and Eq. 3.140, respectively. As with the effective conductivity, the quantities coalesce to the constant conductivity curve as ξ becomes small and diverge for large ξ. The effective volumetric heat capacity defined by Eq. 3.140 is seen to be a more well-behaved function than the quantity defined by Eq. 3.132. The effective volumetric is relatively uniform in the quasi-asymptotic region.

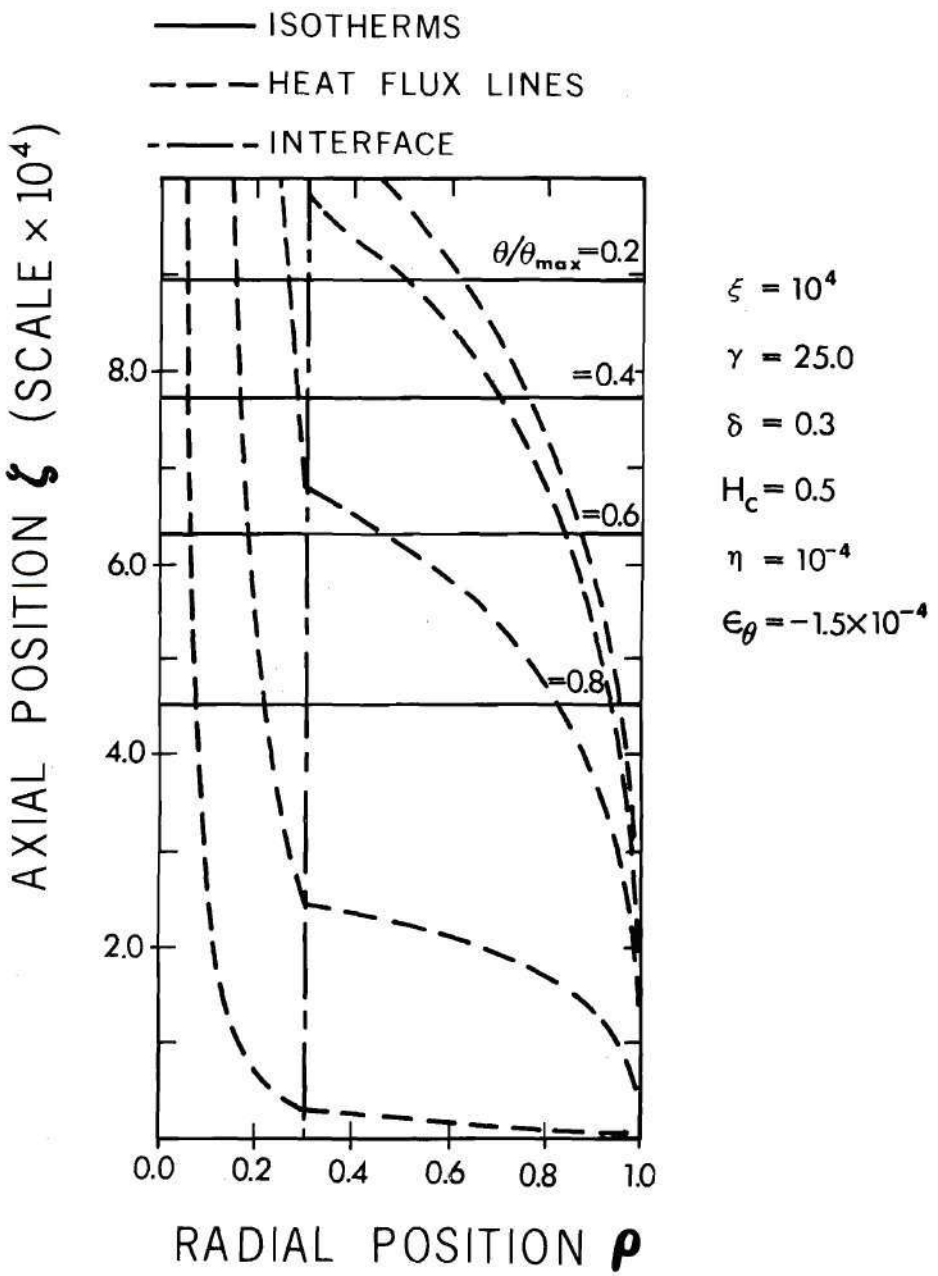

Figure 39. Isotherms and Heat Flux Lines for Linear Conductivity

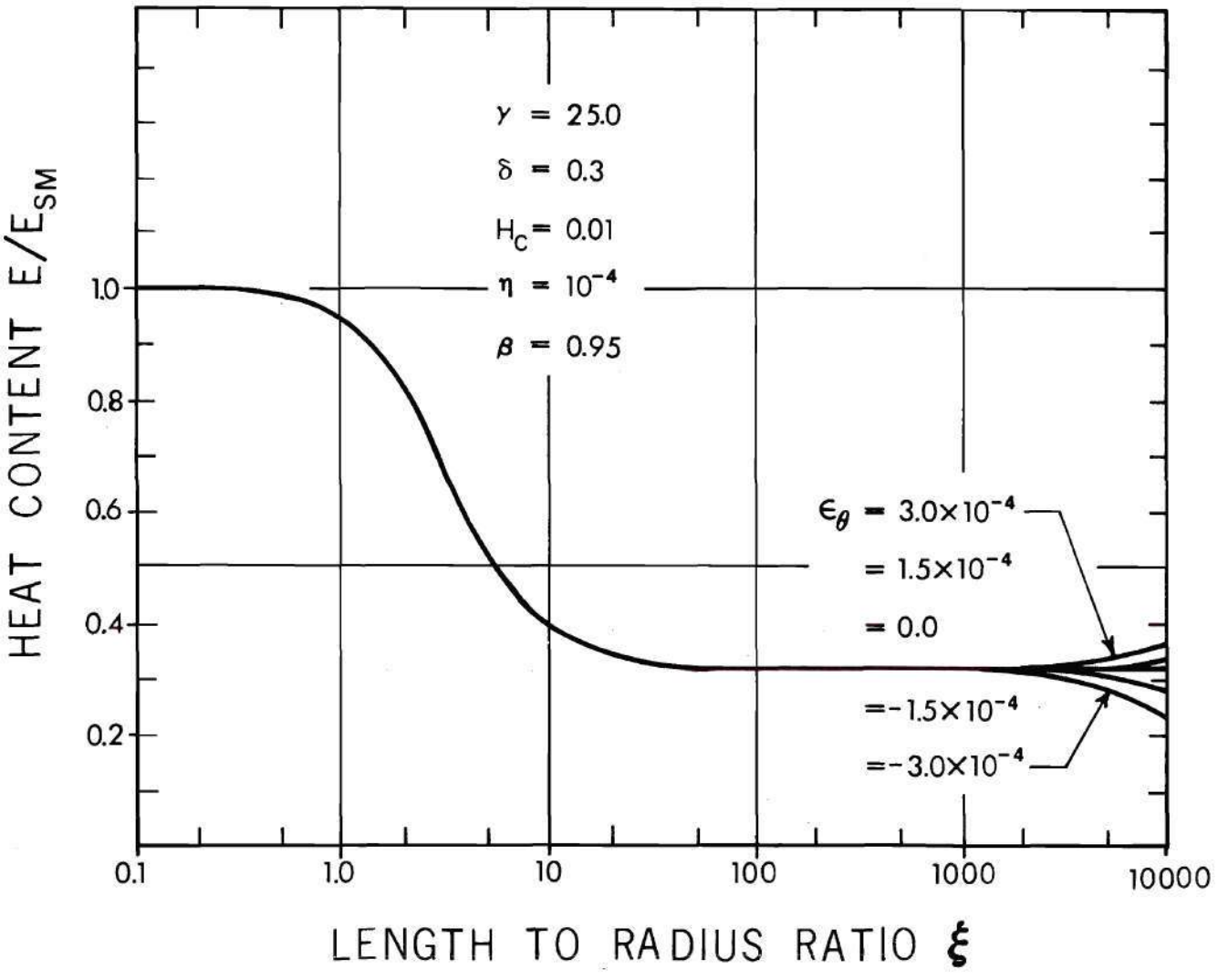

Figure 40. Heat Content versus Length for Various Linear Coefficients

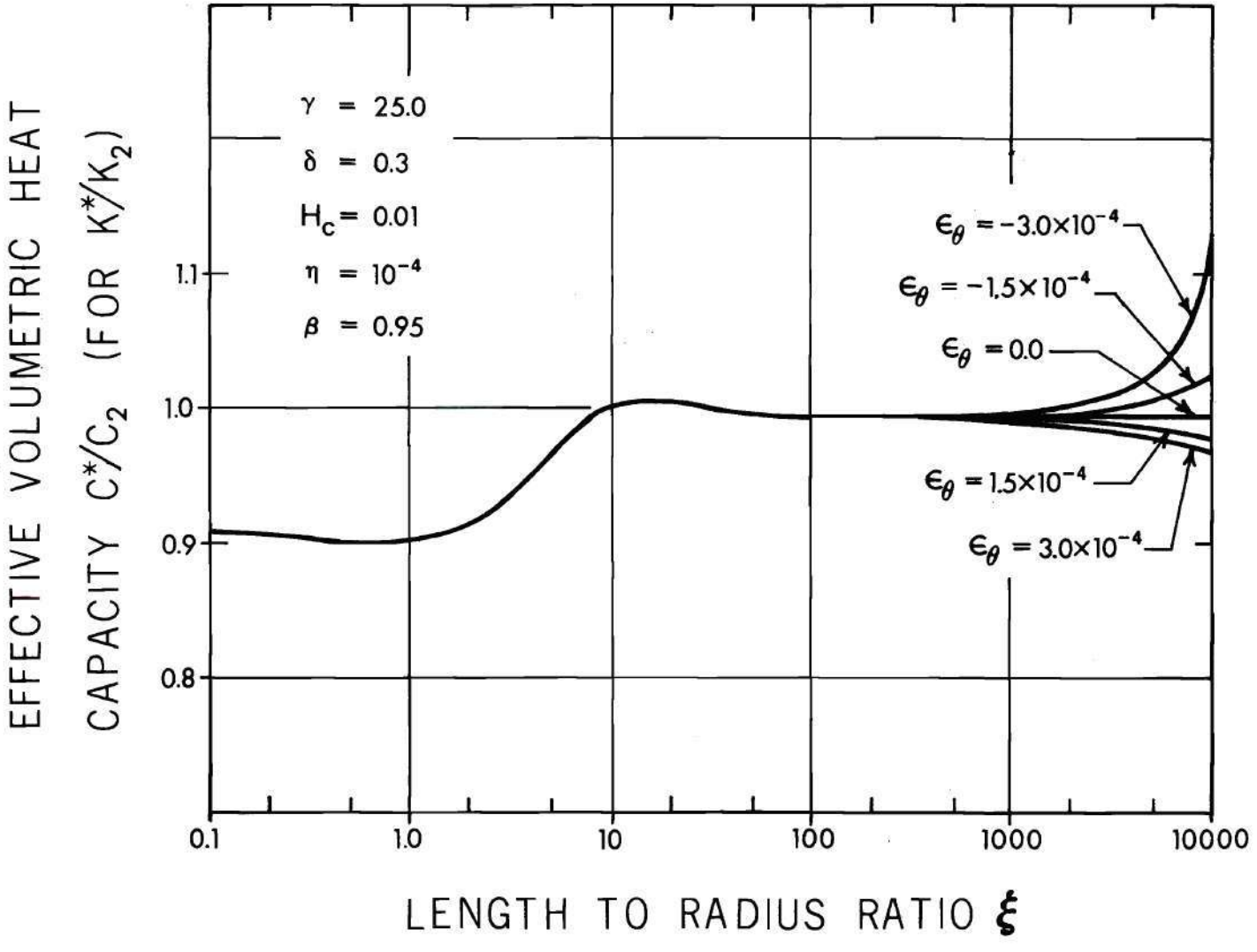

Figure 41. Effective Volumetric Heat Capacity versus Length for Various Linear Coefficients (for Effective Conductivity)

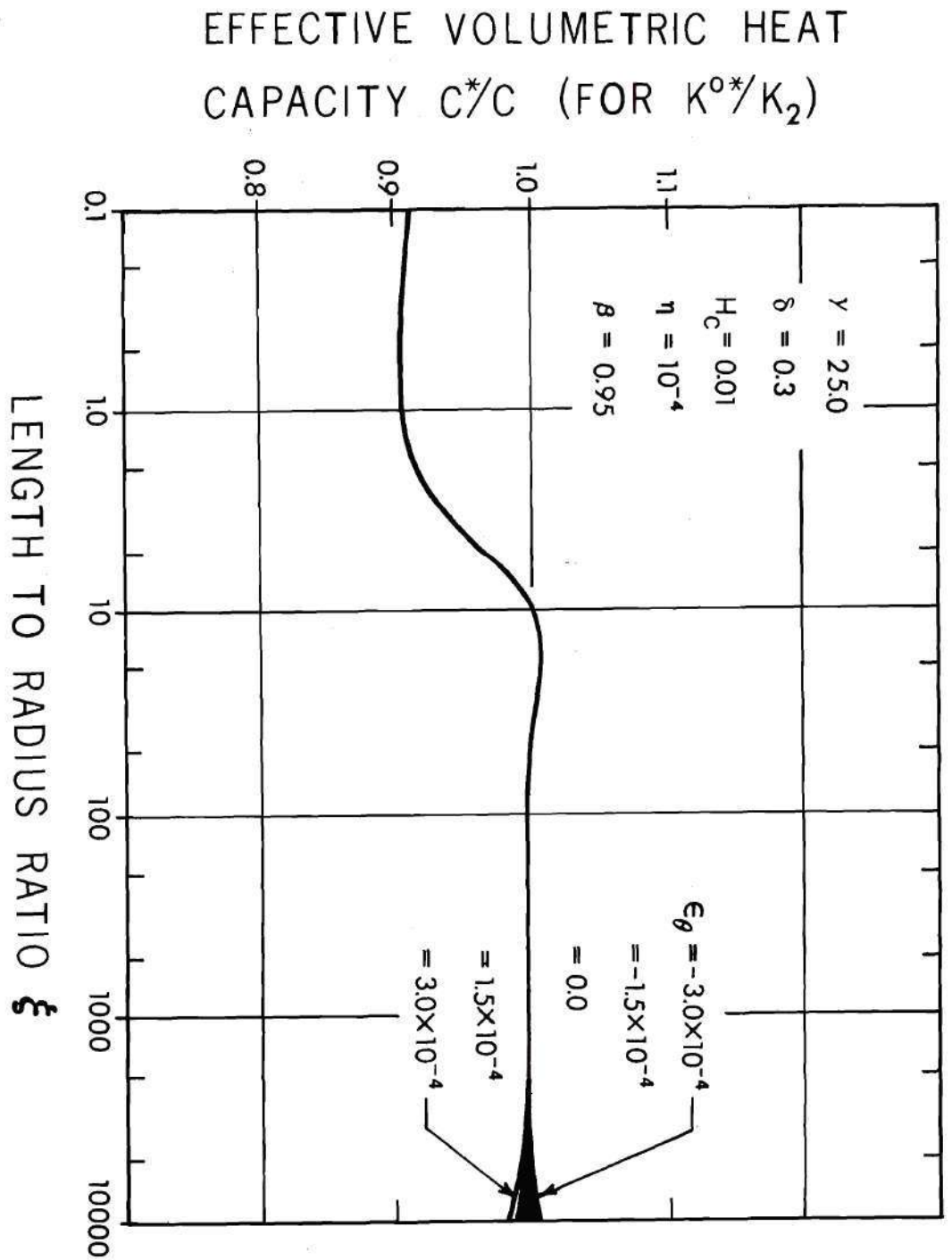

Figure 42. Effective Volumetric Heat Capacity versus Length for Various Linear Coefficients (for Effective Linear Conductivity)

CHAPTER V

CONCLUSIONS

Temperature distributions in composite cells are obtained in exact analytic form for constant conductivity and in approximate form for a linear conductivity by using first-order perturbation theory. The solutions are used to evaluate effective conductivity, heat content, and effective volumetric heat capacity. A computer program evaluating the analytic solutions is very efficient and well suited to perform the large number of cell calculations required for the parametric study. In addition the analytic forms can be used to derive additional information, such as limiting cases and approximate formulas.

From the parametric study, the following conclusions are made about the constant and the linear conductivity problems.

Constant Conductivity Conclusions

1. For large length-to-radius ratios, the effective conductivity approaches asymptotically the volume-averaged formula reported by several other authors [11,14,17] despite heat generation in both fiber and matrix and a gap conductance at the fiber-matrix interface. The effective conductivity also approaches a lower asymptote for small length-to-radius ratios. Formulas for these asymptotes, as well as formulas for the asymptotes of heat content and effective volumetric heat capacity are presented in Table 8.

2. Heat generation in the fiber has a negligible effect on conductivities for fiber-to-matrix heat generation ratios expected in composite nuclear fuels.

3. An approximate formula for asymptotic length, Eq. 4.6, is presented to evaluate whether a doubtful cell is indeed in the upper asymptotic region. Equation 4.5 gives an approximate formula for estimating effective conductivities which are slightly less than the upper asymptote.

4. Because the fiber volume fraction is small, the fraction of heat stored in the fiber is small. As a result, the effective volumetric heat capacity is relatively insensitive to the volumetric heat capacity of the fiber. All values of the effective volumetric heat capacity lie near unity.

5. Heat content is essentially proportional to the reciprocal of effective conductivity.

6. For large length-to-radius ratios, composite temperature distributions are independent of the radial coordinate and have parabolic dependence on the axial coordinate. The radial heat flow is a maximum in this limiting case.

7. Effective conductivities and effective volumetric heat capacities for composite cells are artificial quantities; however, they can be used in engineering calculations as the properties for an equivalent homogeneous material. In these calculations, the effective quantities will conserve maximum temperatures and heat contents of the composite cells. Temperature distributions of composites and their corresponding equivalent homogeneous cells become identical as the length-to-radius ratios become large.

Linear Conductivity Conclusions

1. The linear conductivity model for UO_2 and the first-order perturbation solution of the linear conductivity problem are shown to be adequate approximations for a composite nuclear fuel within a certain range. An acceptability criterion, based on physically reasonable temperatures for UO_2, is proposed, Eq. 3.117.

2. The effective linear conductivity reduces to the constant conductivity for small and intermediate length-to-radius ratios. The linear conductivity term becomes significant as the length-to-radius ratio becomes large, and the effective linear conductivity diverges slightly from the constant conductivity asymptote.

3. While no asymptotic solution exists for the linear conductivity problem, a relatively flat portion of the effective linear conductivity as a function of length-to-radius ratio is designated as the quasi-asymptotic region. This region's lower bound is the asymptotic length defined for constant conductivity Eq. 4.1 and its upper bound, Eqs. 4.12 and 4.13, is given by a restriction based on the acceptability criterion.

4. Within the quasi-asymptotic region, effective linear conductivity and effective volumetric heat capacity are fairly uniform and may be approximated by the same volume-averaged formulas for constant conductivity.

5. Temperature distributions for cells within the quasi-asymptotic range are independent of the radial coordinate and have an axial dependence given by an equivalent material with a linear conductivity.

APPENDIX A

FOURIER SERIES OF $[\theta_2^0]^2$

The temperature function, θ_2^0, derived in Chapter III is given by

$$\theta_2^0 = \sum_{j=1}^{\infty} C_j \left[I_0(\lambda_j \rho) + \frac{I_1(\lambda_j)}{K_1(\lambda_j)} K_0(\lambda_j \rho) \right] \cos \lambda_j \zeta + \frac{fp_2}{2} [\xi^2 - \zeta^2] \quad \text{(A.1)}$$

The Fourier series expansion for the parabolic term is also given in Chapter III.

$$\frac{fp_2}{2} (\xi^2 - \zeta^2) = fp_2 \sum_{j=1}^{\infty} L_j \cos \lambda_j \zeta \quad \text{(A.2)}$$

where

$$L_j = \frac{2}{\xi} \frac{(-1)^{j-1}}{\lambda_j^3} \quad \text{(A.3)}$$

Replacing the parabolic term in Eq. A.1 by its Fourier series, Eq. A.2 yields

$$\theta_2^0(\rho, \zeta) = \sum_{j=1}^{\infty} \left\{ C_j \left[I_0(\lambda_j \rho) + \frac{I_1(\lambda_j)}{K_1(\lambda_j)} K_0(\lambda_j \rho) \right] + fp_2 L_j \right\} \cos \lambda_j \zeta \quad \text{(A.4)}$$

The square of the temperature function at the interface can be

written as

$$\left.\frac{[\theta_2^0]^2}{2}\right|_{\rho=\delta} = \left[\sum_{j=1}^{\infty} H_j \cos\lambda_j \zeta\right]^2 \tag{A.5}$$

where

$$H_j = \frac{1}{\sqrt{2}}\left\{C_j\left[I_0(\lambda_j\delta) + \frac{I_1(\lambda_j)}{K_1(\lambda_j)} K_0(\lambda_j\delta)\right] + f\rho_2 L_j\right\} \tag{A.6}$$

Using the rules for products of cosine functions, Eq. A.5 becomes

$$\frac{[\theta_2^0]^2}{2} = \sum_{j=1}^{\infty}\sum_{k=1}^{\infty} \frac{H_j H_k}{2} \cos(\lambda_j - \lambda_k)\zeta \tag{A.7}$$

$$+\sum_{j=1}^{\infty}\sum_{k=1}^{\infty} \frac{H_j H_k}{2} \cos(\lambda_j - \lambda_k)\delta$$

At this point we note that the sums and differences of λ_j do not give results which are elements of the sequence of λ_j.

$$\lambda_j = \frac{2j-1}{2}\,\frac{\pi}{\xi} \qquad j = 1, 2, 3, \ldots$$

$$\lambda_j + \lambda_k = (j+k-1)\frac{\pi}{\xi} \tag{A.8}$$

$$\lambda_j - \lambda_k = (j-k)\frac{\pi}{\xi} \tag{A.9}$$

The sums and differences comprise another sequence, α_n, and significantly the cosine function series for the new sequence is not orthogonal to the old.

The new sequence is given in the following way:

$$\alpha_n = n\frac{\pi}{\xi} \qquad n = 0,1,2,\ldots \tag{A.10}$$

The new series may be simplified by summing coefficients, $(H_jH_k)/2$, of like cosine functions producing an equation of the following form:

$$\frac{[\theta_2^0]^2}{2} = R_0 + \sum_{n=1}^{\infty} R_n \cos\alpha_n\zeta \tag{A.11}$$

The coefficients, R_n, are evaluated by summing all of the product pairs, H_jH_k, having $\lambda_j+\lambda_k$ or $|\lambda_j-\lambda_k|$ equal to α_n. For clarity, the sums and differences for the first five values of λ_j are listed in Tables 10 and 11. The diagonal lines enclose the combinations which have the same value of α_n.

Formally, all of the summations contain an infinite number of terms. However, the convergence of the series allows truncation to a finite number of terms. Equations A.12 to A.14 list formulas for R_n obtained by tracing the diagonal lines in Tables 10 and 11.

For n = 0,

$$R_0 = \frac{1}{2}\sum_{j=1}^{M} H_j^2. \tag{A.12}$$

For n = 1,2,3,. . ., M-1,

$$R_n = \frac{1}{2}\left[\sum_{j=1}^{n} H_jH_{n+1-j} + 2\sum_{j=n+1}^{M} H_jH_{j-n}\right]. \tag{A.13}$$

Table 10. Sums $\lambda_j + \lambda_k$*

j	λ_j \ k, λ_k	(1) 0.5	(2) 1.5	(3) 2.5	(4) 3.5	(5) 4.5
(1)	0.5	1	2	3	4	5
(2)	1.5	2	3	4	5	6
(3)	2.5	3	4	5	6	7
(4)	3.5	4	5	6	7	8
(5)	4.5	5	6	7	8	9

*Factors $\frac{\Pi}{\xi}$ are omitted for ease of reading.

Table 11. Differences $\lambda_j - \lambda_k$*

j	λ_j \ k, λ_k	(1) 0.5	(2) 1.5	(3) 2.5	(4) 3.5	(5) 4.5
(1)	0.5	0	1	2	3	4
(2)	1.5	-1	0	1	2	3
(3)	2.5	-2	-1	0	1	2
(4)	3.5	-3	-2	-1	0	1
(5)	4.5	-4	-3	-2	-1	0

*Factors $\frac{\Pi}{\xi}$ are omitted for ease of reading.

For n = M,

$$R_M = \frac{1}{2} \sum_{j=1}^{M} H_j H_{n-j} . \tag{A.14}$$

Thus a series of the following form is defined:

$$\frac{[\theta_2^0]^2}{2} = R_0 + \sum_{n=1}^{M} R_n \cos \alpha_n \zeta \tag{A.15}$$

The remaining task is to find a set of coefficientf, F_j, such that

$$R_0 + \sum_{n=1}^{M} R_n \cos \alpha_n \zeta = \sum_{j=1}^{M} F_j \cos \lambda_j \zeta \tag{A.16}$$

This may be accomplished by multiplying Eq. A.16 by $\cos\lambda_j \zeta$ and integrating over the range, $0 \leqq \zeta \leqq \xi$. The result is given by the following:

$$F_j = \frac{2}{\xi} \int_0^{\xi} \cos \lambda_j \zeta \left\{ R_0 + \sum_{n=1}^{M} R_n \cos \alpha_n \zeta \right\} d\zeta \tag{A.17}$$

$$= \frac{2}{\xi} \left\{ \frac{R_0}{\lambda_j} (-1)^{j-1} + \lambda_j \Sigma \frac{R_n (-1)^{j+n-1}}{\lambda_j^2 - \alpha_n^2} \right\}$$

To verify the validity of these formulas, comparisons are made over the range $0 \leqq \zeta \leqq \xi$ in Table 12. The results show agreement within one percent.

Table 12. Comparison of $\frac{1}{2}[\theta_2^0]^2$ for $\xi = 1000$, $\delta = 0.3$, $\gamma = 25.0$, and $\eta = 10^{-4}$ (Multiply all values by 10^3)

ζ	$\frac{1}{2}[\theta_2^0]^2$	$R_0 + \sum_{n=1}^{\infty} R_n \cos \alpha_n \zeta$	$\sum_{j=1}^{\infty} F_j \cos \lambda_j \zeta$
0.0	1.2687	1.2682	1.2686
0.1	1.2427	1.2433	1.2423
0.2	1.1693	1.1687	1.1691
0.3	1.0499	1.0500	1.0500
0.4	0.8953	0.8948	0.8953
0.5	0.7130	0.7136	0.7131
0.6	0.5199	0.5193	0.5199
0.7	0.3295	0.3301	0.3298
0.8	0.1648	0.1642	0.1651
0.9	0.0451	0.0458	0.0446
1.0	0.0000	0.0000	0.0000

APPENDIX B

INTEGRALS OF TEMPERATURE FUNCTIONS

This appendix lists integrals of all the temperature functions required to calculate cell heat content. The heat content formula is

$$\frac{E^*}{E_{SM}} = \frac{\beta \int_{\zeta=0}^{\xi} \int_{\rho=0}^{\delta} \theta_1 \rho d\rho d\zeta + \int_{\zeta=0}^{\xi} \int_{\rho=\delta}^{1.0} \theta_2 \rho d\rho d\zeta}{\int_{\zeta=0}^{\xi} \int_{\rho=0}^{1.0} \theta_{SM} \rho d\rho d\zeta} \tag{B.1}$$

Equation B.1 is too cumbersome to be evaluated as a single expression. The following breakdown is suggested for purposes of organization:

$$I_1 = \int_0^{\xi} \int_0^{\delta} \theta_1 \rho d\rho d\zeta \tag{B.2}$$

$$I_2 = \int_0^{\xi} \int_{\delta}^{1.0} \theta_2 \rho d\rho d\zeta \tag{B.3}$$

$$I_3 = \int_0^{\xi} \int_0^{1.0} \theta_{SM} \rho d\rho d\zeta \tag{B.4}$$

An additional subscript, C or L, will denote constant or linear conductivity solutions, respectively. The constant conductivity is given first.

$$I_{1C} = \int_0^{\xi}\int_0^{\delta}\left[\sum_{j=1}^{\infty} A_j I_0(\lambda_j \rho)\cos\lambda_j \zeta + \frac{fp_1}{2\gamma}(\xi^2-\zeta^2)\right]\rho\, d\rho\, d\zeta \qquad \text{(B.5)}$$

$$= \sum_{j=1}^{\infty} A_j \frac{\delta I_1(\lambda_j \delta)(-1)^{j-1}}{\lambda_j^2} + \frac{fp_1}{6\gamma}\xi^3\delta^2$$

$$I_{2C} = \int_0^{\xi}\int_{\delta}^{1.0}\left\{\sum_{j=1}^{\infty} C_j\left[I_0(\lambda_j\rho) + \frac{I_1(\lambda_j)}{K_1(\lambda_j)}K_0(\lambda_j\rho)\right]\cos\lambda_j\zeta \right. \qquad \text{(B.6)}$$

$$\left. + \frac{fp_2}{2}(\xi^2-\zeta^2)\right\}\rho\, d\rho\, d\zeta$$

$$= \sum_{j=1}^{\infty} C_j \frac{(-1)^j}{\lambda_j^2}\delta\left[I_1(\lambda_j\delta) - \frac{I_1(\lambda_j)}{K_1(\lambda_j)}K_0(\lambda_j\delta)\right]$$

$$+ \frac{fp_2\,\xi^3(1-\delta^2)}{6}$$

$$I_{3C} = \int_0^{\xi}\int_0^{1.0}\frac{1}{2\pi\xi}(\xi^2-\zeta^2)\rho\, d\rho\, d\zeta \qquad \text{(B.7)}$$

$$= \frac{1}{6}\frac{\xi^2}{\pi}$$

The linear conductivity solutions are as follows:

$$I_{1L} = \int_0^{\xi}\int_0^{\delta}\left[(A_j + \epsilon_\theta U_j)I_0(\lambda_j\rho) + \frac{fp_1}{2\gamma}(\xi^2-\zeta^2)\right]\rho\, d\rho\, d\zeta \qquad \text{(B.8)}$$

$$= \sum_{j=1}^{\infty}\left[A_j + \epsilon_\theta U_j\right]\frac{\delta I_1(\lambda_j\delta)}{\lambda_j^2}(-1)^{j-1} + \frac{fp_2\xi^3\delta^2}{6\gamma}$$

$$I_{2L} = \int_0^{\xi} \int_{\delta}^{1.0} \left[\theta_2^0 + \epsilon_\theta \theta_2^0 - \frac{\epsilon_\theta}{2}\left[\theta_2^0\right]^2\right] \rho d\rho d\zeta \qquad \text{(B.9)}$$

Equation B.9 must be split again into two parts

$$I_{21L} = \int_0^{\xi} \int_{\delta}^{1.0} (\theta_2^0 + \epsilon_\theta \theta_2^0) \rho d\rho d\zeta \qquad \text{(B.10)}$$

$$= \int_0^{\xi} \int_{\delta}^{1.0} \left\{ \sum_{j=1}^{\infty} \left[C_j + \epsilon_\theta V_j\right]\left[I_0(\lambda_j \rho) + \frac{I_1(\lambda_j)}{K_1(\lambda_j)} K_0(\lambda_j \rho)\right] + \frac{f p_2}{2}(\xi^2 - \zeta^2) \right\} \rho d\rho d\zeta$$

$$I_{22L} = -\frac{\epsilon_\theta}{2} \int_0^{\xi} \int_{\delta}^{1.0} \left[\theta_2^0\right]^2 \rho d\rho d\zeta \qquad \text{(B.11)}$$

$$= \frac{-\epsilon_\theta}{2} \int_0^{\xi} \int_{\delta}^{1.0} \left[\sum_{j=1}^{\infty} \left[C_j \left[I_0(\lambda_j \rho) + \frac{I_1(\lambda_j)}{K_1(\lambda_j)} K_0(\lambda_j \rho)\right] + f p_2 L_j\right] \cos \lambda_j \zeta\right]^2 \rho d\rho d\zeta$$

$$= \frac{-\epsilon_\theta \xi}{4} \left\{ \sum_{j=1}^{\infty} \left[\frac{C_j^2}{2}\left[\chi_0^2(\lambda_j) - \delta^2\left(\chi_0^2(\lambda_j \delta) - \chi_1^*(\lambda_j \delta)\right)\right] - \frac{2 C_j f p_2 L_j \delta \chi_1^*(\lambda_j \delta)}{\lambda_j} + \frac{f p_2 L_j (1 - \delta^2)}{2} \right\}$$

where

$$\chi_0(\lambda_j \rho) = I_0(\lambda_j \rho) + \frac{I_1(\lambda_j)}{K_1(\lambda_j)} K_0(\lambda_j \rho) \qquad \text{(B.12)}$$

$$x_1(\lambda_j\rho) = I_1(\lambda_j\rho) + \frac{I_1(\lambda_j)}{K_1(\lambda_j)} K_1(\lambda_j\rho) \tag{B.13}$$

$$x_0^*(\lambda_j\rho) = I_0(\lambda_j\rho) - \frac{I_1(\lambda_j)}{K_1(\lambda_j)} K_0(\lambda_j\rho) \tag{B.14}$$

$$x_1^*(\lambda_j\rho) = I_1(\lambda_j\rho) - \frac{I_1(\lambda_j)}{K_1(\lambda_j)} K_1(\lambda_j\rho) \tag{B.15}$$

$$I_{3L} = \int_0^{\xi}\int_0^{1.0} \theta_{SM}\rho d\rho d\zeta \tag{B.16}$$

$$= \int_0^{\xi}\int_0^{1.0} \frac{-1+\sqrt{1+\frac{\epsilon_\theta}{\pi\xi}(\xi^2-\zeta^2)}}{\epsilon_\theta} \rho d\rho d\zeta$$

Equation B.16 has solutions of different form for $\epsilon_\theta < 0$ or > 0.

For $\epsilon_\theta < 0$

$$I_{3L} = \frac{1}{4\epsilon_\theta}\left\{\frac{\xi(\pi+\xi\epsilon_\theta)}{(-\pi\xi\epsilon_\theta)^{1/2}} \ln\left[\frac{(-\epsilon_\theta\xi)^{1/2}+\pi^{1/2}}{(\pi+\xi\epsilon_\theta)^{1/2}}\right] - \xi\right\} \tag{B.17}$$

For $\epsilon_\theta > 0$

$$I_{3L} = \frac{1}{4\epsilon_\theta}\left\{\frac{\xi(\pi+\xi\epsilon_\theta)}{(\pi\xi\epsilon_\theta)} \tan^{-1}\left[\frac{\epsilon_\theta\xi}{\pi}\right]^{1/2} - \xi\right\} \tag{B.18}$$

$$E_{EM} = \frac{C^*}{C_2} \int_{\zeta=0}^{\xi} \int_{\rho=0}^{1.0} \tilde{\theta}_{EM} \rho d\rho d\zeta \tag{B.19}$$

$$= \left(\frac{C^*}{C_2}\right)\left(\frac{1}{2\pi\varepsilon}\right)\left(\frac{k_2^0}{k^{0*}}\right) \int_{\zeta=0}^{\xi} \int_{\rho=0}^{1.0} \left[\xi^2 - \zeta^2\right]\left[1 - \left(\frac{\epsilon_\theta}{4\pi\varepsilon}\right)\left(\frac{k_2^0}{k^{0*}}\right)(\xi^2 - \zeta^2)\right] \rho d\rho d\zeta$$

$$= \frac{C^*}{C_2} \frac{\xi^2}{6\pi} \frac{k_2^0}{k^{0*}} \left[1 - \frac{\epsilon_\theta \xi k_2^0}{5\pi k^{0*}}\right] \tag{B.20}$$

APPENDIX C

LINEAR CONDUCTIVITY OF UO_2

The best linear fit to approximate a function, k(T), over the range T_1 to T_2 minimizes the following integral:

$$\overline{\Delta k^2} = \int_{T_1}^{T_2} \left[aT + b - k(T)\right]^2 dT \tag{C.1}$$

The minimum satisfies the following conditions:

$$\frac{\partial \overline{\Delta k^2}}{\partial a} = \frac{\partial \overline{\Delta k^2}}{\partial b} = 0 \tag{C.2}$$

Thus,

$$0 = \int_{T_1}^{T_2} T\left[aT + b - k(T)\right] dT \tag{C.3}$$

$$0 = \int_{T_1}^{T_2} \left[aT + b - k(T)\right] dT \tag{C.4}$$

Carrying out the integrations gives

$$0 = \frac{a}{3}\left[T_2^3 - T_1^3\right] + \frac{b}{2}\left[T_2^2 - T_1^2\right] - \int_{T_1}^{T_2} k(T)\,dT \tag{C.5}$$

$$0 = \frac{a}{2}\left[T_2^2 - T_1^2\right] + b\left[T_2 - T_1\right] - \int_{T_1}^{T_2} k(T)\,dT \tag{C.6}$$

Equations C.5 and C.6 may be put in the form

$$ac_{11} + bc_{12} = c_{13} \tag{C.7}$$

$$ac_{21} + bc_{22} = c_{23} \tag{C.8}$$

where

$$C_{11} = \frac{1}{3}\,(T_2^3 - T_1^3)$$

$$C_{12} = \frac{1}{2}\,(T_2^2 - T_1^2)$$

$$C_{13} = \int_{T_1}^{T_2} T\,k(T)\,dT$$

$$C_{21} = C_{12} = \frac{1}{2}\,(T_2^2 - T_1^2)$$

$$C_{22} = T_2 - T_1$$

$$C_{23} = \int_{T_1}^{T_2} k(T)\,dT$$

For Bianchieria's equation for conductivity

$$C_{13} = \int_{T_1}^{T_2} \frac{T}{A+BT} + CT(T+D)^3\,dT$$

$$= \frac{T_2 - T_1}{B} - \frac{A}{B^2} \ln\left[\frac{BT_2 + A}{BT_1 + A}\right] + C\left\{\frac{1}{5}\left[(T_2+D)^5 - (T_1+D)^5\right]\right.$$

$$\left. - \frac{D}{4}\left[(T_2+D)^4 - (T_1+D)^4\right]\right\}$$

$$C_{23} = \int_{T_1}^{T_2} \frac{1}{A+BT} + C(T+D)^3 \, dT$$

$$= \frac{1}{B} \ln\left[\frac{BT_2+A}{BT_1+A}\right] + \frac{C}{4}\left[(T_2+D)^4 - (T_1+D)^4\right]$$

From Table 5, the parameters A, B, C, and D are

$$A = .1739$$

$$B = 2.614 \times 10^{-4}$$

$$C = 5.3436 \times 10^{-12}$$

$$D = 459.69$$

The calculated coefficients, a and b, are for $T_1 = 1000$ and $T_2 = 2000$

$$a = -7.807 \times 10^{-4}$$

$$b = 3.013$$

and for $T_1 = 1000$ and $T_2 = 3000$

$$a = -4.890 \times 10^{-4}$$

$$b = 2.580$$

APPENDIX D

APPROXIMATE FORMULA FOR k^*/k_2

A function to satisfy Eq. 4.4 can be obtained by noting that, as ξ gets large, λ_j must get small. Thus, the modified Bessel functions in the effective conductivity expression can be replaced by approximations for Bessel functions with small arguments.

Equations D.1 through D.4 list these approximations for small x.

$$I_0(x) \cong 1.0 \tag{D.1}$$

$$I_1(x) \cong x \tag{D.2}$$

$$K_0(x) \cong -\ln x \tag{D.3}$$

$$K_1(x) \cong \frac{1}{x} \tag{D.4}$$

Equation 3.163 is a convenient form in which to substitute Eqs. D.1 through D.4.

$$\frac{k_2}{k^*} = \frac{2\pi}{\xi}\left[\theta_{comp}\right]_{max} = \frac{-(\eta-\gamma)}{\gamma[(\eta-1)\delta^2+1]} \cdot \sum_{j=1}^{\infty} H_c \frac{\mathcal{L}_j}{G_j} \times \left[I_0(\lambda_j) + \frac{I_1(\lambda_j)}{K_1(\lambda_j)} K_0(\lambda_j)\right] + \frac{1}{(\eta-1)\delta^2+1} \sum_{j=1}^{\infty} \mathcal{L}_j \tag{3.163}$$

Only the first factor depending on λ_j needs to be considered. It may be moved outside the summation.

$$\frac{k_2}{k^*} \cong \left\{ \left[\frac{-(\eta-\gamma)H_C}{\gamma[(\eta-1)\delta^2+1]} \right] \left[\frac{I_0(\lambda_1) + \frac{I_1(\lambda_1)}{K_1(\lambda_1)} K_0(\lambda_1)}{G_1} \right] + \frac{1}{(\eta-1)\delta^2+1} \right\} \sum_{j=1}^{\infty} \mathcal{L}_j \tag{D.5}$$

Substituting the approximations from Eqs. D.1 through D.4 for the Bessel functions yields the following:

$$I_0(\lambda_1) + \frac{I_1(\lambda_1)}{K_1(\lambda_1)} K_0(\lambda_1) \cong 1 - \lambda_1^2 \ln \lambda_1 \tag{D.6}$$

$$G_1 \cong \frac{1}{\gamma}\left[1-\frac{1}{\delta^2}\right]\left[\lambda_1^2\delta + H_C\right] - H_C\left[1-\lambda_1^2 \ln \lambda_1 \delta\right] \tag{D.7}$$

The preceding relations combined with Eq. D.5 yield the following relation after rearranging and simplifying:

$$\frac{k^*}{k_2} \cong \frac{k_U^*}{k_2} \left\{ \frac{1 - \frac{\lambda_1^2\delta^2}{(\gamma-1)\delta^2+1}\left[\gamma \ln \lambda_1 \delta + \frac{\delta}{H_C}(1-\delta^2)\right]}{1 - \frac{\lambda_1^2\delta^2}{(\eta-1)\delta^2+1}\left[\eta \ln \lambda_1 + \gamma \ln \delta + \frac{\delta}{H_C}(1-\delta^2)\right]} \right\} \tag{D.8}$$

The eigenvalue, λ_1, may be replaced by $(\pi/2\xi)$ producing a relation of the required form.

$$\frac{k^*}{k_2} = \frac{k_U^*}{k_2} \cdot \phi(\xi, \gamma, \delta, H_c, \eta) \tag{D.9}$$

$$\phi(\xi,\gamma,\delta,H_c,\eta) = \frac{1-\left(\frac{\pi\delta}{2\xi}\right)^2\left[\frac{\gamma \ln\frac{\pi\delta}{2\xi} + \frac{\delta}{H_c}(1-\delta^2)}{(\gamma-1)\delta^2+1}\right]}{1-\left(\frac{\pi\delta}{2\xi}\right)^2\left[\frac{\gamma\ln\frac{\pi}{2\xi}+\gamma\ln\delta+\frac{\delta}{H_c}(1-\delta^2)}{(\eta-1)\delta^2+1}\right]} \tag{D.10}$$

An approximate formula for the minimum asymptotic length is obtained by substituting Eq. D.10 into Eq. 4.1. The result is the following:

$$\frac{1-\left(\frac{\pi}{2\xi}\right)^2 \ln\left(\frac{\pi}{2\xi}\right)}{\left\{1-\left(\frac{\pi\delta}{2\xi}\right)^2\left[\eta\ln\frac{\pi}{2\xi}+\gamma\ln\delta+\frac{\delta}{H_c}\left(1-\frac{1}{\delta^2}\right)\right]\right\}} = 0.99 \tag{D.11}$$

BIBLIOGRAPHY

1. Chapman, A. T., Clark, G. W., and Hendrix, D. E., "UO_2-W Cermets Produced by Unidirectional Solidification," J. Am. Ceram. Soc., 53, 1, 60-61 (1970).

2. Hulse, C. O. and Batl, J. A., "Preparation of Ceramic Eutectics by the Floating Molten Zone Technique," in Advanced Materials: Composites and Carbon, A Symposium of the American Ceramic Society, Chicago, 132 (1970).

3. Galasso, F. S., "Unidirectional Solidified Eutectics for Optical, Electronic and Magnetic Applications," J. Metals, 19, 6, 17-21 (1967).

4. Liebmann, W. K. and Miller, E. A., "Preparation Phase Boundary Energies, and Thermoelastic Properties of InSb-In Eutectic Alloys with Ordered Microstructures," J. Appl. Phys., 34, 2653 (1963).

5. Loxhall, J. G. and Hellawell, A., "Constitution and Microstructure of Some Binary Halide Mixtures," J. Am. Ceram. Soc., 47, 184 (1964).

6. Viechnicki, D. and Schmid, F., "Eutectic Solidification in the System $Al_2O_3/Y_3Al_5O_{12}$," J. Material Science, 4, 1, 84-88 (1969).

7. Schmid, F. and Viechnicki, D., "Oriented Eutectic Microstructures in the System Al_2O_3/ZrO_2," J. Material Science, 5, 470-473 (1970).

8. Schmid, F. and Viechnicki, D., "Ceramic Eutectics," in Advanced Materials: Composites and Carbon, A Symposium of the American Ceramic Society, Chicago, 96 (1970).

9. Chapman, A. T. and Clark, G. W., "Growth of UO_2 Single Crystals Using the Floating Zone Technique," J. Am. Ceram. Soc., 48, 9, 494-495 (1965).

10. Chapman, A. T., et al., "Substructure and Perfection in UO_2 Single Crystals," J. Am. Ceram. Soc., 48, 9 (1970).

11. Springer, G. S. and Tsai, S. W., "Thermal Conductivities of Unidirectional Materials," J. Composite Materials, 1, 2, 166-173 (1967).

BIBLIOGRAPHY (Continued)

12. Adams, D. F. and Doner, D. K., "Longitudinal Shear Loading of a Unidirectional Composite," J. Composite Materials, 1, 1, 4 (1967).

13. Zinsmeister, G. E. and Purohit, K. S., "Comments on Springer and Tsai's Method of Predicting Effective Thermal Conductivities of Unidirectional Composites," J. Composite Materials, 4, 278 (1970).

14. Behrens, Ernst, "Thermal Conductivity of Composite Media," J. Composite Materials, 2, 1, 2 (1968).

15. Donea, Jean, "Thermal Conductivities Based on Variational Principles," J. Composite Materials, 6, 262 (1972).

16. D'Andrea, G. and Ling, T. F., "On Thermal Conductivity of Composites," Proceedings of the Fourth International Heat Transfer Conference, 1, Paris, France (1970).

17. Rust, J. H. and Boyle, D. R., "Heat Conduction Analysis of Composite Nuclear Fuels," ASME Paper, 75-HT-30 (1975).

18. Chamis, C. C. and Sendeckyj, G. P., "Critique on Theories of Thermoelastic Properties of Fibrous Composites," J. Composite Materials, 2, 3, 332 (1968).

19. Kittel, C., Quantum Theory of Solids, John Wiley and Sons, Inc., New York, pp. 250-254 (1963).

20. Lamarsh, J. R., Nuclear Reactor Theory, Addison-Wesley Publishing Company, Inc., Reading, Mass., p. 374 (1966).

21. Cohen, E. R., "The Thermal Neutron Flux in a Square Lattice," Nuclear Science and Engineering, 1, 268-269 (1956).

22. Carslaw, H. S. and Jaeger, J. C., Conduction of Heat in Solids, Clarendon Press, Oxford, Chapter 1 (1958).

23. Ross, A. M. and Stoute, R. L., "Heat Transfer Coefficient Between Uranium Dioxide and Zircaloy 2," AECL-1552 (1962).

24. Ozizik, M. Necati, Boundary Value Problems of Heat Conduction, International Textbook Company, Scranton, Pennsylvania, p. 181 (1968).

25. Park, D., Introduction to the Quantum Theory, McGraw-Hill Book Company, New York, p. 212 (1964).

BIBLIOGRAPHY (Concluded)

26. Aizen, A. M., Redchits, I. S., and Fedotkin, I. M., "An Engineering Method of Calculating the Transient Heat Flow Through a Multilayer Wall Containing Heat Source and Having Imperfect Thermal Contact," High Temperature, 12, 3, 588-592 (1975) (Translated).

27. Bianchieria, A., et al., Westinghouse (USA) Report, WARD-4135-1, 6 (Sept. 1969).